SECURITY CLASSIFICATION OF THIS PAGE (When Data Entered)

5

REPORT DOCUMENTATION PAGE

READ INSTRUCTIONS BEFORE COMPLETING FORM

1. REPORT NUMBER: AFOSR-TR- 84-1272 (Technical Report)
2. GOVT ACCESSION NO.
3. RECIPIENT'S CATALOG NUMBER

4. TITLE (and Subtitle): Attenuation of Seismic Waves at Regional Distances

5. TYPE OF REPORT & PERIOD COVERED: Final Report, 1 Oct. 82 - 30 Sept. 84

6. PERFORMING ORG. REPORT NUMBER

7. AUTHOR(s): Otto W. Nuttli, Brian J. Mitchell

8. CONTRACT OR GRANT NUMBER(s): F49620-83-C-0015

9. PERFORMING ORGANIZATION NAME AND ADDRESS: Dept. of Earth & Atmospheric Sciences, Saint Louis University, St. Louis, MO 63156

10. PROGRAM ELEMENT, PROJECT, TASK AREA & WORK UNIT NUMBERS: 62714E

11. CONTROLLING OFFICE NAME AND ADDRESS: Defense Advanced Research Projects Agency, 1400 Wilson Blvd., Arlington, VA 27709

12. REPORT DATE: 27 November 1984

13. NUMBER OF PAGES

14. MONITORING AGENCY NAME & ADDRESS (if different from Controlling Office): Air Force Office of Scientific Research, Bolling Air Force Base, Washington, DC 20332

15. SECURITY CLASS. (of this report): Unclassified

15a. DECLASSIFICATION/DOWNGRADING SCHEDULE

16. DISTRIBUTION STATEMENT (of this Report)

Approved for Public Release. Distribution Unlimited.

17. DISTRIBUTION STATEMENT (of the abstract entered in Block 20, if different from Report)

18. SUPPLEMENTARY NOTES

19. KEY WORDS (Continue on reverse side if necessary and identify by block number)

Attenuation, Magnitude, Spectra
Q, Surface Waves, Nuclear Explosions
Lg Waves, Seismic Yield
NTS (Nevada Test Site),

20. ABSTRACT (Continue on reverse side if necessary and identify by block number)

The coda-Q method was applied to determine the anelastic attenuation of 1-sec period Lg waves at NTS, East Kazakh, the Indian subcontinent, and the South American continent.

m_b(Lg) versus explosion yield calibration curves are given for NTS explosions in hard rock and in alluvium. The NTS hard-rock calibration curve,

(continued)

DD FORM 1 JAN 73 1473

85 01 30 025

SECURITY CLASSIFICATION OF THIS PAGE (When Data Entered)

m sub b

20. Abstract (continued)

AFOSR-TR- 84-1272

when applied to explosions in other regions of the United States and in the French Sahara, gives realistic yield estimates. The technique also is applied to selected Soviet explosions in East Kazakh. m_b(Lg) and m_b(P) values were used to estimate the m_b(P) bias between NTS and eastern North America. Assuming that explosions and earthquakes of the same m_b(P) value excite Lg waves of equal amplitude, the P-wave magnitude bias between NTS and eastern North America is 0.31 magnitude units. A tentative value for the bias between NTS and Shagan River is 0.41 magnitude units, but this value may be changed when further study of anelastic attenuation of Lg in Eurasia is completed.

The effects of velocity structure, crustal Q, and sediment Q values on the attenuation of Lg waves were studied using theoretical amplitude spectra and synthetic seismograms for various models. Comparisons with observations suggest that crustal velocity structure can have a significant effect on Lg attenuation and that low-Q sediments have a profound effect of the variation of Lg attenuation in stable regions. By contrast, in areas where crustal Q values are low, there is little effect of sediment Q values on the attenuation of Lg. Low Q values for the crust of the western United States seem to be required in order to match the variation of frequency in the wave forms of Lg.

Frequency-dependence of crustal Q seems significant in regions of high Q, but are small or non-existent in regions of low Q values.

Keywords include: Lg waves, Magnitude, Surface waves, Spectra, Nuclear explosions, and Seismic yield.

AFOSR-TR- 84-1272

Final Technical Report

1 October 1982 - 30 September 1984

ARPA Order:	4397
Program Code:	3D60
Contractor:	Saint Louis University
Effective Date of Contract:	1 October 1982
Contract Expiration Date:	30 September 1984
Amount of Contract:	$279,034.00
Contract Number:	F49620-83-C-0015
Principal Investigators:	Brian J. Mitchell Otto W. Nuttli
Telephone:	314-658-3131
Short Title:	Surface Wave Attenuation

Sponsored by

Advanced Research Projects Agency (DOD)

ARPA Order No. 4397

Monitored by AFOSR under Contract #F49620-83-C-0015

Table of Contents

TECHNICAL SUMMARY

Lg Yield and Magnitude Bias Estimates

The methodology for using 1-sec period Lg amplitudes has been refined for determining yields of underground nuclear explosions at NTS. In particular, special attention was devoted to obtaining the best possible estimates of the coefficient of anelastic attenuation for paths from NTS to the WWSSN stations BKS, DUG, and TUC. In the first iteration the coda-Q method is applied to determine Q_o (1-Hz value of Q) and the parameter η which is a measure of the frequency dependence of Q. Then small corrections to the Q_o values are made so as to minimize the deviations between the station-average $m_b(Lg)$ and the individual $m_b(Lg)$ values. Two problems were encountered and overcome in applying the coda-Q method. The first concerns the interference of low-frequency fundamental-mode Rayleigh waves with the Lg coda waves about 1 to 3 minutes after the onset of Lg, which if not corrected for will give frequency values that are too low at relatively small lapse times. The second concerns the leveling off of frequency for large lapse times, with the lapse time at which the frequency attains a constant value being a function of the magnitude of the explosion. This phenomenon can incorrectly result in too large estimates of wave frequency at long lapse times. Both phenonmena, especially the latter, can result in underestimates of η and overestimates of Q_o values. Nevada earthquakes, for which both $m_b(P)$ and $m_b(Lg)$ were obtained, support the Q_o and η values found in this study.

Lg amplitudes and $m_b(Lg)$ values were obtained for all NTS explosions of announced yield, and calibration curves are presented for shots

in hard rock and in alluvium. The standard deviation of the hard rock m_b(Lg) values is 0.06 magnitude units (equivalent to about a 15% uncertainty in yield value).

Lg amplitudes also were used to estimate yields of non-NTS events in the United States (SALMON, GASBUGGY, RULISON and RIO BLANCA) and in the French Sahara (SAPHIR and RUBIS). The hard-rock NTS calibration curve. when applied to these data, gave yield values close to the announced one. This suggests that there is no magnitude bias in m_b(Lg), in contrast to observed bias for m_b(P), and that the excitation of Lg waves for an explosion of a given yield is the same in all continental areas.

Q_o, η and m_b(Lg) values were obtained for Soviet explosions at the Shagan River and Degelen Mountain regions of the East Kazakh test site. Preliminary results indicate a yield of 200 kt for the largest explosion considered, that of Septemver 14, 1980. For the only Soviet explosion of announced yield at East Kazakh, that of January 15, 1965, the announced yield was 125 kt and the m_b(Lg)-estimated yield was 105 kt.

The m_b(P) and m_b(Lg) values for NTS explosions indicate that the m_b(P) bias of NTS relative to eastern North America is 0.31 magnitude units or larger. depending on whether the excitation of Lg waves is the same for explosions as for earthquakes of the same m_b(P), or whether the Lg excitation for explosions is less.

Tentatively the m_b(P) bias between NTS and Shagan River events is found to be 0.41 magnitude units. However, the Q_o and η values for the Soviet explosions need to be further studied, which will be done in the

work to follow. If the Shagan River P-wave attenuation in the asthenosphere is the same as for eastern North America, the bias between it and NTS will be 0.31 magnitude units.

Lg Attenuation in South America

The coda-Q method was applied to earthquakes occurring in South America and recorded by WWSSN stations across the continent. Amplitude attenuation was used as an independent method of obtaining the same information.

Both methods give low Q_o values (135 to 320) in the northern and wstern coastal areas of South America, the regions of neotectonics. The shield and geologically older areas of eastern South America have an average Q_o value of about 700. Regions of low Q_o have ζ values of 0.4 to 0.7, and regions of high Q_o have ζ values of 0.0 to 0.2.

Lg Attenuation in India and Pakistan

The coda-Q method was applied to earthquakes occurring in India and recorded by WWSSN stations in India and Pakistan. Amplitude attenuation was used to confirm the coda-Q results for selected stations.

The mountainous areas of northern India and Pakistan show relatively low Q_o (300) and relatively high ζ (0.4) average values. The shield area of northern India shows relatively high Q_o (700) and relatively low ζ (0.2) values.

The research of B.J. Mitchell has been concentrated on two major aspects of seismic wave attenuation. First, several factors which influence the attenuation of seismic waves at regional distances have

been thoroughly investigated. These include crustal velocity structure, crustal Q structure, and Q values and thicknesses of surficial sediments. Second, the frequency dependence of shear wave Q in the crust of South America and India have been studied using both 1-Hz Lg and Lg waves at intermediate periods. The results of these studies can be summarized as follows.

Effects of Crustal Velocity Structure on Lg Attenuation

In the eastern United States the presence of low-velocity sediments contributes to the length of the Lg coda and smooths the wave form which for simple crustal models of few layers and no sediments is spikey in appearance. Known differences in velocity structure between the eastern United States and Basin-and-Range province can lead to differences in m_b(Lg) predicted from synthetic seismograms computed for those models. Assuming identical Q models for the two regions, we find magnitude differences of 0.2 to 0.3 units for 1-Hz Lg waves. Magnitude differences remain substantial to periods as large as 6s, but become much smaller at longer periods.

Effect of low-Q Sediments on Lg Attenuation

The large variation observed for Lg Q values at 1-Hz across the eastern United States can be explained as being due to variations in thickness of low-Q sediments. The frequency-dependent Q model of Mitchell (1980) covered with varying thicknesses of sediments having realistic values of Q produced reasonable agreement with observed values of Lg Q in Nebraska, Pennsylvania, and gulf coast Louisiana, where they range between about 1300 and 400. In regions, such as the western

United States, where crustal Q values are thought to be much lower than those in stable regions, the presence of low-Q sediments has a much smaller effect on the attenuation of 1-Hz Lg.

Effect of Crustal Q Structure on Lg Attenuation

Both models with a thick layer of low-Q sediments overlying a high-Q upper crust and models with a low-Q upper crust can explain the attenuation of Lg waves at intermediate periods in the western United States. The observed attenuation of 1-Hz Lg waves, however, appears to require a model for the Basin-and-Range which has low Q values in the upper crust.

Frequency-Dependence of Apparent Shear-Wave Q in the Crust

In both South America and India, the upper crust in the stable portions of those regions is characterized by frequency-dependent values of shear-wave Q. In order to model 1-Hz Lg waves for those stable regions, shear wave Q values in the upper crust must be higher than those needed to explain shear-wave Q values at intermediate periods. By contrast, the upper crust in the tectonically active protions of both continents appear to have low values of shear-wave Q which do not depend upon frequency.

METHODOLOGY OF USING Lg WAVES FOR ESTIMATING EXPLOSION YIELD AND BODY-WAVE MAGNITUDE BIAS BETWEEN TEST SITES

Otto W. Nuttli

INTRODUCTION

Lg waves are short-period, higher-mode surface waves that propagate in the continental crust. They were first described by Press and Ewing (1952), who noted that even a small segment of oceanic crustal path (as little as 200 km) was sufficient to extinguish them. Their group velocity at a period of 1 sec is approximately 3.5 km/sec. They exhibit vertical and radial as well as transverse particle motion, suggesting that they are a combination of higher-mode Rayleigh and Love waves. Nuttli (1973), making use of the fact that Lg waves in general have larger amplitudes than P waves at regional distances in eastern North America, employed them to estimate body-wave magnitude (m_b) of small explosions and earthquakes for which no P-wave data could be obtained. Furthermore, their amplitudes appear to be less sensitive to focal mechanism and focal depth than those of P waves, which results in a smaller uncertainty and standard deviation in the estimated m_b value obtained from Lg amplitudes.

Lg ATTENUATION

In the time domain at regional distances the attenuation of surface-wave amplitudes due to geometric spreading and wave dispersion was shown by Ewing et al (1957) to vary as Δ^{-1} for normally dispersed waves and $\Delta^{-5/6}$ for Airy waves, where Δ is epicentral distance. Observational data for Lg (Nuttli, 1973) suggested that the $\Delta^{-5/6}$ relation is more appropriate. Recently the $\Delta^{-5/6}$ relation was confirmed by numerical modelling of regional waves by Campillo et al (1984), who showed that the Lg amplitudes on synthetic seismograms decayed as $\Delta^{-5/6}$ when no anelastic attenuation (infinite Q) was

assumed.

From earthquake data Nuttli (1973) found that the anelastic attenuation of 1-sec period Lg waves in eastern North America is low, approximately 0.0006 km^{-1} (Q = 1500), compared to a value of about 0.005 km^{-1} (Q = 180) for southern California. This accounts for the fact that Lg waves are much more prominent on regional-distance seismograms for eastern North American earthquakes than for western ones.

Singh and Herrmann (1983) used Herrmann's (1980) extension of Aki and Chouet's (1975) method for estimating Q from the coda of Lg waves to map the apparent Q of 1-sec period Lg waves over the United States. Their map shows extreme values of 140 (California) and 1350 (central United States), along with considerable character or geographical variability. It suggests that if Lg amplitudes are to be used to estimate explosion yield to an accuracy of 30% (m_b to an accuracy of about 0.1), it is inadequate to use an average value of apparent Q of Lg over a region as large as the western United States. Rather it is necessary to estimate, as accurately as possible, the apparent Q value for particular source-to-station paths. This statement takes on increasing significance for regions of low Q (e.g. NTS) and/or for large epicentral distances (e.g. Soviet explosions recorded by WWSSN stations). Therefore, before Lg amplitudes can be used for determining m_b(Lg) and for estimating explosion yield of NTS and Soviet explosions, it is necessary to obtain Q values for specific source-to-station paths. The problem's difficulty is compoundedby the facts that the Lg waves do not always have a period of 1.0 sec and the Q value is frequency or period dependent. In this report it is assumed that the frequency dependence can be written as (Mitchell, 1980)

$$Q(f) = Q_o f^{\eta}$$

where Q_o is the 1-Hz value, f is wave frequency and η is a number between

0 and 1, given to one significant figure.

For the purposes of this study a first approximation of the Q_o and η values was obtained by using the method of Herrmann (1980) for individual source-to-station paths, and then by adjusting the Q_o values (η is not allowed to vary) so as to minimize the deviations of individual station m_b values from the station-average value. Typically these adjustments in Q_o values are found to be less than 10% of the values of the first approximations.

Because the $m_b(Lg)$ and explosion yield estimates depend critically on the Q values employed, careful consideration must be given to the determination of Q. For NTS events, with low Q paths, the WWSSN station TUC as a distance of about 700 km was found from observational data to be the most distant WWSSN station that gave consistent $m_b(Lg)$ values. Data from BKS and DUG also were found to be usable. It would be desirable to have data from more than three stations for estimating an average $m_b(Lg)$, but the uncertainties in amplitude associated with the attenuation corrections for longer paths outweigh the advantages of using more of the existing WWSSN stations. Therefore, because of the limited number of stations, the results of this study are primarily useful for developing a methodology of estimating $m_b(Lg)$ and explosion yield, rather than of obtaining precise values of these quantities for NTS events.

In general the Q values for source-to-station paths of Lg waves from explosions at the East Kazakh test sites recorded by WWSSN stations in Scandinavia and southern Asia are larger than for the NTS region. Therefore stations at larger epicentral distances can be used (more than 4000 km for some of the Scandinavian stations for large explosions). But the distribution of WWSSN stations with respect to the East Kazakh sites is far from ideal for accurate evaluation of $m_b(Lg)$ and yield. Much better results could be obtained from

seismographs located in the geological shield and old plateau regions of the Soviet Union, at distances of no more than 1000 to 2000 km.

The Aki and Chouet (1975) and Herrmann (1980) studies, used in the present analysis, consider the Lg coda to consist of scattered waves. Therefore, they can be expected to give a Q value that is representative of the region over which they are scattered, rather than an average value over a specific source-to-station path. One of the surprising results of this study, as well as related ones using earthquake data for South America, India and the Near East, is that the Lg coda method appears to give reliable average values for specific source-to-station paths. This observation has been tested in a number of independent ways, such as using Lg amplitude data rather than the variation of predominant wave frequency with lapse time to estimate Q.

Nevertheless, it is instructive to look at the consequences of errors in Q values. If, for a given source region, the Q values for all the source-to-station paths are overestimated, the resulting $m_b(Lg)$ will be underestimated. Therefore, the absolute $m_b(Lg)$ values of the explosions would be in error, and in such cases these $m_b(Lg)$ values could not be used to estimate m_b bias (for teleseismic P waves) between two test sites, such as NTS and the East Kazakh sites. However, if the $m_b(Lg)$ data are only to be used for estimating yield for a test site for which adequate announced yield data are available for calibration purposes, errors in $m_b(Lg)$ would not affect errors in yield estimates for that site as long as the yields to be estimated lie in the range of the calibration data. Another way of stating this is to note that even if the proposed methodology successfully predicts the yields of NTS explosions (those whose yields are classified), there is no assurance that the Q values employed and the $m_b(Lg)$ values obtained are the correct values.

After a number of iterations our best Q values for NTS paths to DUG, BKS and TUC are: DUG, $Q_o = 155$, $\gamma = 0.6$; BKS, $Q_o = 139$, $\gamma = 0.6$; TUC, $Q_o = 162$, $\gamma = 0.6$. The data used to obtain these values are given in Tables 1 to 3,

and the data points and the corresponding curves are shown in Figure 1.

Rondout Associates (1984) also applied the coda Q method to WWSSN statins for NTS events. They obtained smaller ζ values and larger Q_o values than those given by Nuttli (1983), namely: DUG, $Q_o = 230$, $\zeta = 0.3$; BKS, $Q_o = 225$, $\zeta = 0.2$; TUC, $Q_o = 300$, $\zeta = 0.2$. As a result their estimates of $m_b(Lg)$ for NTS events are smaller than those obtained by Nuttli (1983).

Although application of the coda-Q method to obtain Q_o and ζ values is fairly straightforward, there are two complicating factors that must be watched out for. First, explosions are excellent exciters of fundamental-mode surface waves because of their shallow depth. Depending on the epicentral distance, the fundamental-mode waves will arrive early in the coda, about one to three minutes after the onset of Lg. They will have larger amplitudes and longer periods than the scattered coda waves. Therefore, it is easy to mistakenly read their wave frequency rather than the higher frequency of coda waves at the time the fundamental-mode waves are arriving. The other problem arises near the end of the coda. In this study it has been observed that beyond some particular lapse time, whose value depends on the size of the explosion, the majority of scattered coda waves show no change in frequency with increasing coda lapse time, rather than continuing to decrease with increasing lapse time. One has to carefully search that part of the coda for the relatively few and somewhat larger amplitude waves that give the low frequency values. If not, the wave frequencies will be overestimated at these larger lapse times. These two complicating factors can lead to smaller estimates of ζ and consequently larger values of Q_o.

The differences between the Q_o, ζ values for paths from NTS to DUG, BKS and TUC obtained by Nuttli (1983) and Rondout Associates (1984) lead to big differences in estimated $m_b(Lg)$. Table 4 illustrates the differences, which amount to about 0.5 magnitude units. Comparison with $m_b(P)$ values published in the Bulletin of the International Seismological Centre lead to two different

interpretations. The Rondout Associates $m_b(Lg)$ values are about 0.2 of a magnitude unit smaller than the $m_b(P)$ values. If the Rondaut Associates $m_b(Lg)$ values are correct, this implies that Lg-wave amplitudes from nuclear explosions are smaller than from earthquakes, and therefore 1-sec period Lg-wave amplitudes can serve as a good discriminant between explosions and earthquakes. On the other hand, if the Nuttli (1983) $m_b(Lg)$ values are correct, $m_b(Lg)$ for NTS is on average about 0.3 magnitude units larger than m_b(P-ISC). If these $m_b(Lg)$ values are the correct ones, it follows that the teleseismic P-wave amplitudes at NTS are being attenuated by at least 0.3 magnitude units in the asthenosphere beneath NTS. (The 0.3 unit value would result if the excitation of 1-sec period Lg amplitudes for earthquakes and explosions of the same $m_b(P)$ values is the same. If the explosion is less efficient in generating Lg waves, the numerical value of P-wave attenuation at NTS would be even larger than 0.3 magnitude units.)

Earthquakes near NTS offer the promise of deciding between the above two possibilities. Dermengian et al (1984) gave a list of small magnitude earthquakes with epicenters near NTS that occurred between 1963 and 1968. Of the ten earthquakes in their list, we had film copies of three in our seismogram library. Table 5 presents the m_b(P-NEIS) and the $m_b(Lg)$ values obtained by using the Nuttli (1983) estimates of Q_o and γ. From the table it can be seen that the $m_b(Lg)$ values are about 0.1 magnitude units larger than the $m_b(P)$ values. As these events are earthquakes, $m_b(Lg)$ is expected to be larger than or equal to $m_b(P)$, i.e. larger if there is anomalous attenuation of P-wave amplitudes in the asthenosphere beneath NTS, and equal if there is no such anomalous attenuation of P-wave amplitudes. On average for the three Nevada earthquakes $m_b(Lg)$ is 0.1 units larger than $m_b(P)$ if the Nuttli (1983) Q_o and γ values are used. If the Rondout Associates (1984) Q_o and γ values are used, the $m_b(Lg)$ values are about 0.4 units smaller than the $m_b(P)$ values for the earthquakes, which is difficult to explain. Although it would be

desirable to have more data, the econcusion is that the Nuttli (1983) values of Q_o and γ are more applicable to the NTS region than the Rondout Associates (1984) values.

NTS STUDIES

Lg amplitudes were measured at DUG, BKS and TUC for all NTS events of announced yield for which seismogram copies were available. The events were grouped into two simple classifications, alluvium and "hard rock", depending upon the characteristics of the source medium as described in Springer and Kinnaman (1971, 1975). The yields also were taken from the papers of Springer and Kinnaman (1971, 1975). P-wave m_b values were obtained from the Bulletin of the International Seismological Centre.

The $m_b(Lg)$ data versus $\log_{10}$ yield are plotted in Figure 2. Over the range of 2 to 1000 kt the data points have been fitted by a quadratic curve, rather than a straight line. If the Lg spectrum can be represented by a long-period segment of zero slope and a short-period segment of slope two (the period at which the two segments of a spectrum intersect is called the corner period), then the curve of Figure 2 should consist of one straight-line segment of unit slope for explosions with a spectral corner period of less than one second and a second straight-line segment of 0.5 slope for the larger explosions. This would present an alternate way of selecting a mathematical relation to fit the data. The equation of the quadratic curve, obtained by a least-squares fit to the data, is

$$m_b(Lg) = 3.868 + 1.181 \log Y - 0.0938 (\log Y)^2 \qquad (1)$$

where Y is the announced yield, in kilotons, The standard deviation of $m_b(Lg)$ is 0.060. The slope of the curve at small yields (10 kt) is 1.01, close to that predicted by theory. The slope at the largest yields shown in the figure (1000 kt) is 0.62.

From Figure 2 it can be seen that the two granite explosions lie above

the curve (about 0.1 magnitude unit) and the dry tuff explosions lie slightly below the curve.

The alluvium data need to be treated separately, as they clearly form a different population than the "hard rock" explosion data. Figure 3 shows the data and a curve constructed to pass through the data and to have the same slopes as the "hard rock" curve at yields of 0.5 and 100 kt, namely 1.05 and 0.80, respectively.

In addition to explosions of announced yield, $m_b(Lg)$ was determined also for selected NTS events whose yield values remain classified information. Of all the NTS "hard rock" events considered in this study, 71 had published m_b(P-ISC) values. For these 71 NTS "hard rock" events it was found that

$$m_b(Lg) - m_b(\text{P-ISC}) = +0.31 \pm 0.02 \qquad (2)$$

Assuming that $m_b(Lg)$ is equal to m_b(P-ISC) in areas where there is no anomalous P-wave amplitude attenuation in the asthenosphere (e.g. eastern North America), equation (2) tells us that the P-wave amplitudes are reduced by 0.31 magnitude units in the asthenosphere beneath NTS. If Lg amplitudes are not excited as strongly for explosions as for earthquakes of the same $m_b(P)$ value, the amplitude loss of P waves in the asthenosphere beneath NTS would be even larger than 0.31 magnitude units.

NON-NTS EXPLOSIONS IN THE UNITED STATES

There are a few explosions of announced yield in the United States not located at NTS. Of these, SALMON in Mississippi, GASBUGGY in New Mexico and RULISON and RIO BLANCA in Colorado were selected for analysis. Table 6 gives the results, where the NTS hard-rock yield curve, given by equation (1), was assumed to be applicable for the explosions off the test site. In general, the agreement between announced yield and the $m_b(Lg)$ yield estimate is quite good, except for RIO BLANCA, an event of three 30 kt explosions, for which $m_b(Lg)$ underestimated the total yield by 27%. However, it should be noted that only one WWSSN station could be used for GASBUGGY, RULISON and

and RIO BLANCA, and that the anelastic attenuation coefficient value from the source to the individual station was obtained, therefore, only from the coda of one seismogram. Most of the regional stations for these events could not be used because the Lg amplitudes were too large, with the trace going off the seismogram.

FRENCH SAHARA EXPLOSIONS

Marshall et al (1979) gave yields of several French Sahara explosions. The nearest WWSSN station haveng a continental path was HLW in Egypt, at a distance beyond 3000 km. Fortunately, the anelastic attenuation of Lg across Africa is low, so that two of the explosions, SAPHIR and RUBIS, had measureable Lg-wave amplitudes. Figure 4 gives an example of Lg waves of SAPHIR recorded at AAE in Ethiopa, at a distance of 3947 km. The onset of Lg is sharp, at $11^h\ 48^m\ 55^s$. The maximum sustained amplitude was read at $11^h\ 49^m\ 08^s$. The seismogram was enlarged to approximately six times its original size, and the Lg waveform was traced from the image on a film viewer.

Table 7 lists the data for RUBIS and SAPHIR. Station HLW is in Egypt, and SDB in Angola. Both shots were in granite. For the Nevada explosions SHOAL and PILEDRIVER, also in granite, the $m_b(Lg)$ was about 0.15 units larger than for the typical hard-rock shot. If such a correction were applied to the Sahara events, the estimated yield from $m_b(Lg)$ for RUBIS would be 46 kt and for SAPHIR would be 73 kt. The data are too few to argue whether the French Lg data are better satisfied by an NTS hard-rock or NTS granite $m_b(Lg)$ versus yield relation, although the SAPHIR data would argue for the former, even if the SDB value were not used. The conclusion can be made, however, that for the limited available data, the NTS hard-rock $m_b(Lg)$ versus yield relation will give French Sahara explosion yields no more than 50% in error.

EXPLOSIONS AT EAST KAZAKH TEST SITE

Regional Lg waves can be observed at WWSSN stations in southern Asia and Scandinavia from explosions at the East Kazakh Test Site in the USSR. Table 8 lists the stations utilized in the study, along with the Q_o and η values obtained by applying Herrmann's (1980) method to the Lg coda. Also included are revised Q_o values, which were obtained by applying station corrections based on average $m_b(Lg)$ values for the events. In three cases (KBL, NIL and UME) the revised Q_o value falls outside the bounds obtained by application of the coda method. In all three cases the revised Q_o is lower than the lower-bound value. This indicates that the Lg amplitudes at these stations are somewhat smaller than expected.

Figure 5 presents m_b(P-ISC) versus $m_b(Lg)$ for 30 selected Shagan River events at the East Kazakh Test Site. Contrary to NTS events, m_b(P-ISC) is larger than $m_b(Lg)$ for Shagan River explosions. The average difference is 0.10 units, with a standard deviation of 0.14. The straight-line curve drawn in the figure is the best-fitting line with unit slope. Figure 6 shows similar data for 24 selected Degelen Mountain explosions at the East Kazakh Test Site. Again m_b(P-ISC) is larger than $m_b(Lg)$, but the average is 0.24 units, with a standard deviation of 0.14. The difference in average values of the magnitude difference for the two sites at East Kazakh is surprising. It is difficult to explain, if it is real. The value of m_b(P-ISC) - $m_b(Lg)$ for PILEDRIVER, which is in granite at NTS, is similar to the values for the other hard-rock events at that site. Therefore, the different source-rock types at Degelen Mountain and Shagan River likely are not the explanation. The difference in m_b(P-ISC) - $m_b(Lg)$ values at the two East Kazakh sites, namely 0.24 - 0.10, corresponds to about a 38% difference in estimated yield values based on $m_b(Lg)$.

Tables 9 and 10 present estimated yields of selected explosions at the Shagan River and Degelen Mountain sites, respectively. They are not intended to be taken as actual estimates of the true yields of the events, but rather to demonstrate the methodology for using $m_b(Lg)$ to obtain yield. Before they can be accepted, it must be demonstrated that the NTS hard-rock relation, given by equation (1), applies equally well to East Kazakh explosions. Also, the effect, if any, of different source crustal structures on the excitation of Lg waves needs to be investigated. Finally, more data should be scrutinized to obtain, if possible, better Q_o and values for the various paths from East Kazakh to the WWSSN station.

Marshall et al (1979) list one East Kazakh explosion of announced yield. It is the event of January 15, 1965 that cratered in a wet sandstone, for which a yield of 125 kt was given. The estimated yield obtained by $m_b(Lg)$, namely 105 kt, is 16% less than the announced yield. One example is inadequate for attempting to provide explanations for the difference. It even is possible that the relatively close agreement is fortuitous.

The data of Tables 9 and equation (2) give an $m_b(P)$ bias between NTS and Shagan River of 0.41 magnitude units, subject to the same limitations as the yield estimates discussed above. This bias value can be compared with a value of 0.24 obtained by Murphy and Tzeng (1982) by comparing the spectra of Alaskan earthquakes as obtained from seismograms recorded at NTS and near the Semipalatinsk site, and of 0.25 obtained by Dermengian et al (1984) by means of m_b/K analysis of earthquakes with epicenters near the Semipalatinsk site and NTS. Sykes and Ciufentes (1984) used 20-sec period surface waves from NTS events to obtain an M_S versus yield calibration curve, which they then applied to East Kazakh explosions to estimate yields. They also calculated m_b values for the NTS and East Kazakh events which, when combined with yield values, can give the m_b bias between the two test sites. Although they did not explicitly state the value of the bias, their data suggest a value of at least 0.35 magnitude units.

The distribution of WWSSN stations is far from ideal for determining $m_b(Lg)$ and for estimating yields of East Kazakh explosions. The southern Asian stations, which are closest to the test site, are located in or beyond mountainous, neotectonic areas. The paths to the Scandinavian stations are more uniform, but the distances are all 3500 km and greater. Both of these problems lead to scatter in $m_b(Lg)$ values. A 0.1 unit error in $m_b(Lg)$ translates into about a 30% error in estimated yield. The ideal data would come from stations in the interior of Asia, at distances of 500 to 2000 km from the source.

ACKNOWLEDGMENTS

I wish to thank Donald L. Springer of the Lawrence Livermore National Laboratory for helpful discussion concerning source conditions at NTS, Paul W. Pomeroy of Rondout Associates for exchange of information concerning Q values at NTS, John R. Murphy and T. Joseph Bennett of S-Cubed for making available reports containing their estimates of magnitude bias, and Lynn R. Sykes for providing a reprint of his paper.

REFERENCES

Aki, K. and B. Chouet (1975). Origin of coda waves: Source, attenuation, and scattering effects, Jour. of Geoph. Res., 80, 3322-3342.

Campillo, M., M. Bouchon and B. Massinon (1984). Theoretical study of the excitation , spectral characteristics, and geometrical attenuation of regional seismic phases, Bull. Seism. Soc. Amer., 74, 79-90.

Dermengian, J. M., J. R. Murphy and T. J. Bennett (1984). Estimation of Magnitude/Yield Bias through m_b/K Analyses of Earthquakes with Epicenters near the Semipalatinsk and Nevada Test Sites, Final Report, S-Cubed, ACDA Contract No. AC2MC105.

Ewing, M., W. S. Jardetzky and F. Press (1957), Elastic Waves in Layered Media, McGraw-Hill, pg. 358.

Herrmann, R. B. (1980) Q estimates using the coda of local earthquakes, Bull. Seism. Soc. Amer., 70, 447-468.

Marshall, P. D., D. L. Springer and H. C. Rodean (1979). Magnitude corrections for attenuation in the upper mantle, Geophysical Journal, 57, 609-638.

Mitchell, B. J. (1980). Frequency dependence of shear wave internal friction in the continental crust of eastern North America, Jour of Geoph. Res., 85, 5212-5218.

Murphy, J. R. and T. K. Tzeng (1982). Estimation of Magnitude/Yield Bias between the NTS and Semipalatinsk Nuclear Testing Areas, Final Report, S-Cubed, ACDA Contract No. ACOMC107.

Nuttli, O. W. (1973). Seismic wave attenuation and magnitude relations for eastern North America, Jour. of Geophys. Res., 78, 876-885.

Nuttli, O. W. (1983). Illustration of use of coda Q method to obtain anelastic attenuation values for paths from Salmon (Mississippi) and NTS events, in Mitchell, B. J. and O. W. Nuttli, Attenuation of Seismic Waves at Regional Distances, Semi-Annual Report, Saint Louis University, DARPA Contract F49620-83-C-0015.

Press, F. and M. Ewing (1952). Two slow surface waves across North America, Bull. Seism. Soc. Amer, 42, 219-228.

Rondout Associates (1984). The Use of Regional Seismic Waves for Yield Determination, Semi-Annual Technical Report No. 1, 1 Oct 1982-31 Mar 1983, DARPA Contract F49620-83-C-0017.

Singh, S. and R. B. Herrmann (1983). Regionalization of crustal coda Q in the continental United States, Jour. of Geophys. Res., 88, 527-538.

Springer, D. L. and R. L. Kinnaman (1971). Seismic source summary for U.S. underground nuclear explosions, 1961-1970, Bull. Seism. Soc. Amer., 61, 1073-1098.

Springer, D. L. and R. L. Kinnaman (1975). Seismic source summary for U.S. underground nuclear explosions, 1971-1973, Bull. Seism. Soc. Amer., 65, 343-349.

Sykes, L. R. and I. L. Cifuentes (1984). Yields of Soviet underground nuclear explosions from seismic surface waves: Compliance with the Threshold Test Ban Treaty, Proc. Natl. Adad. Sci. USA, 81, 1922-1925.

TABLE 1

WAVE FREQUENCY, f_p, VERSUS LAPSE TIME, t, FOR NTS EVENTS RECORDED AT BKS ON WWSSN SHORT-PERIOD, VERTICAL-COMPONENT SEISMOGRAMS

Date	Event	m_b(Lg)	f_p(Hz)	t (sec)
02/08/67	WARD	4.77	1.17	171
			0.90	200
			0.82	213
			0.84	260
			0.65	297
06/12/69	TAPPER	4.85	0.98	213
			0.84	261
			0.78	310
			0.73	351
12/17/69	LOVAGE	4.96	0.59	389
			0.56	430
			0.47	500
08/31/67	DOOR MIST	5.05	1.07	188
			0.86	220
07/27/67	STANLEY	5.19	1.01	199
			0.95	214
			0.78	233
			0.62	290
06/26/67	MIDI MIST	5.20	0.98	202
			0.84	266
			0.65	320
01/30/69	VISE	5.23	0.90	287
			0.76	305
			0.49	390
			0.42	440
05/10/67	MICKEY	5.26	0.65	377
			0.59	444
			0.50	487
			0.43	563
05/27/69	TORRIDO	5.44	1.07	185
			0.84	205
			0.84	299
01/19/67	NASH	5.51	0.90	240
			0.59	355
			0.53	395
01/15/69	WINESKIN	5.58	0.59	295
			0.49	367
			0.43	426
			0.37	484
			0.29	498
10/29/69	CALABASH	5.88	0.49	335
			0.42	387
			0.39	437
09/27/67	ZAZA	6.00	0.45	391
			0.39	430
			0.33	530

TABLE 1 (continued)

Date	Event	m_b(Lg)	f_p(Hz)	t(sec)
02/21/68	KNOX	6.01	0.40	426
			0.39	476
			0.29	496
09/06/68	NOGGIN	6.08	0.39	383
			0.39	457
			0.31	526
06/06/73	ALMENDRO	6.31	0.29	435
			0.33	453
			0.24	514
			0.26	548
			0.26	635
			0.22	674
			0.23	737
			0.22	810
			0.23	848
01/03/76	MUENSTER	6.53	0.24	678
			0.22	753
			0.22	780
03/14/76	COLBY	6.53	0.29	463
			0.26	502
			0.24	524
			0.23	545
			0.21	608
			0.20	679

TABLE 2

WAVE FREQUENCY, f_p, VERSUS LAPSE TIME, t, FOR NTS EVENTS RECORDED AT DUG ON WWSSN SHORT-PERIOD, VERTICAL-COMPONENT SEISMOGRAMS

Date	Event	m_b(Lg)	f_p(Hz)	t(sec)
02/23/67	PERSIMMON	4.25	1.17	165
			1.07	179
			0.98	224
			0.78	263
05/01/70	BEEBALM	4.73	0.95	235
			0.59	350
08/31/67	DOOR MIST	5.05	0.73	320
			0.78	357
			0.69	388
07/27/67	STANLEY	5.19	0.73	314
			0.73	369
			0.59	447
06/26/67	MIDI MIST	5.20	0.84	302
			0.72	373
			0.51	489
01/19/67	NASH	5.51	0.59	374
			0.53	433
			0.39	496
			0.45	510
			0.31	574
02/23/67	AGILE	5.91	0.98	261
			0.53	455
			0.39	475
			0.28	870
09/06/68	NOGGIN	6.08	1.17	150
			0.98	187
			0.90	274
			0.69	337
			0.45	392
			0.37	465
06/06/73	ALMENDRO	6.31	0.37	500
			0.34	533
			0.28	574
			0.24	593
09/16/69	JORUM	6.52	0.37	489
			0.32	508
			0.24	592
			0.26	610
			0.22	680

TABLE 3

WAVE FREQUENCY, f_p, VERSUS LAPSE TIME, t, FOR NTS EVENTS RECORDED AT TUC ON WWSSN SHORT-PERIOD, VERTICAL-COMPONENT SEISMOGRAMS

Date	Event	$m_b(Lg)$	f_p(Hz)	t(sec)
02/23/67	PERSIMMON	4.25	0.99	233
			0.90	296
			0.84	316
02/08/67	WARD	4.77	0.84	285
			0.78	310
			0.73	355
06/29/67	UMBER	4.82	0.82	316
			0.65	410
			0.59	438
08/18/67	BORDEAUX	5.01	0.73	274
			0.62	382
			0.51	455
07/27/67	STANLEY	5.19	0.84	297
			0.65	372
			0.49	491
			0.42	555
06/26/67	MIDI MIST	5.20	0.67	390
			0.49	425
			0.43	450
01/30/69	VISE	5.23	0.53	393
			0.45	426
			0.45	475
05/10/67	MICKEY	5.26	0.65	377
			0.59	444
			0.50	487
			0.43	563
01/19/67	NASH	5.51	0.53	440
			0.51	487
			0.36	573
05/07/69	PURSE	5.98	0.25	622
			0.23	668
			0.20	793
10/08/69	PIPKIN	6.06	0.53	427
			0.42	433
			0.28	510
			0.39	535
			0.33	625
			0.28	665
			0.23	753
09/16/69	JORUM	6.52	0.21	701
			0.20	1080
			0.20	1140
			0.20	1290
01/03/76	MUENSTER	6.53	0.20	708
			0.17	770
			0.19	890

TABLE 5

m_b(P-NEIS) AND m_b(Lg) VALUES FOR EARTHQUAKES NEAR NTS

Date	Origin Time	Latitude (^oN)	Longitude (^oW)	m_b(P)	m_b(Lg)
08/21/64	22-03-51.65	37.0	115.1	3.8	3.78
11/17/65	09-41-28.3	37.6	115.2	3.7	3.88
04/06/66	17-56-32.1	37.28	115.38	4.1	4.23

TABLE 5

ESTIMATED $m_b(Lg)$ FOR SELECTED NTS EVENTS USING DIFFERENT ATTENUATION VALUES

Date	Event	m_b(P-ISC)	$m_b(Lg)$ Rondout expnt'l	$m_b(Lg)$ Rondout linear	$m_b(Lg)$ Nuttli
09/13/63	BILBY	---	5.59	5.57	6.1
02/24/66	REX	5.0	4.86	4.78	5.28
05/06/66	CHARTREUSE	5.4	5.24	5.22	5.76
05/20/67	COMMODORE	5.8	5.52	5.50	6.04
05/23/67	SCOTCH	5.7	5.44	5.44	6.00
12/19/68	BENHAM	6.3	6.13	6.01	6.65
04/26/73	STARWORT	5.6	5.35	5.33	5.85

TABLE 6

ESTIMATES OF YEILD OF NON-NTS EXPLOSIONS IN CONTINENTAL U. S.

Event	Date	Stations Used	m_b(Lg)	m_b(P-ISC)	Announced yield (kt)	Yield from m_b(Lg) (kt)*
SALMON	10/22/64	BLA, DAL, FLO, OXF, RCD	4.66	4.6	5.3	5.1
GASBUGGY	12/10/67	DUG	5.38	4.8	29	28
RULISON	09/10/69	TUC	5.56	5.0	40	45
RIO BLANCA	05/17/73	TUC	5.71	5.1	90	66

*Uses NTS hard-rock relation, equation (1).

TABLE 7

FRENCH SAHARA EXPLOSIONS

Event	Date	Station	Δ (km)	Q_o	η	m_b(Lg)	Announced yield (kt)	Yield from m_b(Lg) (kt)*
RUBIS	10/20/63	AAE	3947	750	0.3	5.72	52	68
SAPHIR	02/27/65	AAE	3947	750	0.3	5.96		(135)
		HLW	3146	700	0.3	5.92		(120)
		SDB	4414	720	0.4	5.79		(82)
		average				5.89	120	111

*Uses NTS hard-rock relation, equation (1).

TABLE 8

ATTENUATION PARAMETERS FOR PATHS FROM EAST KAZAKH TEST SITE TO SELECTED WWSSN STATIONS

Station	Approximate Distance (km)	Q_o	Coda Method Upper & Lower Bounds	η	Revised Q_o
KBL	1850	360	(340, 380)	0.6	336
KEV	3500	580	(550, 620)	0.4	554
KON	4350	700	(650, 760)	0.4	700
MHI	2100	380	(360, 410)	0.5	380
NDI	2350	300	(270, 320)	0.6	312
NIL	1850	380	(370, 400)	0.6	354
NUR	3500	580	(520, 650)	0.4	580
QUE	2150	300	(280, 330)	0.6	318
SHL	2950	340	(325, 350)	0.6	340
UME	3700	620	(610, 640)	0.4	591

TABLE 9

TENTATIVE YIELD ESTIMATES FOR SELECTED SHAGAN RIVER EXPLOSIONS OBTAINED FROM $m_b(Lg)$ VALUES

Note: The estimated yields are given only for a demonstration of the methodology, and should not be interpreted or used as measures of actual yields. A number of presently unverified assumptions were made in obtaining the estimated yields.

Date	$m_b(P)$*	$m_b(Lg)$	Number of Stations	Estimated** Yield (kt)	Announced*** Yield (kt)
01/15/65	5.8	5.87	2	105	125
11/02/72	6.1	6.04	1	170	
12/10/72	6.0	6.09	2	200	
07/23/73	6.1	6.13	6	229	
05/31/74	5.9	5.68	4	62	
10/16/74	5.5	5.26	3	20	
12/27/74	5.6	5.69	6	63	
04/27/75	5.6	5.47	4	35	
10/29/75	5.8	5.45	2	33	
12/25/75	5.7	5.83	4	93	
04/21/76	5.3	5.19	1	17	
06/09/76	5.3	5.27	3	21	
07/04/76	5.8	5.90	2	112	
08/28/76	5.8	5.60	5	49	
12/07/76	5.9	5.71	2	66	
05/29/77	5.8	5.58	5	47	
06/29/77	5.3	5.15	3	16	
09/05/77	5.8	5.51	2	39	
11/30/77	6.0	5.71	5	66	
06/11/78	5.9	5.75	4	74	
07/05/78	5.8	5.67	1	59	
08/29/78	5.9	5.80	3	87	
09/15/78	6.0	5.87	3	105	
11/04/78	5.6	5.57	2	46	
04/05/79	5.8	5.84	2	96	
06/23/79	6.2	5.92	2	120	
07/07/79	5.8	5.87	3	105	
08/04/79	6.1	6.01	4	157	
08/18/79	6.1	6.03	5	166	
09/14/80	6.2	6.09	5	200	

*$m_b(P)$ values from International Seismological Centre Bulletin.

** Uses NTS hard-rock relation, equation (1).

***Announced yield value given in Marshall et al (1979).

TABLE 10

TENTATIVE YIELD ESTIMATES FOR SELECTED DEGELEN MOUNTAIN EXPLOSIONS OBTAINED FROM $m_b(Lg)$ VALUES

Note: The estimated yields are given only for a demonstration of the methodology, and should not be interpreted or used as measures of actual yields. A number of presently unverified assumptions were made in obtaining the estimated yields.

Date	$m_b(P)$*	$m_b(Lg)$	Number of Stations	Estimated Yield (kt)**
04/19/73	5.4	5.12	2	15
07/10/73	5.2	5.14	2	15
10/26/73	5.2	4.88	1	8.3
01/30/74	5.4	5.11	2	14
05/16/74	5.2	4.89	2	8.2
07/10/74	5.2	4.75	2	6.2
09/13/74	5.2	4.74	1	6.2
12/16/74	4.8	4.15	2	1.7
02/20/75	5.7	5.40	3	30
03/11/75	5.4	5.23	2	19
06/08/75	5.5	5.04	2	12
08/07/75	5.2	4.90	2	8.7
01/15/76	5.2	4.92	2	9.3
04/21/76	5.1	5.21	1	18
05/19/76	5.0	4.92	2	9.3
07/23/76	5.1	4.96	2	10
12/30/76	5.2	4.99	1	11
03/29/77	5.4	5.36	4	26
04/25/77	5.1	4.94	2	9.5
07/30/77	5.1	4.76	3	6.3
12/26/77	4.9	4.73	2	6.0
03/19/78	5.2	4.90	2	8.7
03/26/78	5.6	5.39	5	29
04/22/78	5.3	5.19	4	17
11/29/78	6.0	5.74	4	72

*$m_b(P)$ values from International Seismological Centre Bulletin.

** Uses NTS hard-rock relation, equation (1).

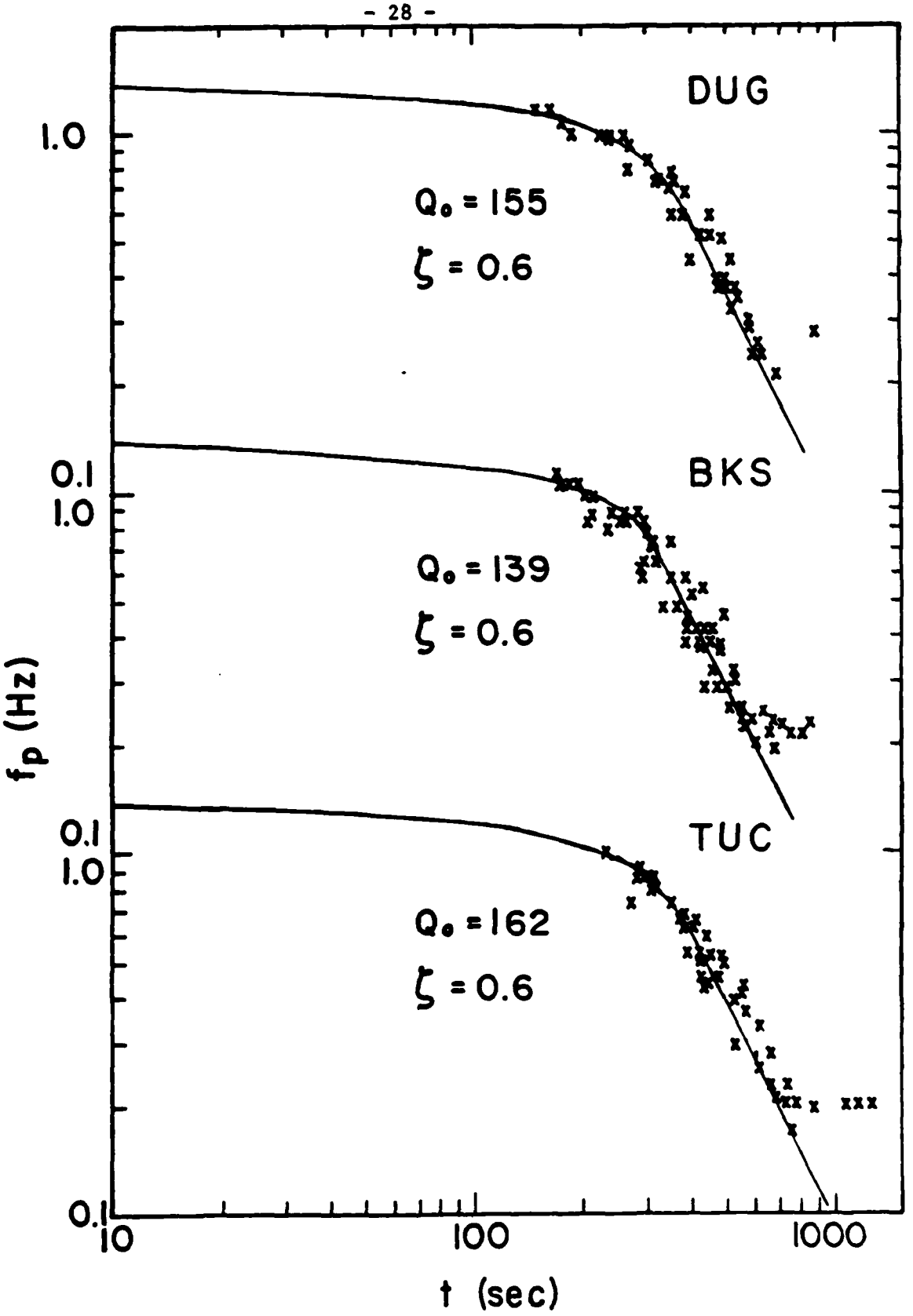

Fig. 1. Q_o and ζ Values for Paths from NTS to BKS, DUG and TUC.

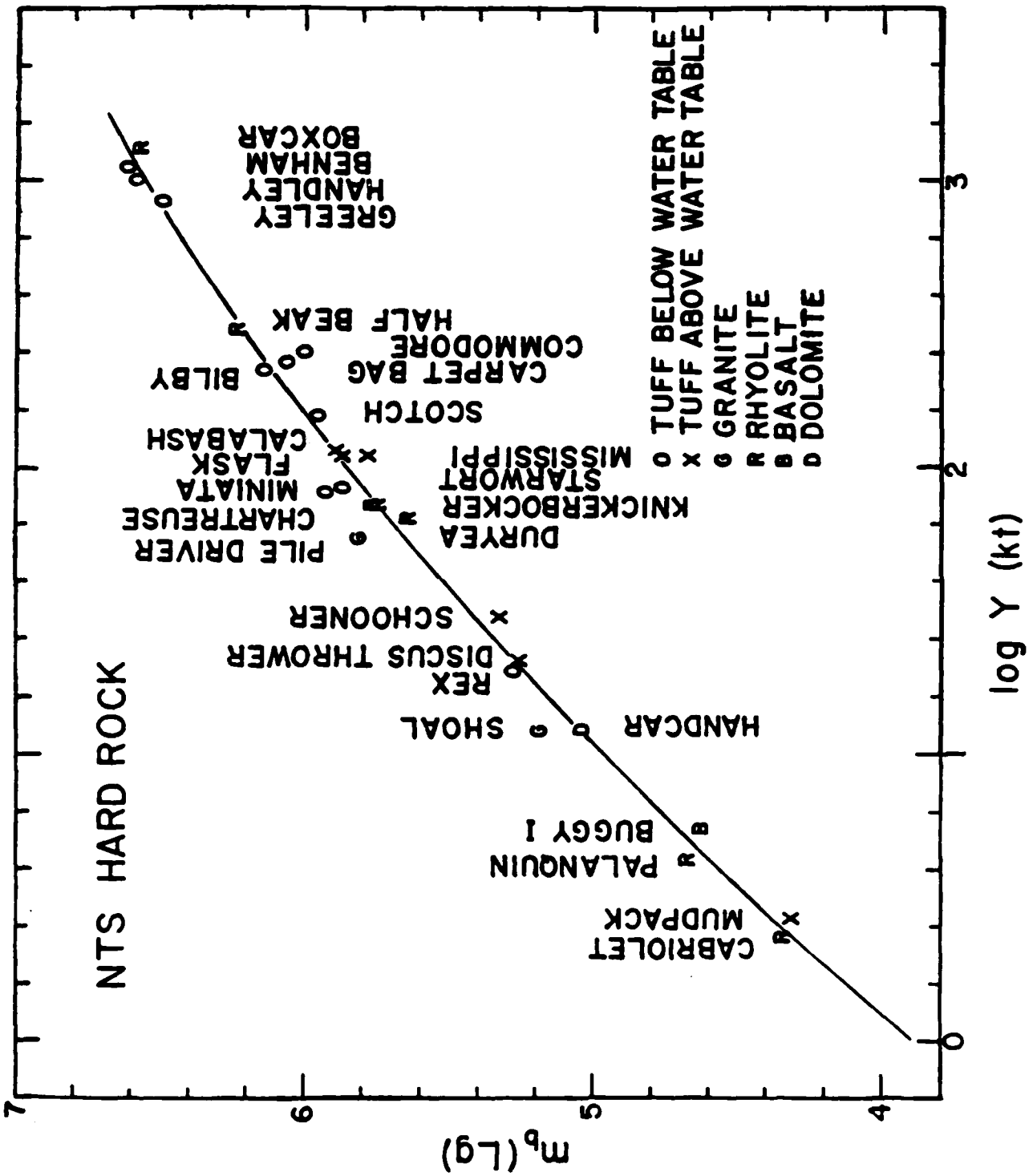

Fig. 2. m_b(Lg) Versus Explosion Yield for Sources in Hard Rock at NTS. The curve is a least-squares quadratic fit to the data.

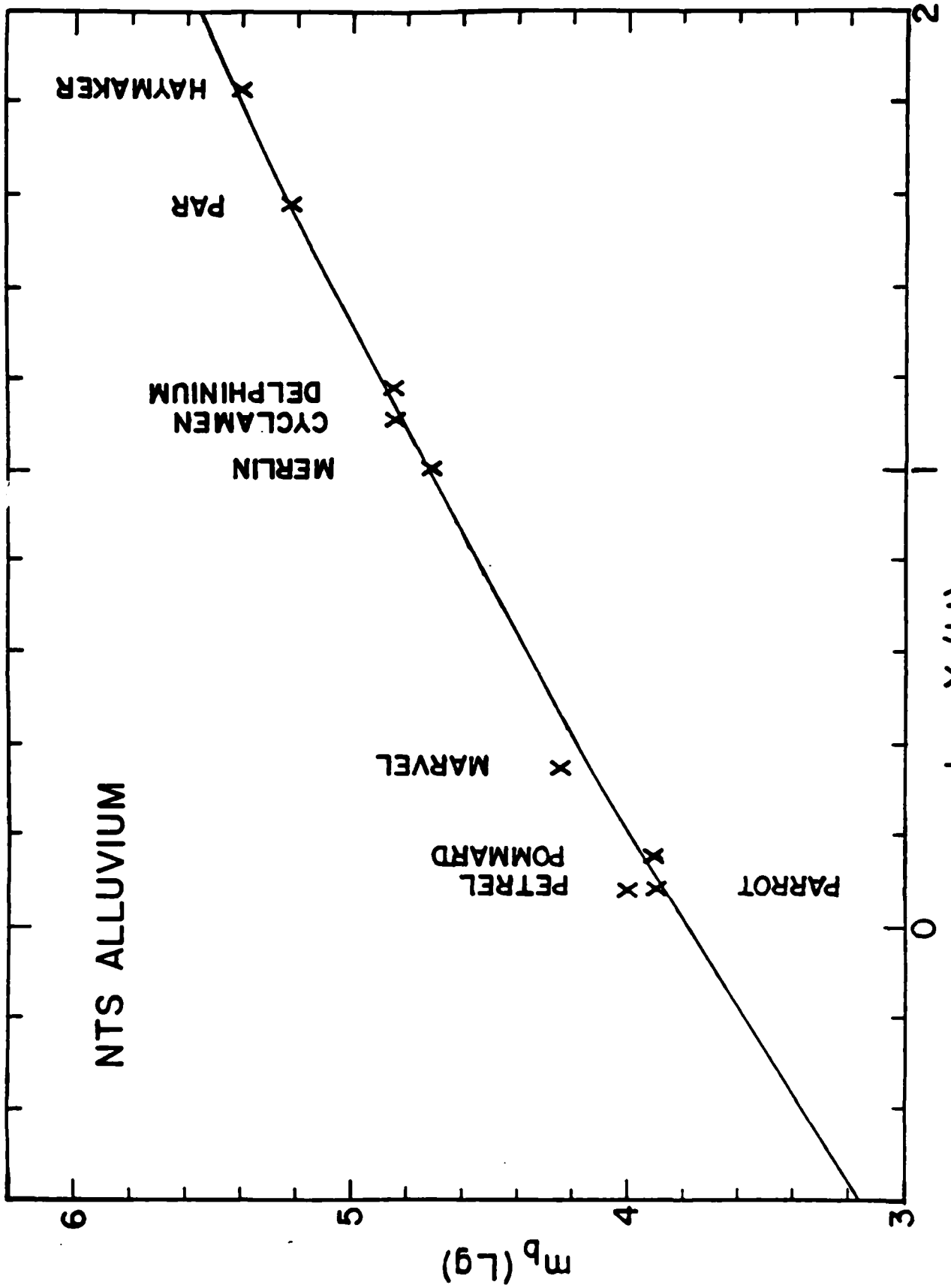

Fig. 3. $m_b(Lg)$ Versus Explosion Yield for Sources in Alluvium at NTS.

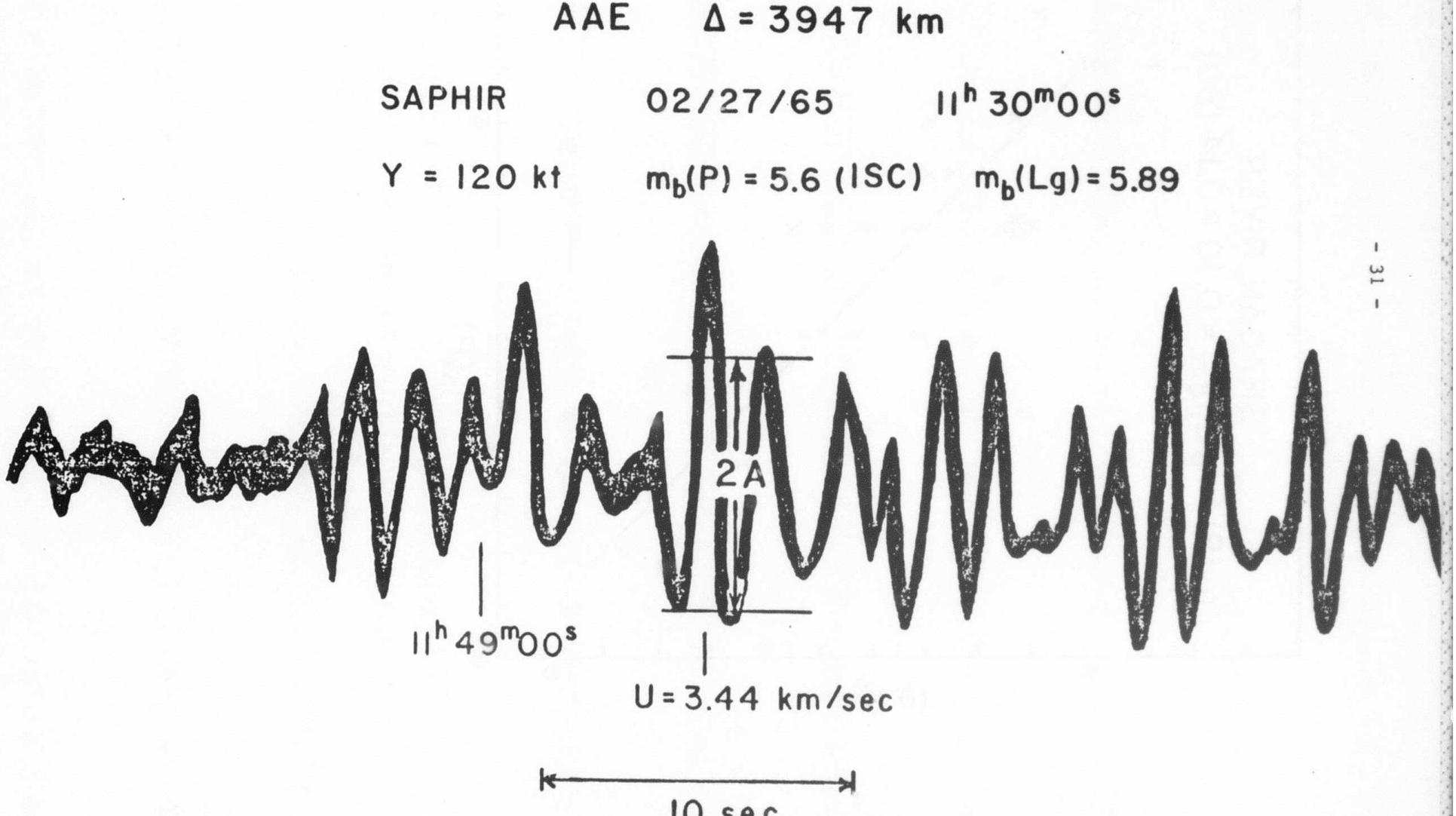

Fig. 4. Trace of AAE Seismogram Showing Beginning of Lg Waves from SAPHIR in French Sahara.

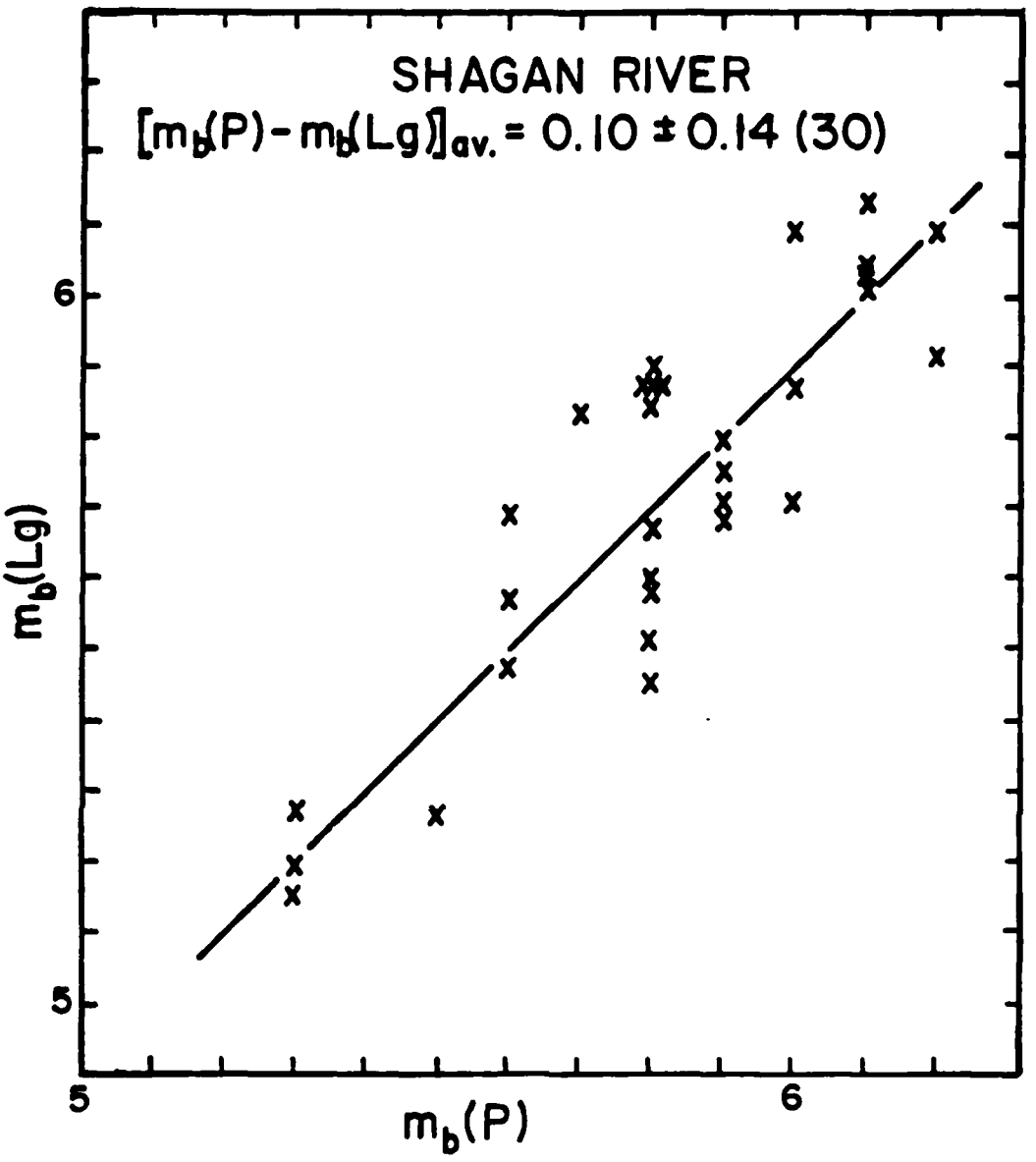

Fig. 5. $m_b(P)$ Versus $m_b(Lg)$ Values for Explosions at Shagan River, East Kazakh.

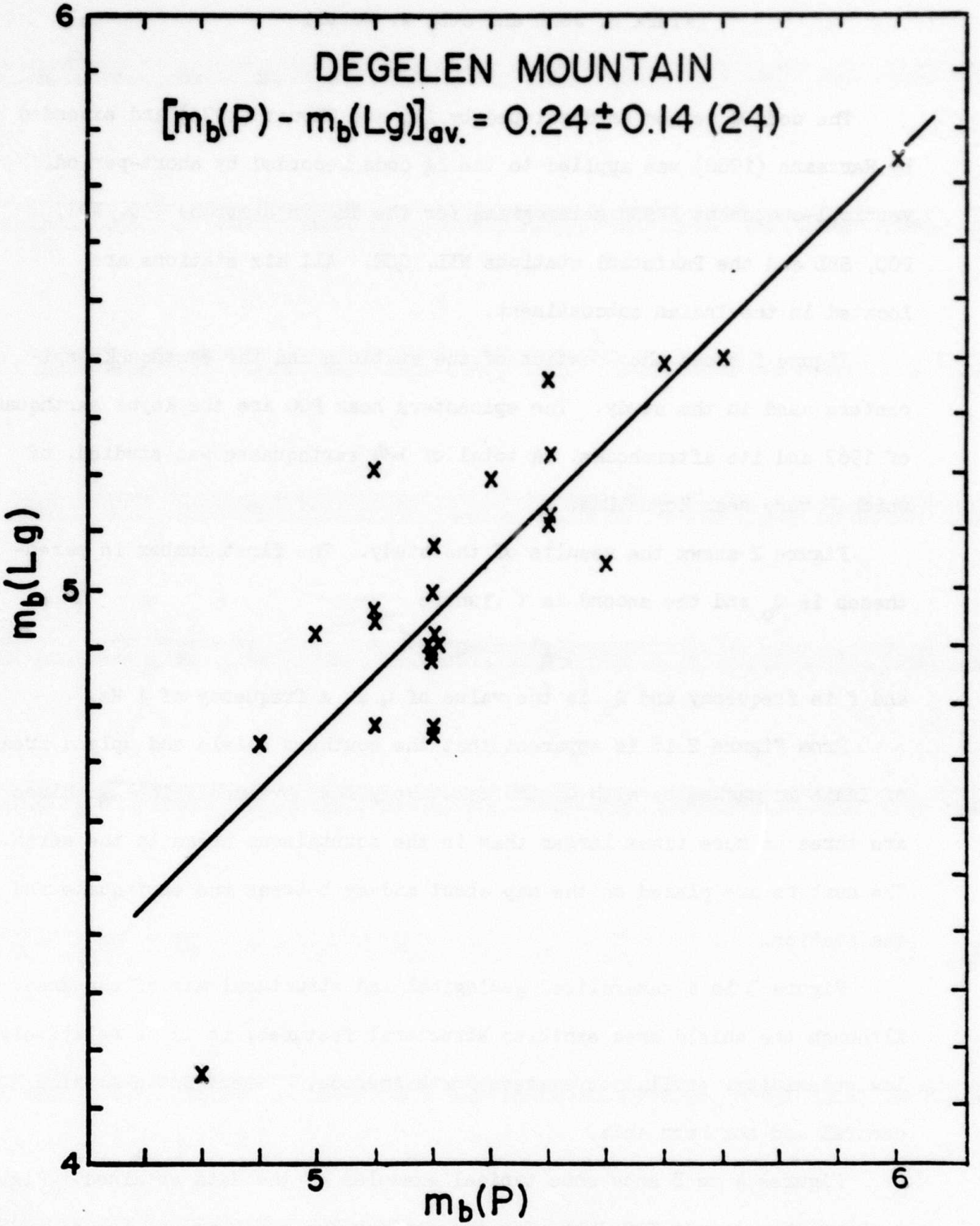

Fig. 6. m_b(P) Versus m_b(Lg) Values for Explosions at Degelen Mountain, East Kazakh.

CODA-Q STUDIES FOR THE INDIAN SUBCONTINENT

Viera M. John and Otto W. Nuttli

The coda-Q method as developed by Aki and Chouet (1975) and extended by Herrmann (1980) was applied to the Lg coda recorded by short-period, vertical-component WWSSN seismograms for the Indian stations KOD, NDI, POO, SHL and the Pakistani stations NIL, QUE. All six stations are located in the Indian subcontinent.

Figure 1 shows the location of the stations and the earthquake epicenters used in the study. The epicenters near POO are the Koyna earthquake of 1967 and its aftershocks. A total of 134 earthquakes was studied, of which 7 were near Koyna Dam.

Figure 2 shows the results of the study. The first number in parentheses is Q_o and the second is γ, where

$$Q(f) = Q_o f^{\gamma}$$

and f is frequency and Q_o is the value of Q at a frequency of 1 Hz.

From Figure 2 it is apparent that the southern shield and upland area of India is marked by high Q_o and relatively low γ values. The Q_o values are three or more times larger than in the mountainous areas to the north. The numbers are placed on the map about midway between the earthquake and the station.

Figure 3 is a generalized geological and structural map of the area. Although the shield area exhibits structural features, it is of relatively low seismicity, similar to eastern North America, eastern South America and central and northern Asia.

Figures 4 to 8 show some typical examples of the data obtained. Figure 4 shows the plot of KOD data, for the earthquakes which are to the northeast of station SHL. Figure 5 presents the NIL data as obtained from earthquakes with epicenters near 39° N, 73° E. Figure 6 shows the data at POO for the

nearby 1967 Koyna earthquakes. Figure 7 presents QUE data for earthquakes near 39° N, 73° E. The Q_o value of 265 is noticeably smaller than the value of 640 obtained from QUE seismograms for the Koyna epicenters at 17° N, 73° E. The phenomenon exhibited in Figures 7 and 8, namely different Q_o and ζ values for earthquakes from different source regions recorded at the same station, also was observed at NDI, NIL, POO and SHL.

As a check on the coda Q values, Lg amplitudes were observed at the same station for a number of earthquakes at different distances and equalized to $m_b = 5.0$ values. The resulting Lg amplitude versus distance data were plotted and fitted by a curve in which γ, the coefficient of anelastic attenuation, is a parameter. The quantity γ is related to Q by

$$\gamma(f) = \pi f/U(f)Q(f)$$

where U is group velocity. The value of γ obtained by amplitude fall-off for waves of a given frequency was compared to that obtained from the Q_o and ζ values by means of the coda analysis. As an example, for station NIL the Lg amplitude attenuation method gave a Q_o of 300, compared to a value of 330 obtained by the coda-Q method. The agreement is considered sufficiently good to justify the previously arrived at conclusion (Herrmann, 1980) that coda-Q methods give Q_o values which are equal to the apparent Q_o values of Lg waves.

REFERENCES

Aki, K. and B. Chouet (1975). Origin of coda waves: Source, attenuation, and scattering effects, Jour. of Geoph. Res., 80, 3322-3342.

Herrmann, R. B. (1980). Q estimates using the coda of local earthquakes, Bull. Seism. Soc. Amer., 70, 447-468.

Khattri, K. N., A. M. Rogers, D. M. Perkins and S. T. Algermissen (1983). A Seismic Hazard Map of India, U. S. Geological Survey, Golden, Colorado.

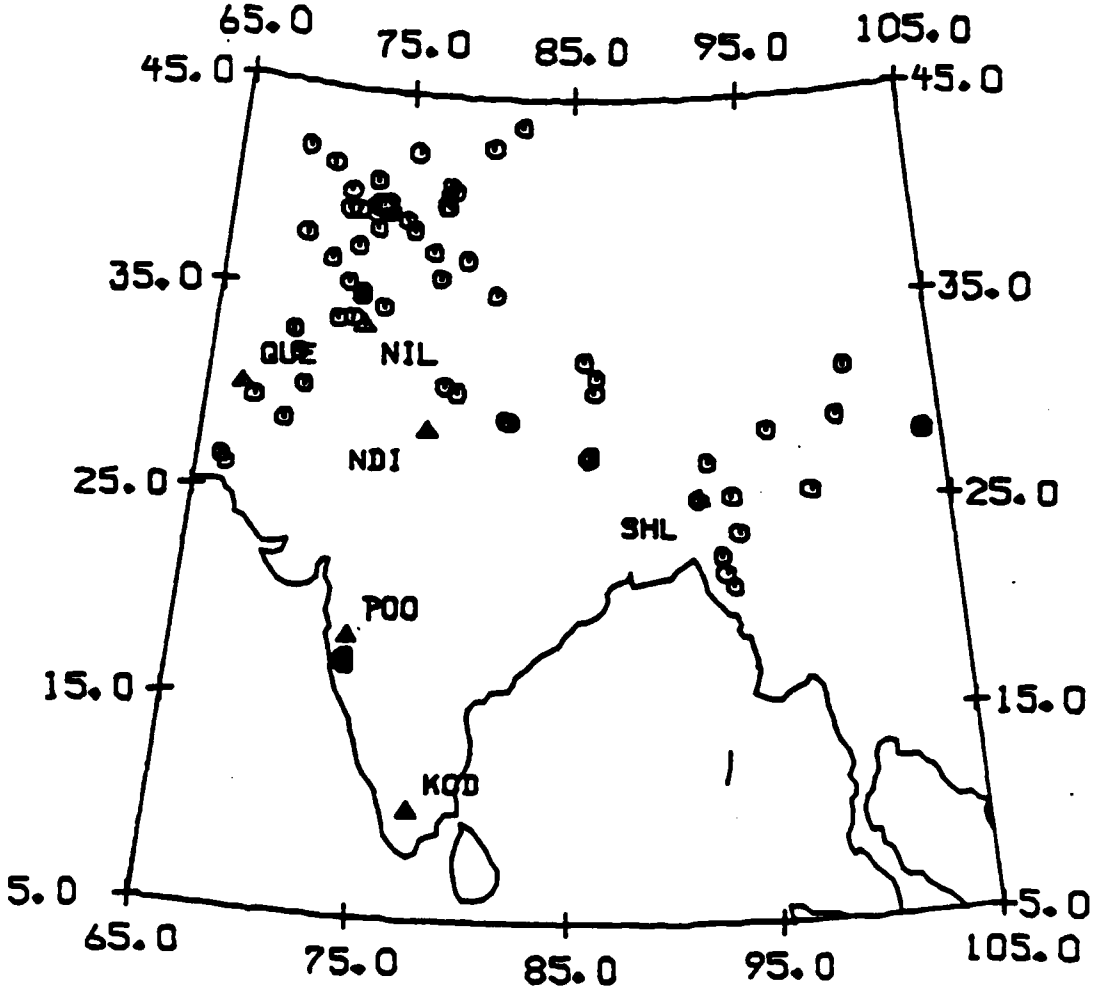

Figure 1. A Map Showing the WWSSN Stations Used and the Earthquake Epicenters.

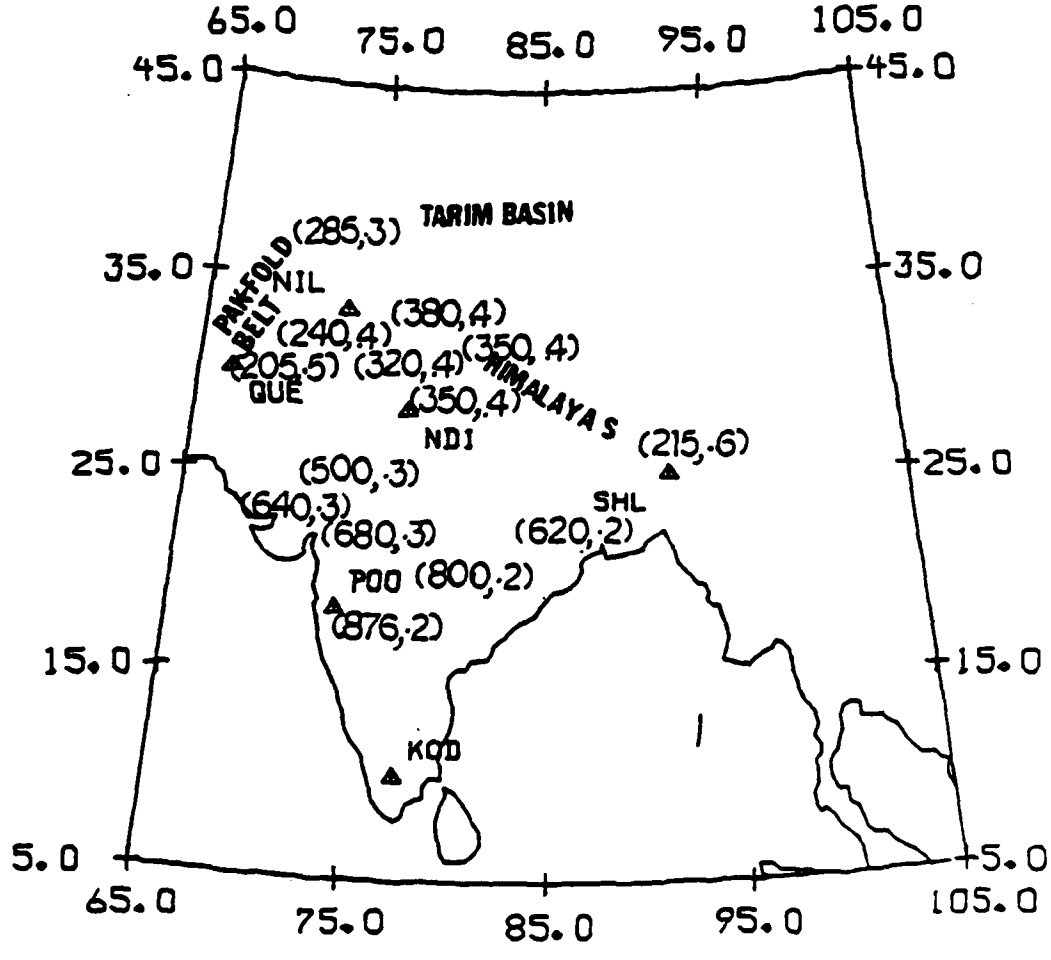

Figure 2. A Map of India Showing the Q_o and $ Values.

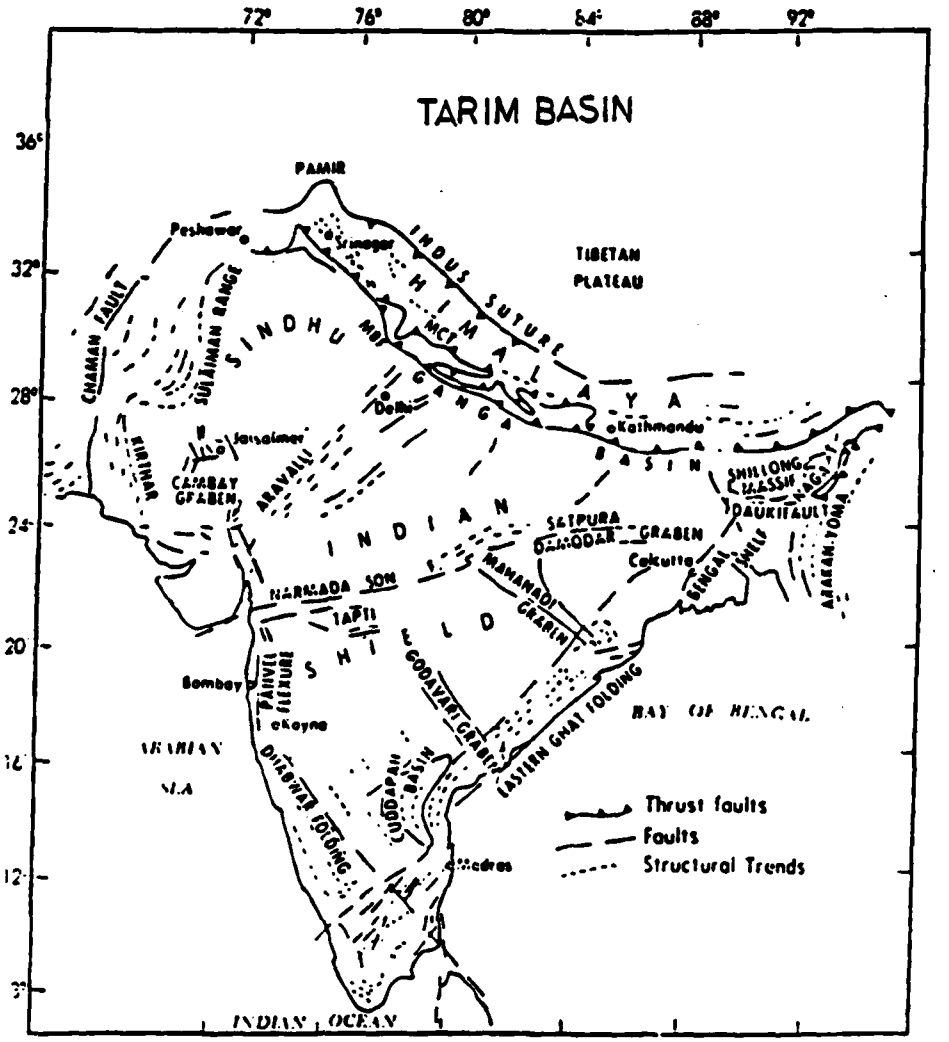

Figure 3. Major Geological and Structural Features of Himalayas, Tibet, and Surrounding Regions (Khattri et al , 1983).

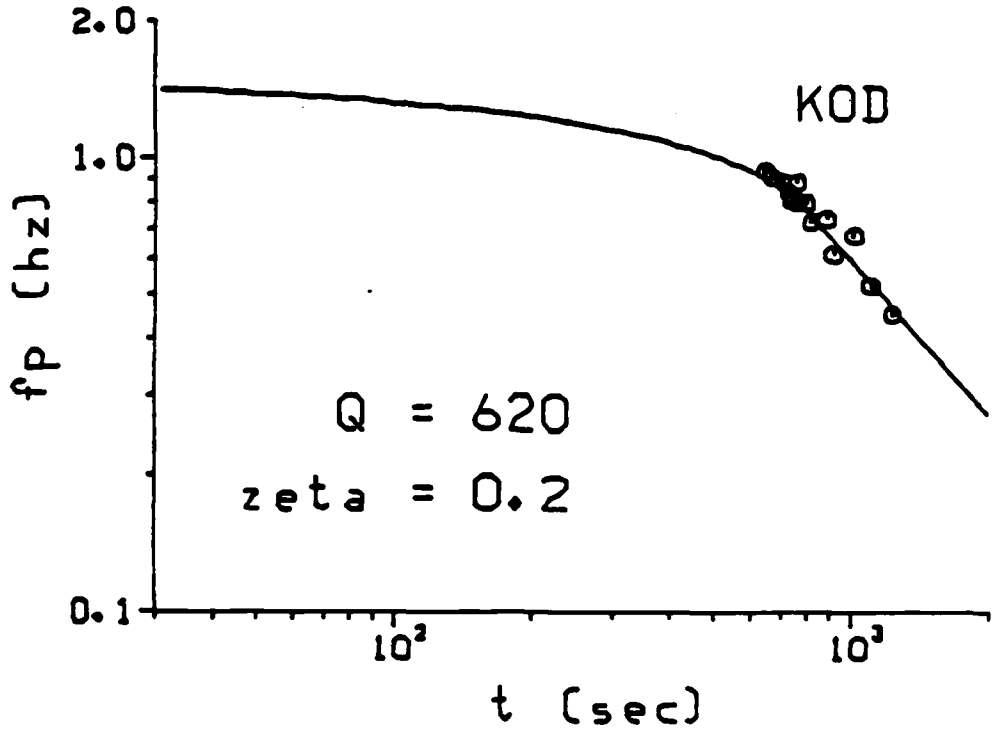

Figure 4. Plot of f_p (Hz) versus t (sec) for KOD. Theoretical Curve for $Q_o = 620$, $\zeta = 0.2$

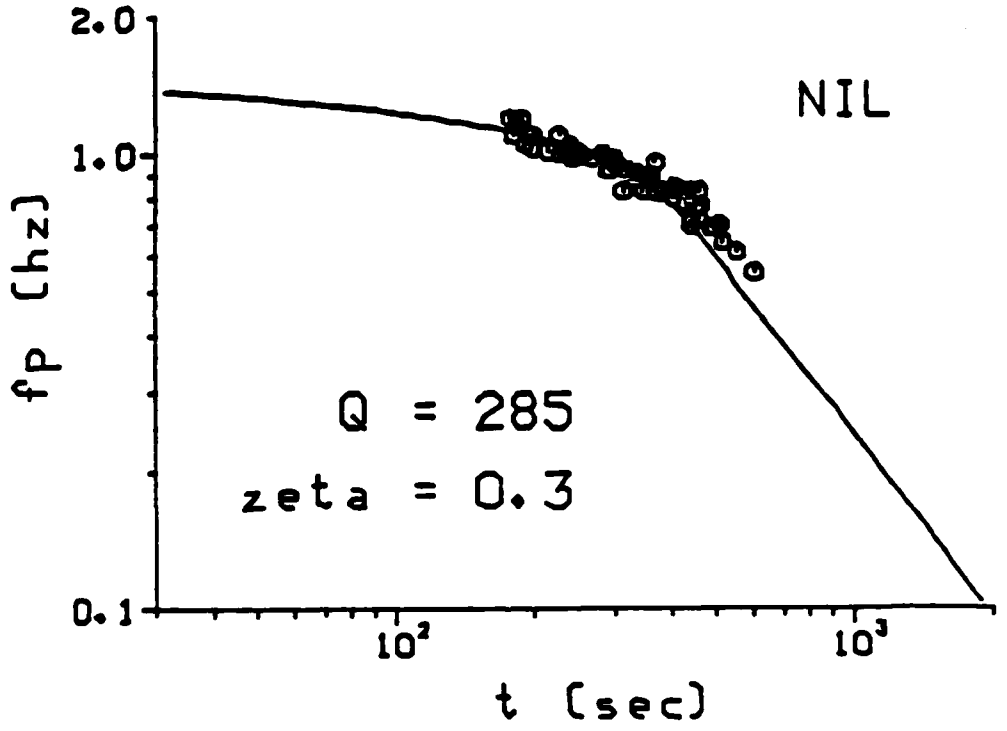

Figure 5. Plot of f_p(Hz) versus t (sec) for NIL. Theoretical Curve for $Q_o = 285$, $\zeta = 0.3$. The Epicenter Location of the Earthquakes Plotted is 39° N, 73° E.

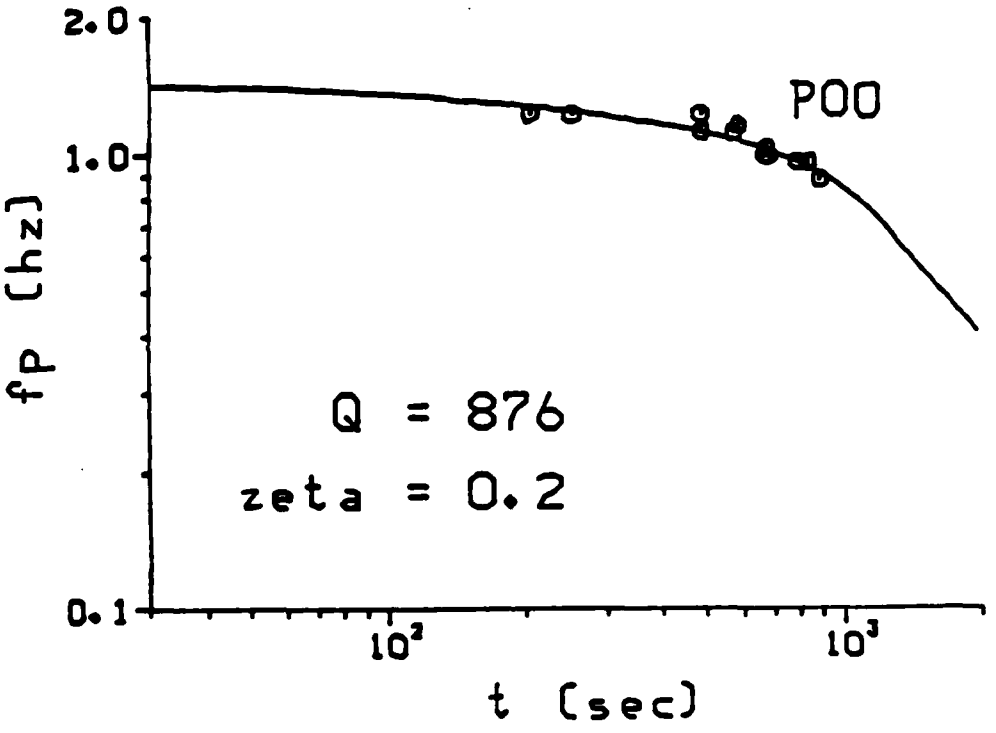

Figure 6. Plot of f_p (Hz) versus t (sec) for POO. Theoretical Curve for Q_o = 876, ζ = 0.2. The Epicenter Location of the Earthquakes Plotted is 17° N, 73° E.

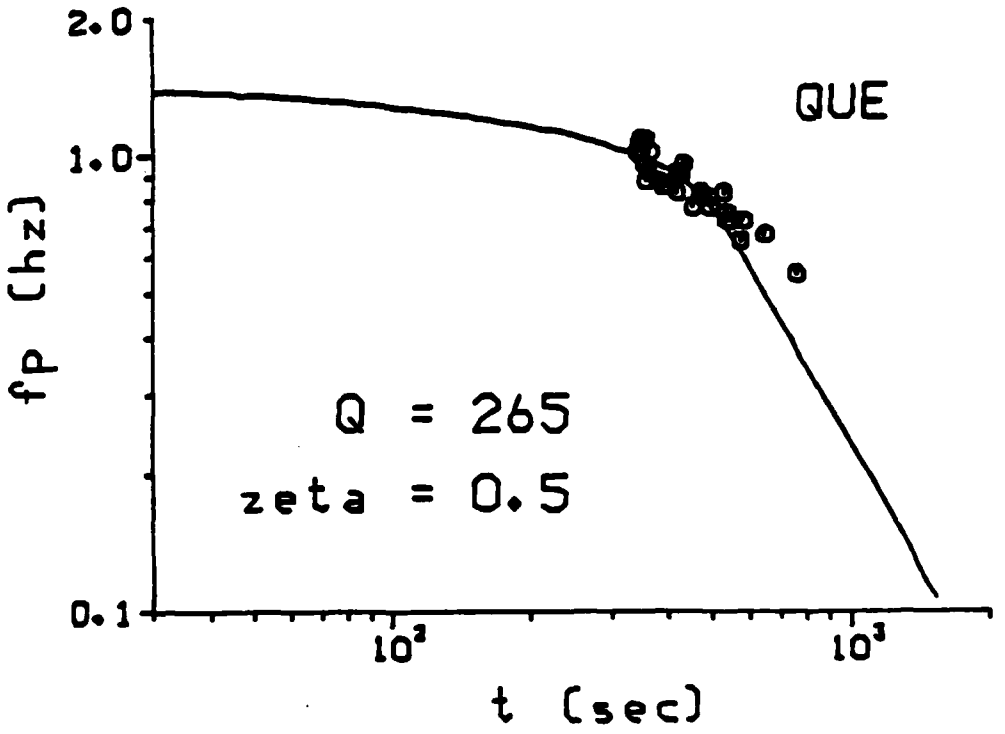

Figure 7. Plot of f_p (Hz) versus t (sec) for QUE. Theoretical Curve for Q_o = 265, ζ = 0.5. The Epicenter Location of the Earthquakes Plotted is 39° N, 73° E.

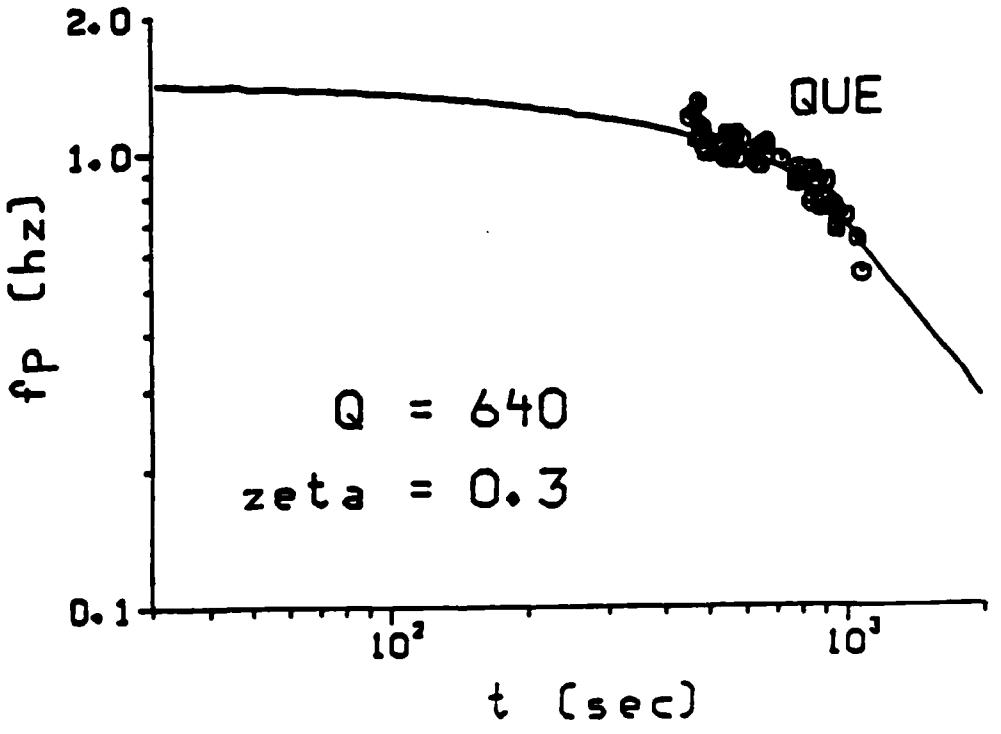

Figure 8. Plot of f_p (Hz) versus t (sec) for QUE. Theoretical Curve for $Q_o = 640$, $\zeta = 0.3$. The Epicenter Location of the Earthquakes Plotted is 17° N, 73° E.

Attenuation of High Frequency Earthquake waves in South America

Mehdi M. Raoof and Otto W. Nuttli

ABSTRACT

Earlier attenuation studies for the South American continent indicate that there is low attenuation for Sn and Lg waves in the shield region east of the Andes, whereas in the west of South America, with some exceptions, there is high attenuation for Sn and Lg waves.

However, these studies were non-quantitative. In this study, Q_o (1-Hz values) for Lg waves for South America are presented, based on a scattering model of Aki (1969) as extended by Herrmann (1980) for the coda waves of shallow local and near-regional earthquakes. The results of the coda Q method are compared with those obtained using Nuttli's (1973) method. These coda-Q_o values are in good agreement with the apparent Q_o of Lg waves obtained by the latter method. The data were obtained from over 100 local and regional earthquakes recorded by 12 WWSSN stations throughout continental South America. These data provided a range of frequencies from 0.4 to 1.4 Hz. Frequency dependence of Q was investigated for the observed range of frequencies by assuming $Q = Q_o (f/f_o)^{\zeta}$. The observed data indicate that the tectonic region of western South America

Department of Earth and Atmospheric Sciences, Saint Louis University, St. Louis, Missouri 63103.

is characterized by low Q_o and a large value of the frequency dependent factor, ζ, with values ranging from 150 to 350 and 0.4 to 0.7, respectively. Q_o values increase in the shield region east of the Andes but frequency dependence decreases. Average crustal Q_o values obtained for north and central Argentina range from 420 to 580 and ζ ranges between 0.2 and 0.3. The Q_o values are larger in the Brazil region, ranging from 580 to 980, with ζ varying from 0.0 to 0.2. In the lower attenuation region of eastern South America, higher values of attenuation correlate with greater thickness of the sedimentary layers.

INTRODUCTION

The study of the anelasticity of various regions of the earth is of major importance for earthquake seismology. In the continental United States and in Eurasia, lateral variations in attenuation and frequency dependence of the quality factor Q have been observed. In particular, the short-period surface waves used to study the earth's crust suffer strongly from lateral heterogeneities in the crust. Therefore, a practical analysis method is required to deal with the problem of a laterally heterogeneous earth.

To deal with this problem, Aki (1969) proposed a statistical treatment for the waves which are backscattered due to lateral heterogeneity. These waves are found in the coda of local earthquakes. He suggested that the seismic coda waves of local earthquakes are backscattered waves from numerous randomly distri-

buted heterogeneities in the earth. Using coda waves of local earthquakes, Aki and Chouet (1975), Aki (1980a, b), Herrmann (1980), Rautian and Khalturin (1978), and Singh (1981) investigated the quality factor (Q) of seismic waves for frequencies greater than 0.1 Hz. Herrmann's (1980) Q values for selected United States locations are consistent with Q values calculated from the anelastic attenuation coefficient (γ) by Nuttli (1973). Because coda Q values are consistent with apparent Q values of Lg waves in the crust, they give some measure, at least in a relative sense, of the Q structure of the crust.

The purpose of this study is to obtain apparent Q values for high frequency Lg waves (approximately 1 Hz) traveling in the South American crust by using Herrmann's (1980) coda Q method. These results will be compared with those obtained by using a different method, the amplitude decrease with distance, which was used by Nuttli (1973) for eastern North America.

Previous anelastic attenuation studies have been primarily concerned with the mantle beneath the South American continent. Body wave attenuation studies by Sacks (1971), Isacks and Barazangi (1980), Chinn *et al.* (1980) and others indicate that there are some high attenuation zones in the west of South America.

Crustal studies in South America indicate great change in the crustal thickness from the coast towards the central Andes. As can be seen in Figure 1, the thickness of the crust changes from about 7 km sea-ward of the trench in western South Amer-

ica (Whitsett, 1975) to a maximum of 70 km under the western high plateau (Altiplano) of the Andes (James, 1971). The crust then thins toward the interior of the continent, with a value of 25-40 km to the east of the eastern cordillera. Such variations in the thickness have a great influence on the propagation of phases such as Lg. Since there has been a limited number of Lg attenuation studies for the South American continent, with no Q_{Lg} values reported, this study was undertaken to provide a generalized Q_o map for Lg waves of about 1-Hz frequency for the South American continent, as well as a contoured Q_o map of South America.

THEORY AND METHOD

Aki (1969) observed that short-period surface waves, which were used in crustal studies, suffered strongly from lateral heterogeneities in the crust. Therefore, he proposed a statistical treatment to deal with the heterogeneity of the earth, and defined the seismic coda waves of local earthquakes as backscattered waves from numerous randomly distributed heterogeneities in the earth. Such waves can be found even near the epicenter after the passage of all the primary waves. Therefore, the later portions of a seismogram should be the result of averaging over many samples of heterogeneities.

Some important characteristics of the coda are its independence of epicentral distance and azimuth and the fact that useful properties of it can be simply measured from seismograms

without any sophisticated calculations.

For the average peak-to-peak amplitude observed around time t, Aki (1969) proposed the following relation:

$$\frac{A(t)}{\sqrt{8}} = I(f_p) Q^{1/4} t^{-1/2} \left[\frac{dt}{df_p}\right]^{-1/4} exp(-\pi f_p \frac{t}{Q}) M_o B(f_p) \qquad (1)$$

where $I(f_p)$ is the instrument magnification at predominant frequency observed at time t, Q is the anelastic attenuation quality factory for the surface wave comprising the coda, M_o is seismic moment and $B(f_p)$ is defined as

$$B(f_p) = [2N(r_o)]^{1/2} \Phi_o(f_p, r_o) \qquad (2)$$

where $N(r_o)$ is the number of scatterers within a radius of r_o. $\varphi_o(f_p, r_o)$ is a function of frequency only, defined by

$$\Phi_o(w|r) = |F(w|r)/M_o exp(wt/2Q) \qquad (3)$$

where F(w|r) expresses the expected absolute value of the Fourier transform of secondary waves coming from a scatterer at distance r. So φ_o(w|r) expresses the excitation of the secondary scattered waves. The unit of φ_o(w|r) is cm per Hz per dyne cm.

Equation (1) was developed by Aki to analyze earthquakes in central California for a particular value of Q. Herrmann (1980) expressed equation (1) in terms of another time variable $t^* = t/Q$, to be applicable in other areas, as follows:

$$\frac{A(t^*)}{\sqrt{8}} = Q^{-1/2} M_o B(f_p) C(f_p, t^*) \qquad (4)$$

where the term $C(f_p, t^*)$ is called the coda shape function and is equal to

$$C(f_p,t^*)=I(f_p)t^{*\frac{-1}{4}}\left[\frac{df_p}{dt^*}\right]^{1/4}exp(-\pi f_p t^*) \qquad (5)$$

For the application of equation (5), there should be a change of predominant frequency of the coda with time, df_p/dt^*.

In Table 1, the predominant frequency f_p and the coda shape function $C(f_p, t^*)$ are given as a function of t^* for the short period WWSSN instrument system with a peak magnification at 1.35 Hz, and a relative magnification of 1.0 at 1 Hz. Since $t^* = t/Q$, if predominant frequency f_p and coda shape are plotted as a function of t^*, they result in theoretical master curves for determination of Q for different regions.

By assuming a source-spectrum corner frequency greater than the peak frequency of the instrument response, the effect of source spectrum can be ignored in the above calculation. Frequency dependence of Q can be investigated by assuming that

$$Q(f) = Q_o(f/f_o)^{\zeta} \qquad (6)$$

assigning a value to ζ, and then plotting f_p as a function of t^*. Master curves for different values of ζ are given in Figure 2.

Methods of Q Estimation

There are several methods that have been proposed for estimating Q, some of which are: f_p versus t and coda shape

methods (Q coda) by Herrmann (1980), and Q inferences from gamma (Q_{L_g}) by Nuttli (1973).

In this study the f_p versus t method will be used first by plotting the predominant frequency of the coda as a function of time after the origin, including the Lg arrival. The predominant frequency can be calculated by simply counting the number of zero crossings of the seismic trace within a given time interval. We use a smaller window or time interval shortly after the Lg arrival but a larger one for later parts of the coda because of the decreasing frequency content in the coda. The number of zero crossings is divided by twice the window length to obtain f_p. Next, the plot of observational data is superimposed on the master curves of Figure 2.

We obtain the frequency dependence parameter ζ from the best-fit curve, and Q_o is obtained from that value of t which maps into $t^* = 1$, since $t^* = t/Q$.

Figure 3 is the plot of predominant frequency f_p (Hz) as a function of time t (sec) after the origin at the Peldehue (PEL) station. The theoretical curve for Q_o equal to 260 and $\zeta = 0.4$ is also shown.

Since the f_p versus t data plot shows considerable scattering for most of the stations in South America, which sometimes makes it impossible to estimate the frequency dependence factor ζ, and thus the best value of Q_o, a test of the validity of the results obtained from the f_p versus t method will be made by using also Nuttli's (1973, 1980) method.

The amplitude of dispersed surface waves in the time domain is given by Ewing *et al.* (1957) as

$$A_1 = A_{o_1}\Delta^{-1/2}(R_o \sin\Delta^\circ)^{-1/2}\exp(-\gamma\Delta) \qquad (7)$$

and for the Airy phases, which Nuttli (1973) concluded gave the best fit to Lg amplitude attenuation, as

$$A_2 = A_{o_2}\Delta^{-1/3}(R_o \sin\Delta^\circ)^{-1/2}\exp(-\gamma\Delta) \qquad (8)$$

where A_1 and A_2 are observed amplitudes at an epicentral distance Δ, A_{01} and A_{02} are constants, R_o is the radius of the earth model, and γ is the coefficient of anelastic attenuation. Nuttli (1973) used the fact that γ is related to Q, frequency f, and group velocity, U, by

$$\gamma = \frac{\pi f}{QU} \qquad (9)$$

The group velocity, U, for the Lg phase is assumed to be 3.5 km/sec. The term Δ^{-n} represents a decrease in amplitude due to dispersion effects, with n equal to 1/2 for ordinary dispersed surface waves and 1/3 for an Airy phase. The next term $(R_o \sin\Delta^\circ)^{-1/2}$ represents the amplitude decrease due to geometrical spreading, where Δ is the epicentral distance in degrees and R_o is the radius of the earth. The last term in both equations, $\exp(-\gamma\Delta)$, represents attenuation due to absorption. Equation (9) can be written as

$$A \approx (\sin\Delta)^{-1/2}\Delta^{-1/3}\exp(-\gamma\Delta) \qquad (10)$$

For a given amplitude A at an epicentral distance Δ and an amplitude A_{10} at a distance of 10 km, we have

$$A_{10}(f)=A(\Delta,f)\left[\Delta\frac{(km)}{10}\right]^{\frac{1}{3}}\left[\frac{\sin(\Delta^{\circ})}{\sin(\frac{10}{111.1})}\right]^{\frac{1}{2}}\exp\left[\gamma(\Delta-10)\right] \qquad (11)$$

where f is Lg wave frequency.

To study the attenuation of Lg amplitude with distance, Nuttli (1973) used equation (10) to get a set of master curves, consisting of log-log plots of amplitude (A) versus distance (Δ), where each curve represents a different value of γ (Figure 4). If the Lg amplitude is plotted as a function of epicentral distance for an event on the same log-log scale as the master curves, we can determine the value of γ by fitting the curves to the data, such as was done by Nuttli (1973), Nuttli and Dwyer (1978), and Bollinger (1979). If γ is determined in this manner for 1-Hz Lg waves, Q_o can be obtained from equation (9). By applying the same procedure to Lg waves of various frequencies, ζ also can be obtained from the variation of γ and Q with frequency.

After γ (1 Hz) has been determined, equation (11) can be used to extrapolate A(Δ) to obtain A_{10}. For eastern North America, Nuttli (1973) found that A_{10} (1 Hz) = 110 microns for m_b = 5.0, where m_b is the teleseismic P-wave magnitude. Making this assumption

$$\log A_{10} = \log A_{\mu} + (m_b + \Delta m_b - 5.0) \qquad (12)$$

where $A_{\mu} = A_{10}$ for m_b = 5.0. Δm_b

is the m_b correction parameter. Therefore, for a given earthquake, if m_b is known from teleseismic P-wave amplitudes, A_{10} can be calculated. If the excitation of Lg waves is independent of crustal structure, as shall be assumed, A_μ = 110 microns everywhere. However, for the same strength of source excitation, m_b varies geographically because of variation in the anelastic attenuation of P-wave amplitudes in the asthenosphere. This is accounted for by adding a Δm_b term to the value of m_b in equation (12). If the Δm_b value can be found for a geographic region, equation (12) will give a 1-Hz, vertical component Lg amplitude at 10 km distance. This value can be compared with that obtained from equation (11), and the best set of Q_o, ζ values (to make the two A_{10} values agree) of the permissible set of values from the coda Q method can be chosen. This procedure helps to reduce the uncertainty in estimating ζ when the range of f_p, t values is not large enough, or when there is scatter in the data points, so that Q_o and ζ values cannot be determined uniquely from the coda data.

DATA ANALYSIS

In this study two main difficulties were encountered. They are the scarcity of data due to low instrument magnification and the scatter of the data. Therefore several thousands of shallow and deep events recorded by 12 WWSSN stations were tested, from which over 240 local and regional earthquakes, occurring mostly in the west of the South American continent, were

selected for the determination of Q. It was found that the deep earthquakes didn't give results consistent with shallow earthquakes. Therefore, the deep earthquakes were removed from the selected earthquake list. Thus the data base for this study consists of about 100 continental shallow local and regional earthquakes recorded by 12 WWSSN stations in South America during the period 1972-1974, with a range of body-wave magnitude of 4.0 to 6.0.

The epicentral information was obtained from the Bulletin of the International Seismological Centre. In the selection of the data, only the short-period, vertical-component microfilm records were used.

Figure 5 shows the location of the events used in this study. It also shows the epicenter-station paths for all the WWSSN stations and earthquakes considered. As can be seen in this figure, most of the paths are along or across the Andes Mountains and only a few paths pass through the shield region. The present available data show no usable earthquakes in the eastern and southern part of the continent, even though some parts of this region are covered by paths due to earthquakes which have occurred in the west and were recorded by three stations (NAT, BDF, and LPA) in the east. Two big gaps (north-northeast and southern parts of continent) still exist.

In this study we used first the f_p versus t method that was described earlier for different earthquakes recorded at each station. In fact, to get less scatter of the data and a more accurate

value for Q_o, rather than finding an average over a larger area, the area surrounding each station was divided into different zones, and then the predominant frequency f_p was plotted against time t after the earthquake origin for each zone. These plots gave different Q_o and ζ values for different directions about the station. In order to get reliable Q_o values, it is essential that the observed predominant f_p versus time t values should cover the sharp curvature portion of the master curves of Figure 2. Otherwise there can be large uncertainties in the Q_o values.

The results of the above process for some stations are presented and shown in Figures 6 through 8. In these figures, circles denote the observed data points and the solid line is the theoretical curve chosen "by eye" to satisfy the data. The Q_o and ζ values are also given for each plot.

In each figure, two plots are presented for each station, which serve to show the quality of their fitness to the theoretical master curve. As an example, in Figure 3 the upper plot is for the four events north of PEL, whereas the lower plot is for the three events to the south of the station. Frequency dependent theoretical curves for $Q_o = 260$ and $\zeta = 0.4$ (upper plot) and $Q_o = 190$, $\zeta = 0.4$ (lower plot) are shown.

In Figures 9 through 12 the events recorded by each station are shown on the separate maps, along with the Q_o values.

A common feature of the plots shown earlier is that they are well fitted by the theoretical master curves, whereas for some stations, like for example TRN in Figure 12, the scatter is consid-

erable enough to make it possible for several curves with different ζ values to be fitted to the data, resulting in different Q_o and ζ values. This is true even if one considers the shield-type paths only. This may be due to two possible factors: either the areas designated as shields are more heterogeneous than expected, or because the shield paths in South America are from earthquakes located in the mountains, the scattering in the data is caused by the portion of the path that crosses the mountain region.

To deal with the problem of high degree of scatter in the data for some stations like TRN, for which the f_p versus t method fails to give accurate results, and to check the results obtained from Herrmann's (1980) f_p versus t method, Nuttli's γ-estimation method also was used.

This method can be simply applied to all the earthquakes by taking one station and one earthquake and measuring the predominant frequency and amplitude versus time after origin time, starting from the Lg arrival. As explained earlier, equations (11) and (12) have been used to obtain Q_o and ζ for different paths. For the magnitude correction factor (Δm_b) in equation (12), we used 0.4-0.6 for the western part, 0.2-0.3 for the northern part, and 0.0-0.1 for the eastern part of South America. Figures 13 through 16 present the results obtained by using Nuttli's method.

Results of Q_o values obtained by Herrmann's (1980) and Nuttli's (1973) methods are shown on Figure 17 and 18, respec-

tively. By general analysis of these maps, one can easily realize that there are lateral variations in Q_o across continental South America. The results obtained by application of the two different methods give very much the same Q_o values for the western part of the continent, whereas for the eastern part the f_p versus t method gives higher values for crustal Q_o than the γ-estimation method. Figure 19 shows the variation of the frequency dependent parameter ζ throughout the continent, by using coda method. Nuttli(1973) method give higher ζ values for eastern South America.

The Q_o values discussed above are obtained from long wave paths (long travel times) which make up the very tail of the seismogram. To investigate whether these Q_o values agree with Q_o values obtained from shorter wave paths (shorter travel times), a similar study was done for short wave paths with the results shown in Figure 20. The important conclusion that we can get from this comparison is that the Q_o values obtained from short and long epicenter to station paths are highly consistent. This map shows an average Q_o value of 160 to 220 for the western part, a value of 550 for the southeast and an average Q_o value of 900 for the eastern part. Figure 21 shows the different zones of Q_o and frequency dependent ζ in South America.

Recently Osagie and Mitchell (1983) studied the attenuation of Q_β in South America at periods between 20 and 80s and found that there is high attenuation for Q_β in the west of South America but lower in the east. It is very interesting that, in their study,

Osagie and Mitchell used a simple crustal Q model, Figure 22, to compute the attenuation and Q values for 1 Hz Lg for South America. Their numerical value is similar to that of this study for the west of South America. However, for the east of South America they obtained a somewhat lower value for Q_o than found in this study. The similarities of these two studies are very important, for they provide more validation of the results of this study.

Finally, by using the Q_o maps obtained from the f_p versus t method and the γ-estimation methods, a contour map of Q_o for the South American continental crust is given in Figure 23. This figure represents one of the important goals of this study.

Comparison of Q_o Values with Tectonics, Geology and Gravity

The South American continent can be divided into three tectonic regions, with different origins and ages: the South American Platform, Patagonian Platform and the Andean Cordillera Belt. The central and a large part of the eastern area of the continent is called the South American Platform, which is the oldest, and its basement is well exposed in the three major shields (Guyana shield, Central Brazil shield and the Atlantic shield in the eastern part of the continent) (Figure 24). Q values obtained in this study show that in the Guyana shield Q_o varies from 400 to 600 and in the Central Brazilian shield from 700 to 1000 (Figures 17 and 18).

The Patagonian Platform is found entirely in Argentina and

extends over the broad continental margin. It is a young platform (Middle Paleozoic onwards). Q_o values obtained for this platform are in the range of 420-580 (Figures 17 and 18).

The first two platforms are bounded by the Andean Cordillera Belt, which is the youngest and extends along the northern boundary of the South American Platform. (Explanatory note of tectonic map of South America by National Department of Mineral Production of Brazil with the collaboration of UNESCO.) Our Q map shows Q_o values of 115 to 350 for this region.

Correlation of Q Values with Geology of the Continent

A geological map of South America is shown in Figure 25. The sedimentary cover of the continent can be compared with the result of our attenuation studies in South America. Generally, in the active region of the west of South America there is no exact relation between attenuation and the thickness of the sedimentary rocks, whereas in the stable region east of South America, the thickness of the sedimentary rocks increases as Q decreases. This result is similar to what Mitchell (1983) observed in the central and eastern United States. Figure 26 shows the variation of the sediment thicknesses in the eastern part of South America.

Comparison of the Q Map with the Gravity Map of South America

The contoured Q_o map presented in this study shows the same pattern as the gravity map of South America (Figures 27).

and indicates that the low Q_o values found in the west of South America correlate with the low gravity values. Also, the high Q_o region of the East correlates with the high gravity anomaly in the crust. This correlation suggests that in the region of high tectonic activity we have high temperatures and high attenuation, and since high temperatures result in rocks of low density, we expect to get relatively low Bouguer gravity values in this regions.

DISCUSSION AND CONCLUSIONS

Previous Sn attenuation studies in South America indicate that, with some exceptions, there is high attenuation in the crust and upper mantle beneath western South America and lower attenuation for the shield regions in the central and eastern parts of the continent (Molnar and Oliver, 1969). Recent attenuation studies by Chinn *et al.* (1980) gave similar results for Sn and Lg in South America. However, their work was focused on Sn propagation. In this study, a generalized Q_o map for Lg waves of about 1 Hz frequency for the South American continent, as well as contoured Q_o maps of South America, are provided by using data from 12 WWSSN stations distributed throughout the continent, at which over 100 local and regional earthquakes with m_b magnitude about 4 to 6 were recorded.

There are two techniques which were used for the determination of Q: 1) f_p versus t method proposed by Herrmann (1980) which is based on a scattering model by Aki (1969); 2) γ-

estimation method by Nuttli (1973).

The Q_o values for the high frequency Lg waves are presented as obtained by using both methods. The coda Q_o values are in good agreement with the Q_o values obtained from Lg amplitudes.

The two different techniques should give approximately similar results if we have no substantial scatter in the data and if there are sufficient data. Although there was some scattering in the f_p versus t data for some stations, Q_o values that resulted from both methods are highly consistent in the west of South America, a high attenuation region, but in the east of South America the Q_o values obtained by Herrmann's (1980) method are somewhat higher than those obtained using Nuttli's (1973). In the western part of the continent, except for the region south of station PEL, Q_o data for short epicenter-station paths give maximum coverage of the region. However, in eastern South America, due to the limited number of and the epicentral location of earthquakes recorded by eastern stations, the Q_o values are averaged over larger areas. In addition, similar to the southern part of the continent, the north-northeastern section of the continent remains a gap.

Data of this study cover the range of frequencies from 0.4 to 1.4 Hz. A frequency dependence of Q was investigated for this range of frequencies by assuming $Q = Q_o (f / f_o)^{\zeta}$.

Generally, results of this study show there are three different zones of attenuation with different frequency dependence in South America, as follows:

1. A high attenuation zone with large frequency dependence in the west, where Q_o varies from 130 to 350 and the frequency-dependence factor (ζ) lies in the range of 0.4 to 0.7, which corresponds to the Andean belt. This also correlates with low gravity values.
2. An intermediate attenuation zone with average frequency dependence in the southwest, central and northern parts of Argentina, where Q_o varies from 420 to 580 and the frequency dependence factor (ζ) lies in the range of 0.2 to 0.3, which corresponds to the Patagonian Platform.
3. A low attenuation zone with low frequency dependence in the east of South America with Q_o of 580 to 980 and with a frequency-dependence factor (ζ) in the range of 0.0 to 0.2, which corresponds to the South American Platform. This also correlates with more positive gravity anomalies.

Earlier studies indicate that there are higher Q_β for the Peru region than north of Chile. Results of this study also agree with higher Q_o values for the Peru and Colombia regions than for the northern part of Chile.

The Q_o maps obtained from short and long paths in this study give similar results, which is considered to be proof that the typical Lg coda is consistent with the very late part of the coda.

Recent results of Lg-wave attenuation obtained from synthetic seismograms by Osagie and Mitchell (1983) indicate similar Q_o values for the west but lower Q_o values for the east than

this study does.

The attenuation map for South America is compared with the thickness of sediment cover for the continent. High attenuation in the west of South America can be correlated with 6000 to 15,000 m of sediment thickness. Generally, in the active region of the west of South America there is no exact relation between attenuation and the thickness of the sedimentary rocks, whereas in the stable region east of South America Q_o decreases as the thickness of the sedimentary rocks increases. This important result is similar to what Mitchell (1983) observed in the central and eastern United States.

As noted by Singh (1981) for North America, the South American Q_o values correlate with geological age, tectonic activity and Bouguer gravity. In this sense the contour map of Q_o for South America (Figure 25) resembles the contoured Q_o map of the United States obtained by Singh and Herrmann (1983).

The crustal Q_o values given in this study, as well as the contour Q_o map, might be useful for studies of earthquake hazard and for earthquake engineering studies in South America.

ACKNOWLEDGEMENTS

The authors wish to thank Drs. Robert Herrmann and Brian Mitchell for their comments and many helpful suggestions. The research reported in this study was supported by Contract F49620-83-C-0015 of the Defense Advanced Research Projects Agency, and was monitored by the Air Force Office of Scientific Research.

REFERENCES

Aki, K. (1969). Analysis of the seismic coda of local earthquakes as scattered waves, *J. Geophys. Res. 74,* **615-631.**

Aki, K. and B. Chouet (1975). Origin of coda waves: source, attenuation, and scattering effects, *J. Geophys. Res. 80,* **3322-3342.**

Aki, K. (1980a). Attenuation of shear waves in the lithosphere for frequencies from 0.05 to 25 hz, *Phys. Earth Planet. Interiors 21,* **50-60.**

Aki, K. (1980b). Scattering and attenuation of shear waves in the lithosphere, *J. Geophys. Res. 85,* **6496-6504.**

Chinn, D.S., Isacks, B.L. and Barazangi, M. (1980). High frequency seismic wave propagation in western South America along the continental margin, in the Nazca plate across the Altiplano, *Geophys. R. Abstract Soc., 60,* **209-244.**

Condie, K.C. (1976). *Plate Tectonics and Crustal Evolution,* **Pergamon Press, New York.**

Defense Mapping Agency Aerospace Center, (1977). Bouguer gravity anomaly, *Map - GAM 1,Third Edition,* **St. Louis Air Force Station, Missouri 63118.**

Goudarzi, G.H. (1977). Geologic map of south America, *Miscellaneous Field Studies Map MF-868 A,* **Department of**

interior United States Geological Survey.

Herrmann, R.B. (1980). Q estimates using the coda of local earthquakes, *Bull. Seism. Soc. Am. 70*, 447-468.

Isacks, B.L. and M. Barazangi (1973). High frequency shear waves guided by a continuous lithosphere descending beneath western South America, *R. Astron. Soc. Geophys. J. 33*, 129-139.

James, D.E. (1971). Andean crustal structure, *Carnegie Inst. Wash. Yearb. 69*, 447-460.

Mitchell, B.J. (1983). Effect of crustal velocities and Q on the amplitudes of Lg at short and intermediate periods, Semi-Annual Report, No. 1, 31 March 1983, ARPA Order No. 4397, Saint Louis University.

Molnar, P., and J. Oliver (1969). Lateral variations of the attenuation in the upper mantle and discontinuities in the lithosphere, *J. Geophys. Res. 74*, 2648-2682.

National Department of Mineral Production, Brazil (1978) Tectonic map of South America (explanatory notes)

Nuttli, O.W. (1973). Seismic wave attenuation and magnitude relations for eastern North America, *J. Geophys. Res. 78*, 876-885.

Nuttli, O.W. (1978). A time-domain study of the attenuation of 10-hz waves in the New Madrid seismic zone, *Bull. Seis*

Soc. Am. 68, 343-355.

Nuttli, O.W. and J. Dwyer (1978). State-of-the-Art for Assessing Earthquake Hazards in the United States; "Attenuation of High Frequency Seismic Waves in the Central Mississippi Valley." Miscellaneous Paper S-73-1, Report 10, U.S. Army Engineer Waterways Experiment Station, CE, Vicksburg, MS.

Nuttli, O.W. (1980). The excitation and attenuation of seismic crustal phases in Iran, *Bull. Seis. Soc. Am. 70*, 469-485.

Osagie, E. and B.J. Mitchell (1983). Regional variation of Q_β and its frequency dependence in the crust of South America, Semi-Annual Report No. 2, 30 November 1983, ARPA Order No. 4397, Saint Louis University.

Rautian, T.G. and V.I. Khalturin (1978). The use of the coda for determination of earthquake source spectrum, *Bull. Seis. Soc. Am. 68*, 928-948.

Sacks, I.S. (1971). The Q structure of South America, *Carnegie Inst. Wsh. Yearb. 70*, 340-343.

Singh, S. (1981). Regionalization of crustal Q in the continental United States, *Ph.D. Dissertation*, Saint Louis University, St. Louis, MO.

Singh, S. and R.B. Herrmann (1983). Regionalization of crustal Q in the continental United States, *JGR 88, B1*, 527-538.

Whitsett, R. (1975). Gravity measurement and their structural implications for the continental margin of southern peru, *Ph.D. thesis*, Dept. of Geophysics,Oregon State University.

FIGURE CAPTIONS

Figure 1. Cross section of the Andes and the coastal region (after James, 1971).

Figure 2. Master curves for different frequency dependencies (ζ) for the short-period WWSSN instruments.

Figure 3. f_p vs t: Upper plot for four events north of PEL. Lower plot for three events south of PEL.

Figure 4. Time-domain amplitude attenuation of Lg waves, with γ as parameter. The units of γ are km^{-1}.

Figure 5. Map showing the epicenter-station paths for all the WWSSN stations and earthquakes considered.

Figure 6. f_p vs t: Upper plot for four events southwest of NAT. Lower plot for two events west of NAT.

Figure 7. f_p vs t: Upper plot for three events southeast of ANT. Lower plot for five events southwest of ANT.

Figure 8. f_p vs t: Upper plot for three events west of TRN. Lower plot for four events southwest of TRN.

Figure 9. Epicenter-station paths and Q_o values for earthquakes (■) recorded at station ANT. Q_o values are obtained by using Herrmann's (1980) method.

Figure 10. Epicenter-station paths and Q_o values for earthquakes (■) recorded at station PEL. Q_o values are obtained by

using Herrmann's (1980) method.

Figure 11. Epicenter-station paths and Q_o values for earthquakes (•) recorded at station NAT. Q_o values are obtained by using Herrmann's (1980) method.

Figure 12. Epicenter-station paths and Q_o values for earthquakes (•) recorded at station TRN. Q_o values are obtained by using Herrmann's (1980) method.

Figure 13. Epicenter-station paths and Q_o values for earthquakes (•) recorded at station ANT. Q_o values are obtained by using Nuttli's (1973) method. (Refer to Figure 9 for the coda Q estimates.)

Figure 14. Epicenter-station paths and Q_o values for earthquakes (•) recorded at station NAT. Q_o values are obtained by using Nuttli's (1973) method. (Refer to Figure 11 for the coda Q estimates.)

Figure 15. Epicenter-station paths and Q_o values for earthquakes (•) recorded at station PEL. Q_o values are obtained by using Nuttli's (1973) method. (Refer to Figure 10 for the coda Q estimates.)

Figure 16. Epicenter-station paths and Q_o values for earthquakes (•) recorded at station TRN. Q_o values are obtained by using Nuttli's (1973) method. (Refer to Figure 12 for the coda Q estimates.)

Figure 17. Average crustal Q_o values for the WWSSN stations by using Herrmann's (1980) method.

Figure 18. Average crustal Q_o values from the WWSSN stations by using Nuttli's (1973) method.

Figure 19. Distribution of ζ values throughout the South American continent, by using coda method.

Figure 20. Average crustal Q_o values from the WWSSN stations obtained from shorter wave paths using Herrmann's (1980) method.

Figure 21. Map showing different zones of Q and frequency dependence of ζ in South America.

Figure 22. Models of anelasticity for eastern and western South America (from Osagie and Mitchell, 1983).

Figure 23. Contour map of crustal Q_o for the entire South American continent.

Figure 24. Tectonic map of South America compiled by Kent C Condie (1982).

Figure 25. Geologic map of South America compiled by Gus H Goudarzi (1977).

Figure 26. Map showing the variations of the sediment thicknesses in eastern South America.

Figure 27. Bouguer gravity map of South America showing the

regions of high and low gravity (by Defense Mapping Agency,1977).

TABLE 1

Coda Shape Function for Short Period WWSSN Seismograph

t^*	f_p(Hz)	$C(f_p\ t^*)$
0.01	1.45	1.25E + 1
0.02	1.44	1.20E + 1
0.03	1.42	8.72E + 0
0.04	1.41	6.50E + 0
0.05	1.40	5.28E + 0
0.06	1.38	4.52E + 0
0.07	1.37	4.48E + 0
0.08	1.36	3.87E + 0
0.09	1.35	3.33E + 0
0.1	1.34	3.00E + 0
0.2	1.26	1.31E + 0
0.3	1.19	6.97E - 1
0.4	1.13	4.01E - 1
0.5	1.08	2.51E - 1
0.6	1.02	1.72E - 1
0.7	0.97	1.15E - 1
0.8	0.92	7.97E - 2
0.9	0.86	5.70E - 2
1	0.80	4.14E - 2
2	0.43	3.68E - 3
3	0.30	8.29E - 4
4	0.23	2.70E - 4
5	0.18	1.13E - 4
6	0.15	5.73E - 5

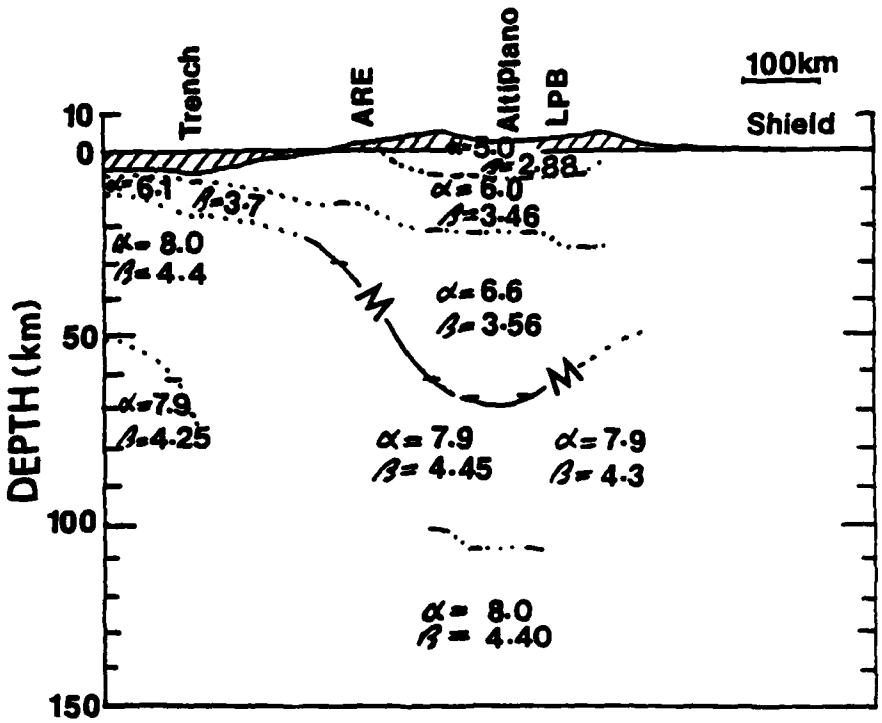
Trench
ARE
Altiplano
LPB
100km
Shield
10
0
50
100
150
DEPTH (km)
α=6.1 β=3.7
α= 8.0 β= 4.4
α=7.9 β=4.25
α=5.0 β=2.88
α= 6.0 β=3.46
α=6.6 β=3.56
α= 7.9 β= 4.45
α=7.9 β= 4.3
α= 8.0 β= 4.40

#1

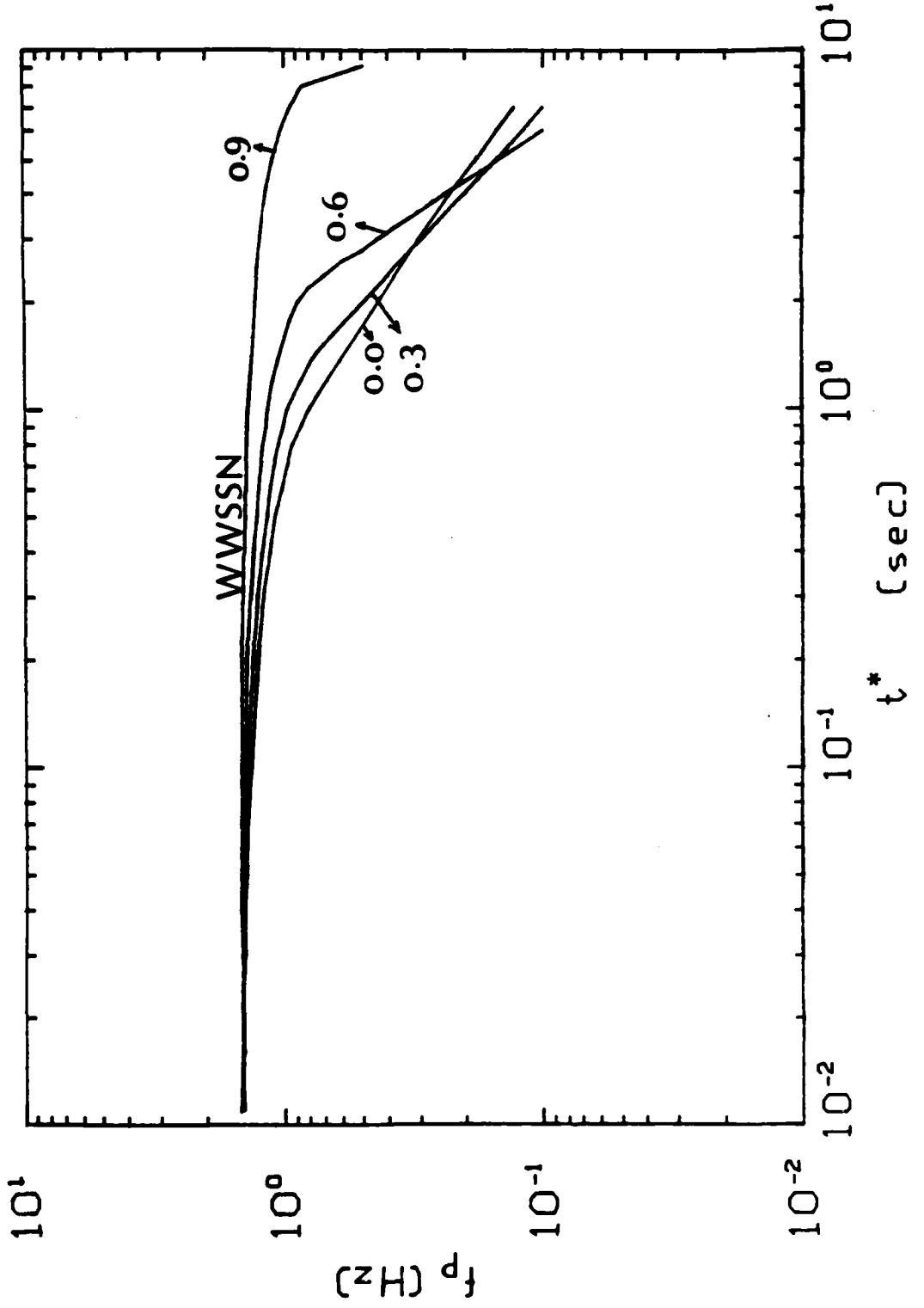

#2

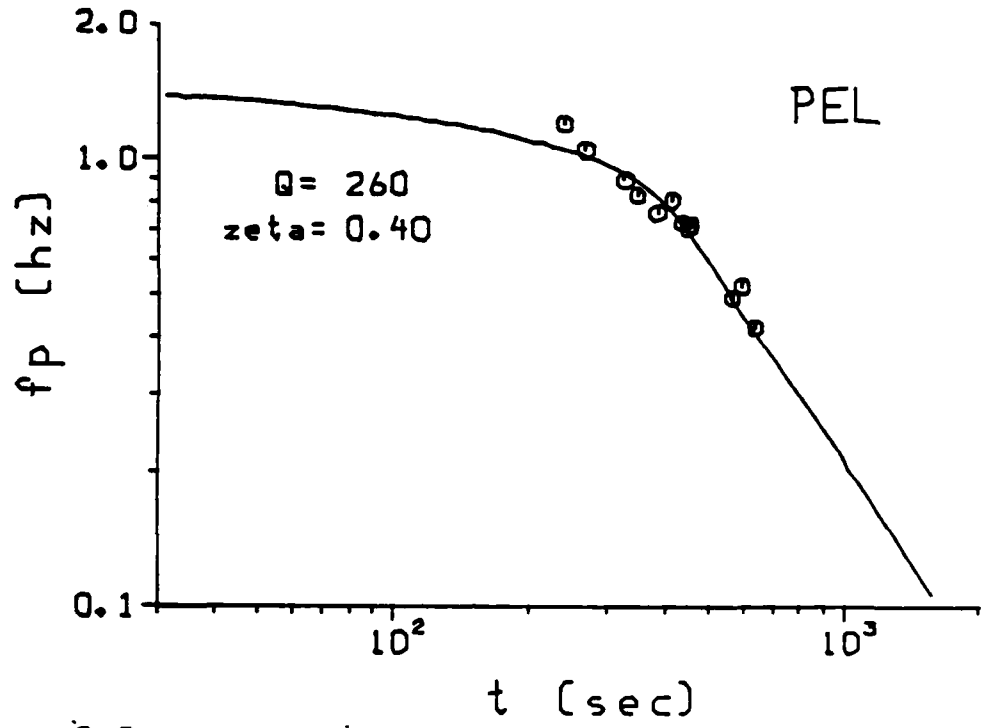
2.0
1.0
0.1
PEL
Q= 260
zeta= 0.40
fp (hz)
10^2
10^3
t (sec)

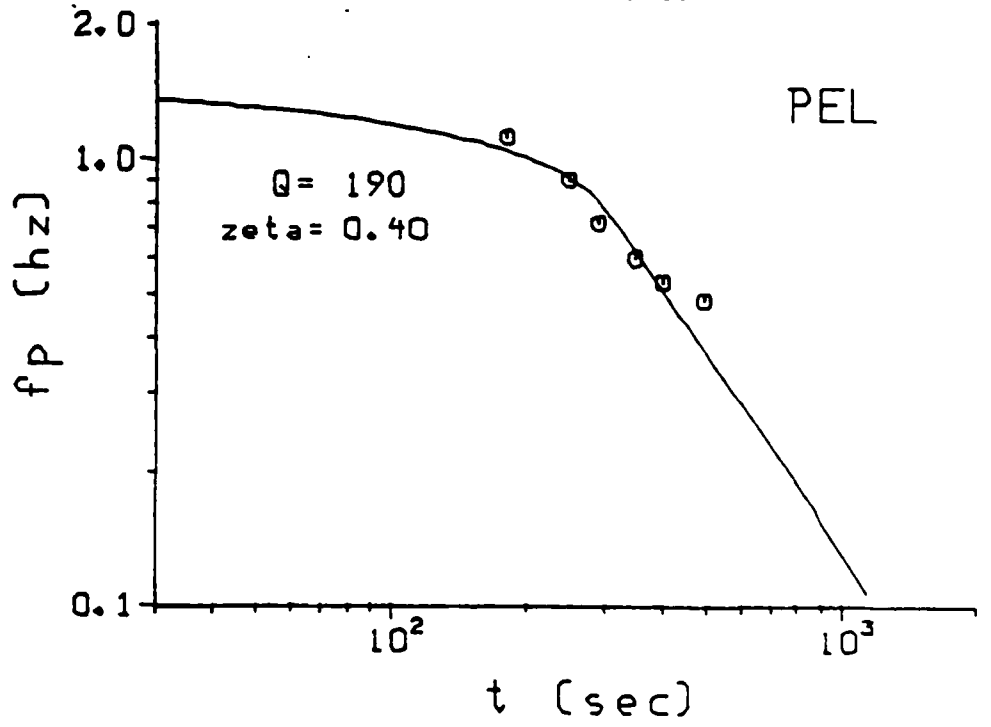
2.0
1.0
0.1
PEL
Q= 190
zeta= 0.40
fp (hz)
10^2
10^3
t (sec)

#3

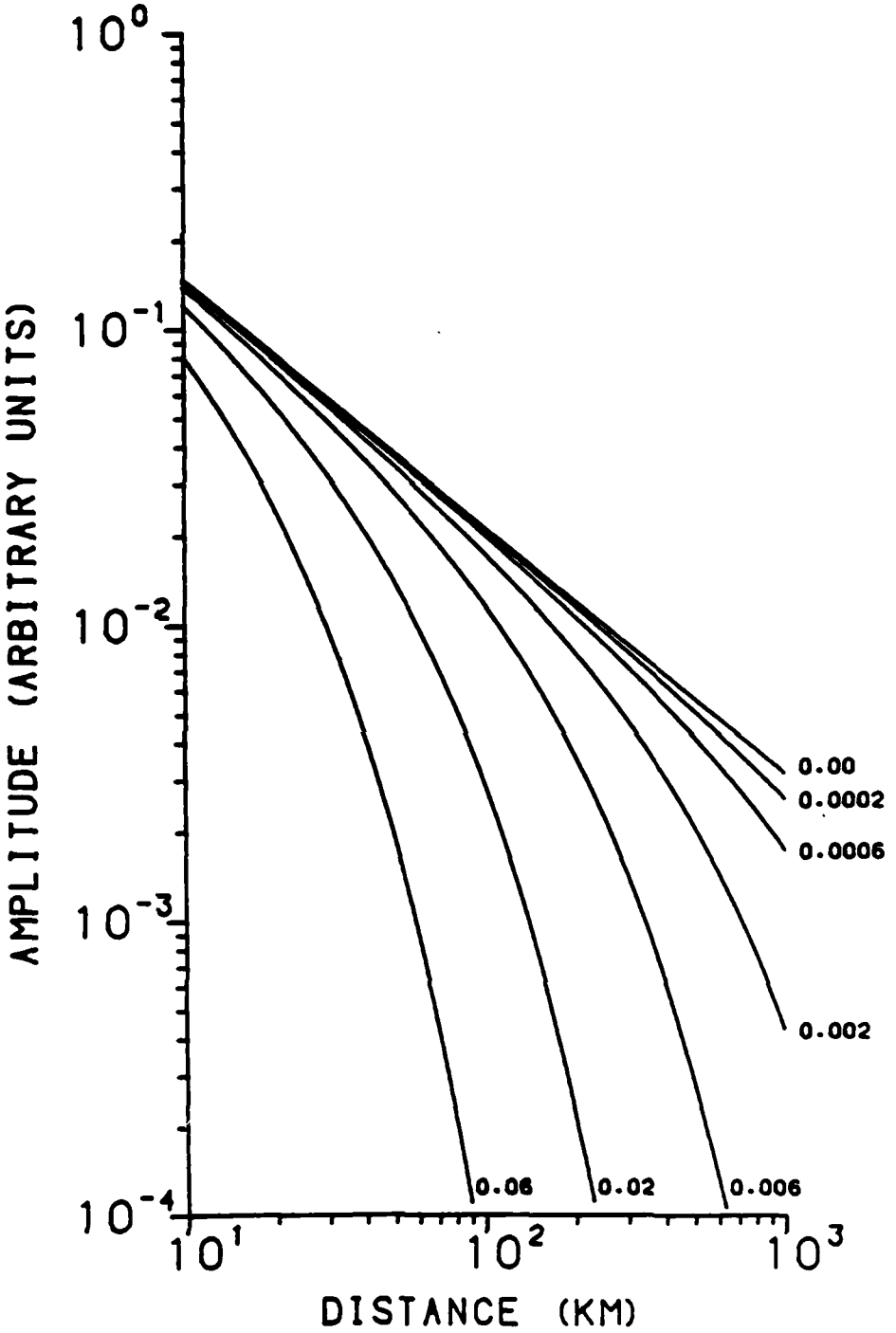
AMPLITUDE (ARBITRARY UNITS)
10^0
10^{-1}
10^{-2}
10^{-3}
10^{-4}
10^1
10^2
10^3
DISTANCE (KM)
0.00
0.0002
0.0006
0.002
0.06
0.02
0.006

#4

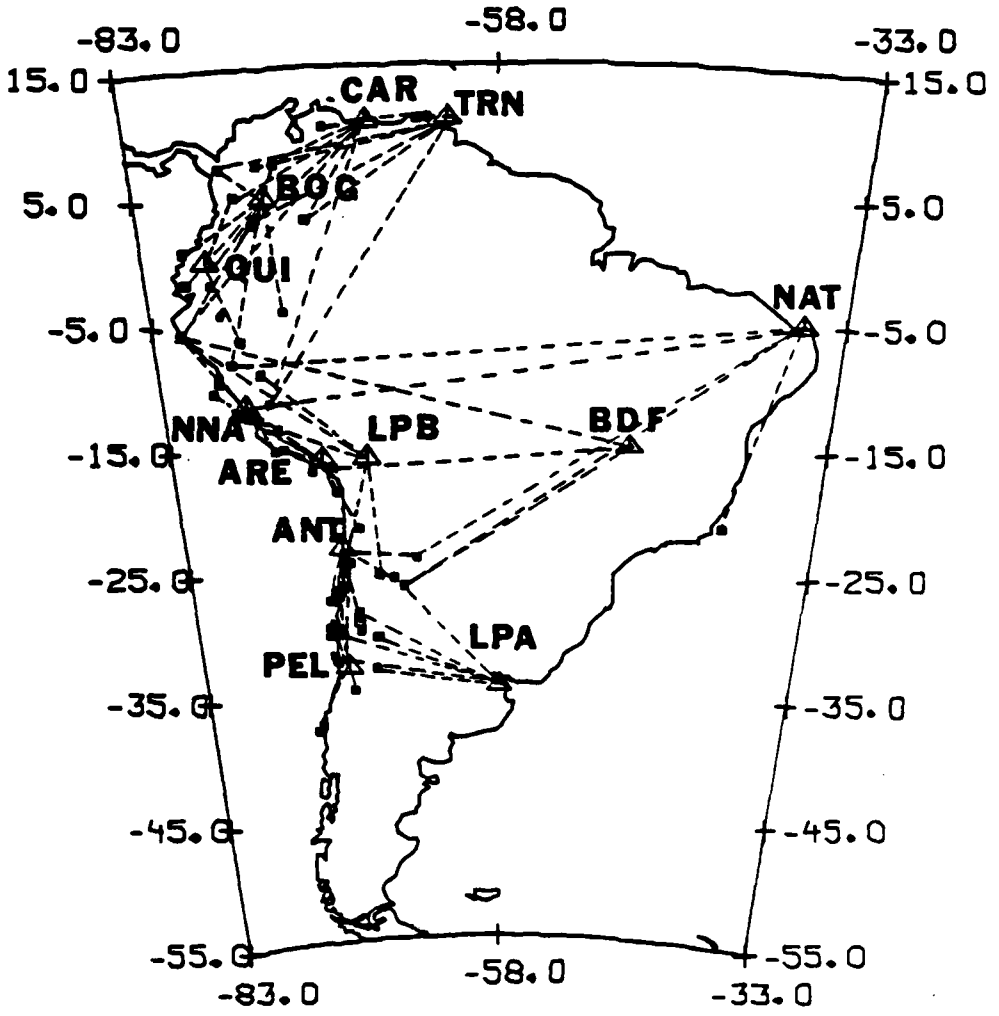
-83.0
-58.0
-33.0
15.0
5.0
-5.0
-15.0
-25.0
-35.0
-45.0
-55.0
CAR
TRN
BOG
QUI
NAT
NNA
LPB
BDF
ARE
ANT
LPA
PEL

#5

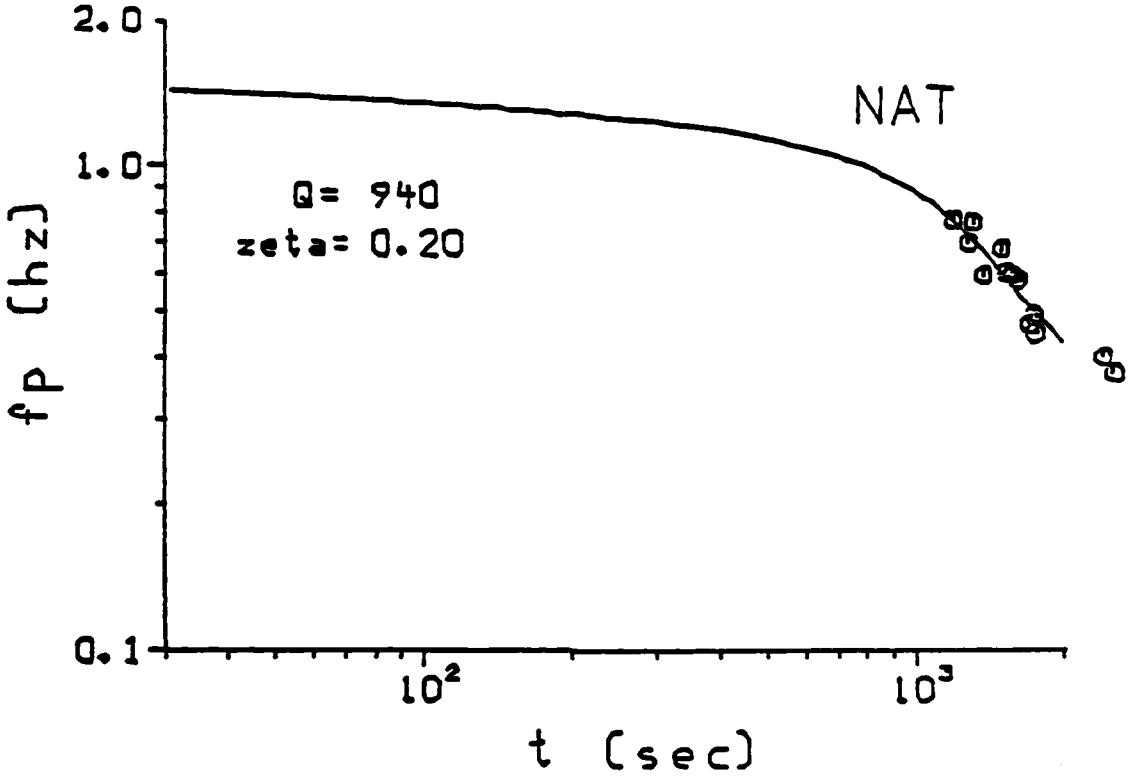
2.0
1.0
0.1
NAT
Q= 940
zeta= 0.20
fp (hz)
10²
10³
t (sec)

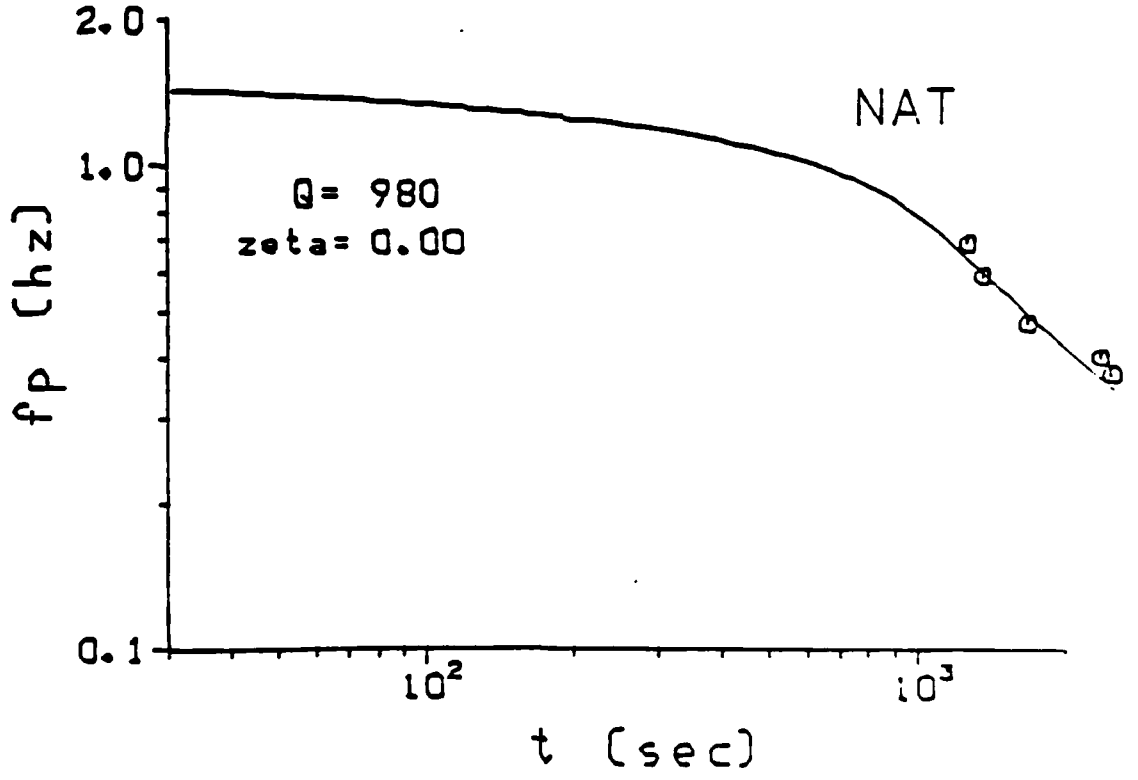
2.0
1.0
0.1
NAT
Q= 980
zeta= 0.00
fp (hz)
10²
10³
t (sec)

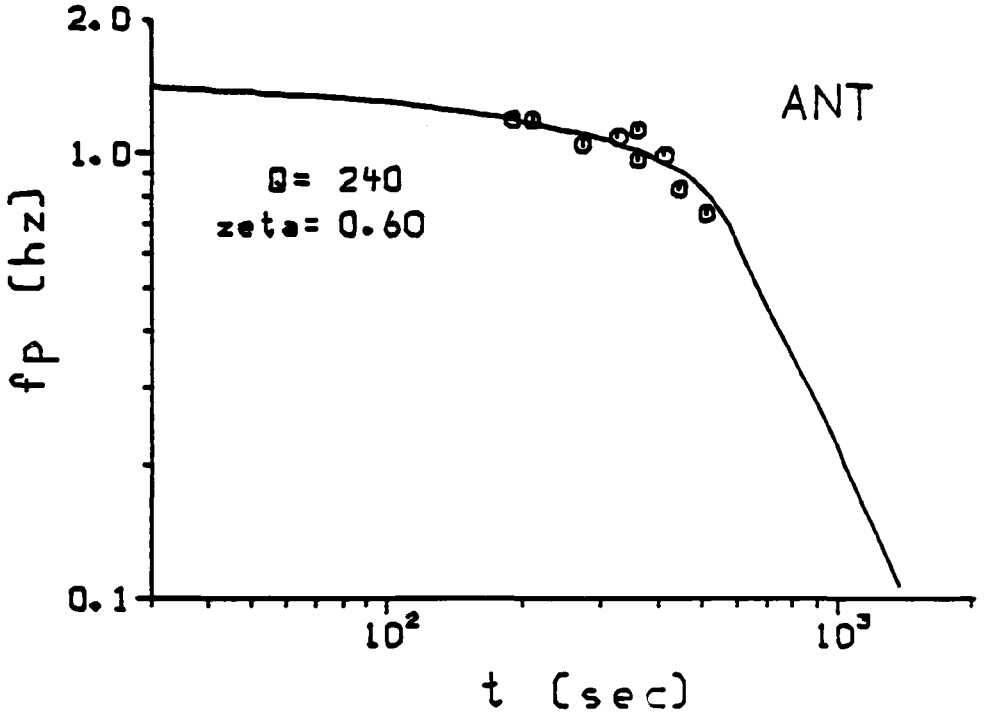
2.0
1.0
0.1
fp (hz)
ANT
Q= 240
zeta= 0.60
10^2
10^3
t (sec)

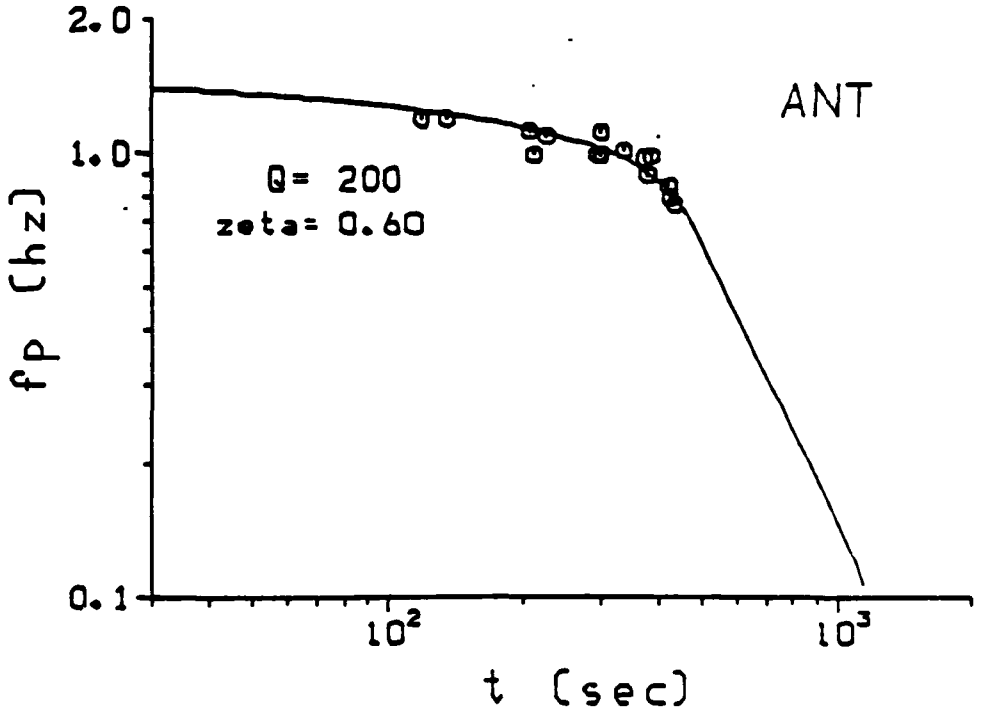
2.0
1.0
0.1
fp (hz)
ANT
Q= 200
zeta= 0.60
10^2
10^3
t (sec)

#7

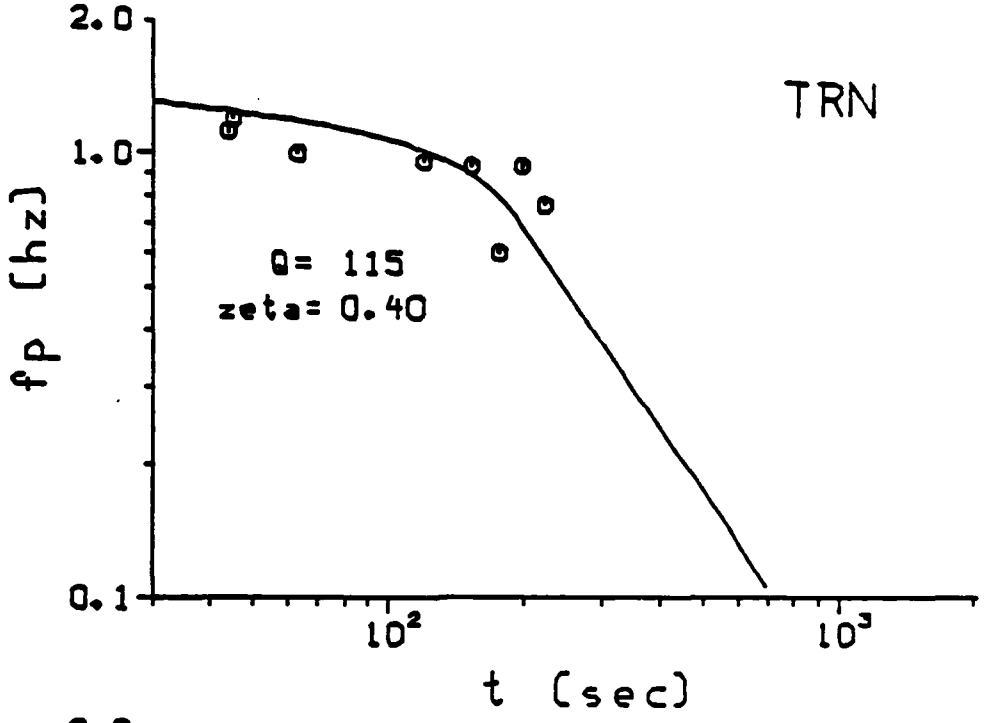
2.0
1.0
0.1
fp (hz)
TRN
Q= 115
zeta= 0.40
10²
10³
t (sec)

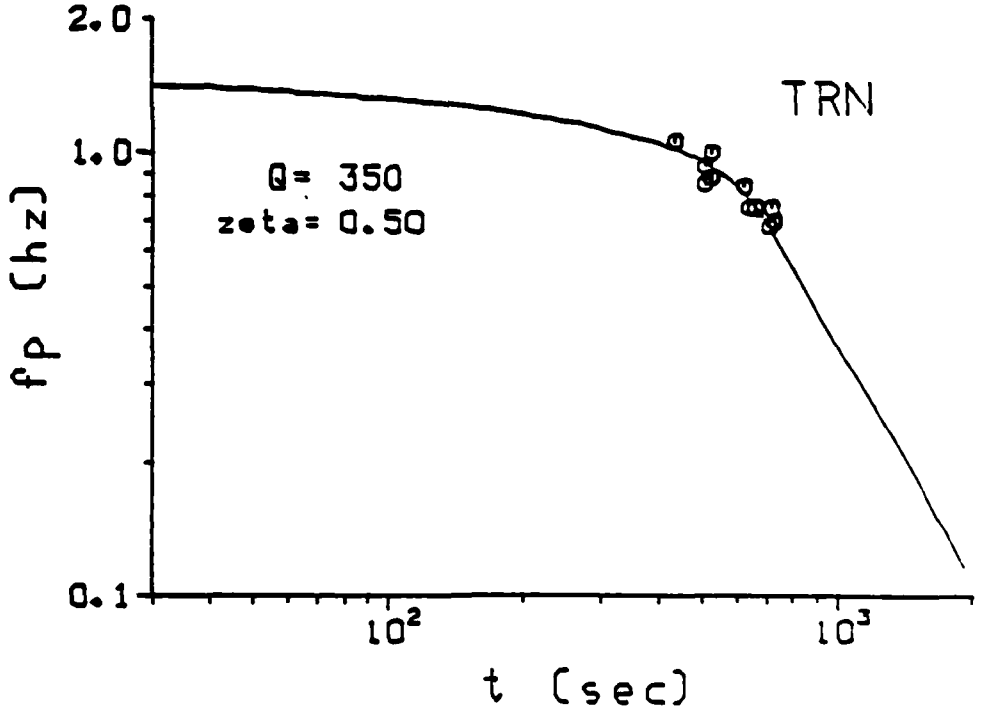
2.0
1.0
0.1
fp (hz)
TRN
Q= 350
zeta= 0.50
10²
10³
t (sec)

#8

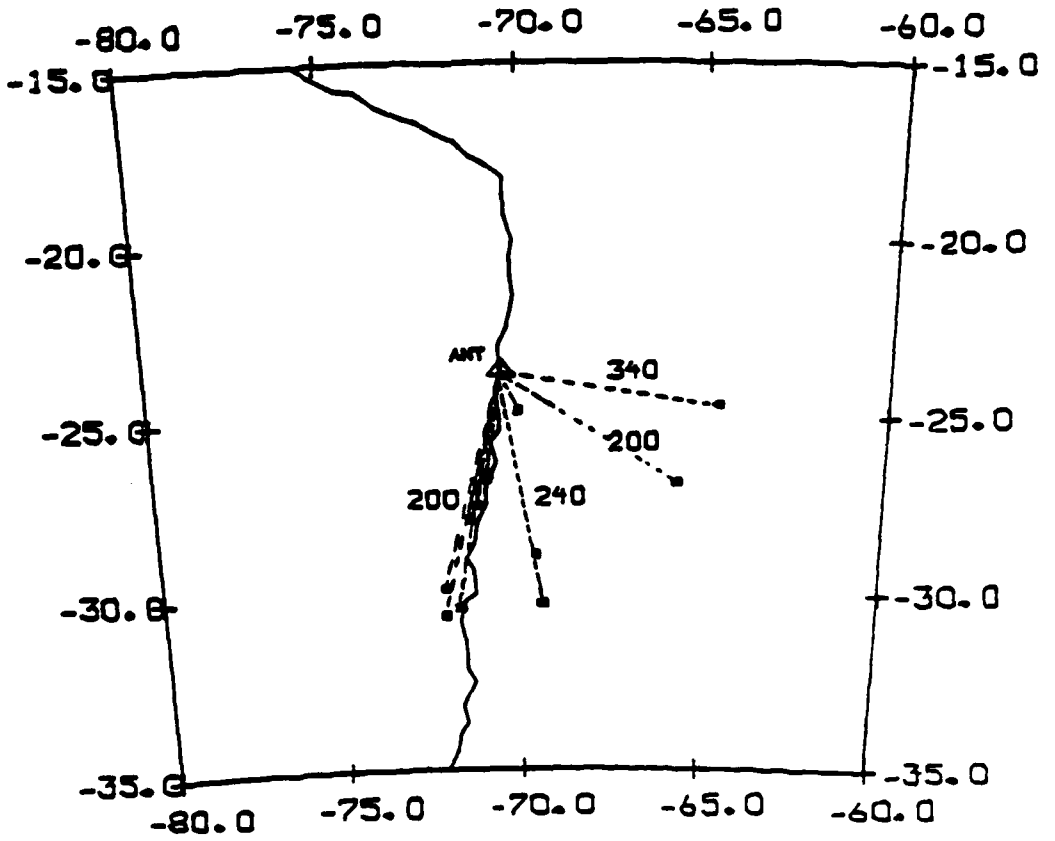

#9

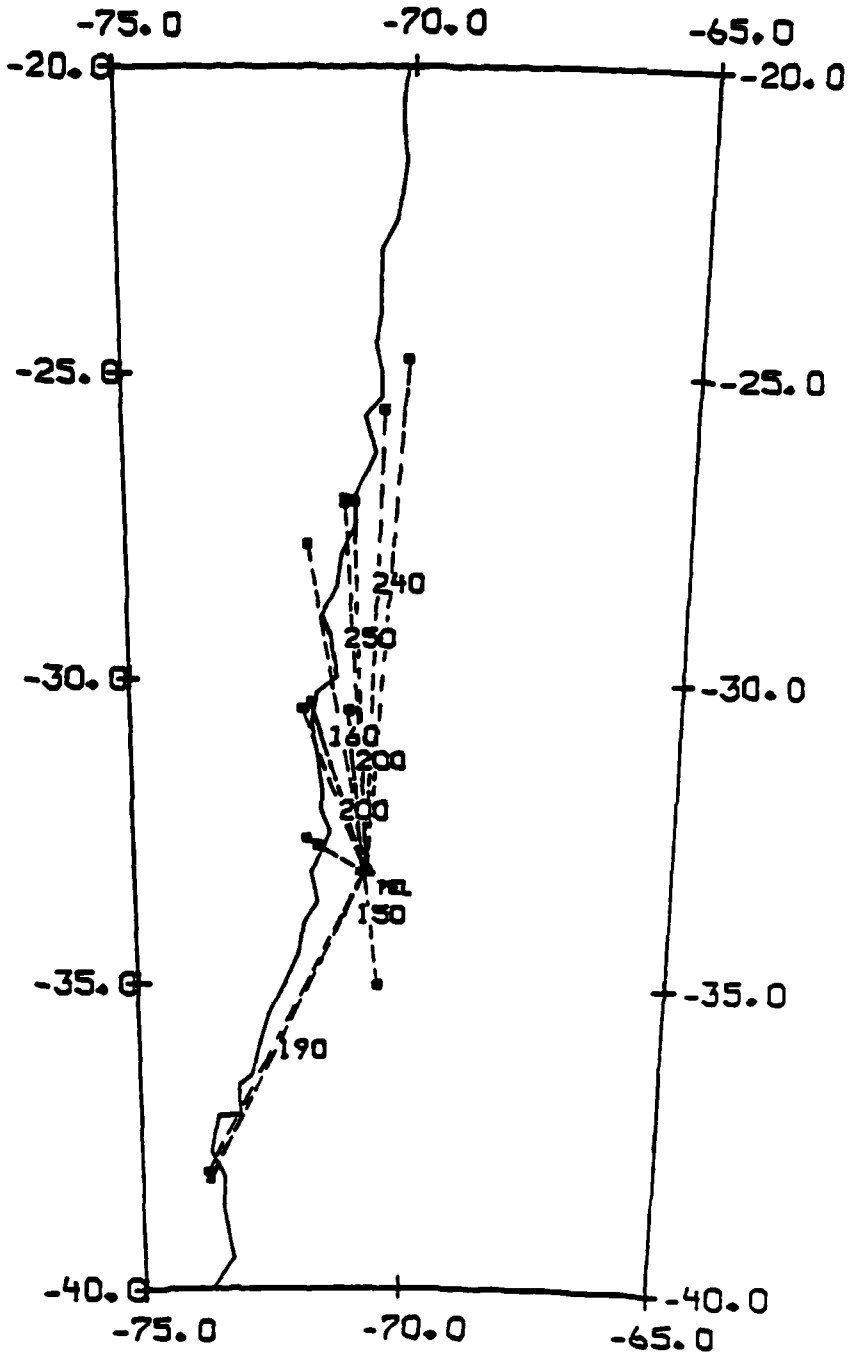
-75.0
-70.0
-65.0
-20.0
-20.0
-25.0
-25.0
-30.0
-30.0
-35.0
-35.0
-40.0
-40.0
-75.0
-70.0
-65.0
240
250
160
200
200
150
190

#10

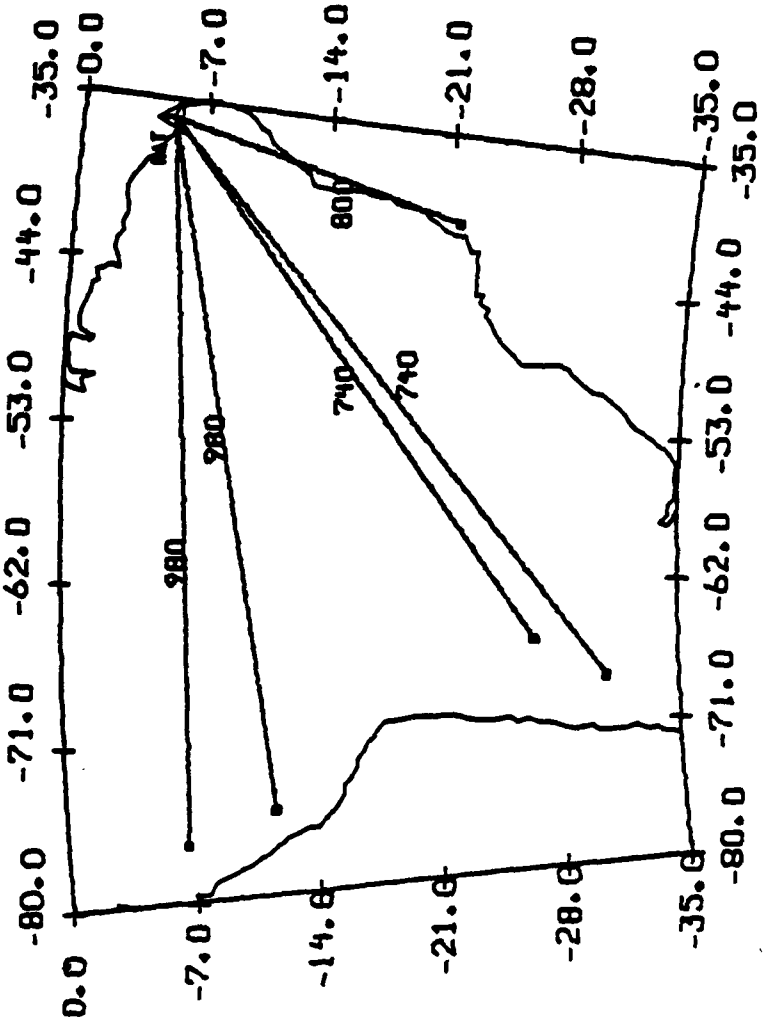

#11

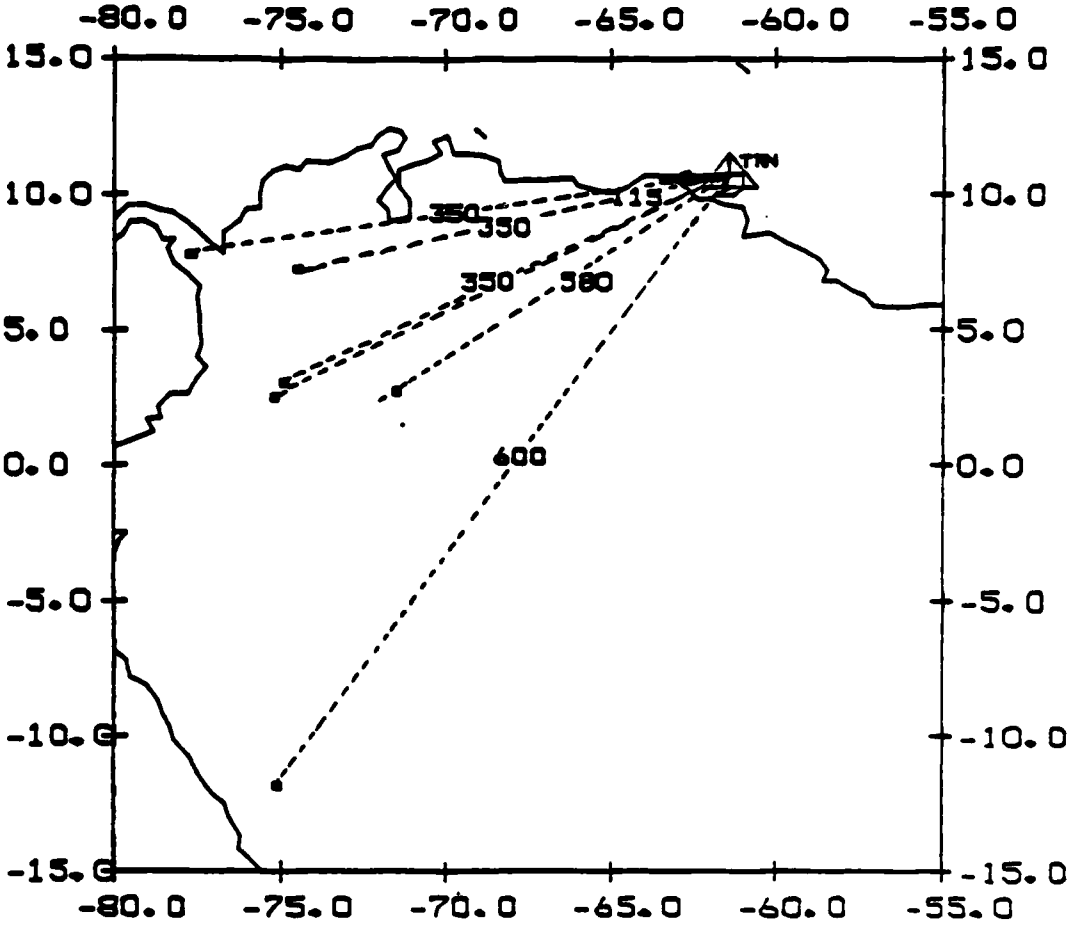
-80.0
-75.0
-70.0
-65.0
-60.0
-55.0
15.0
10.0
5.0
0.0
-5.0
-10.0
-15.0
TRN
350
350
350
350
600

#12

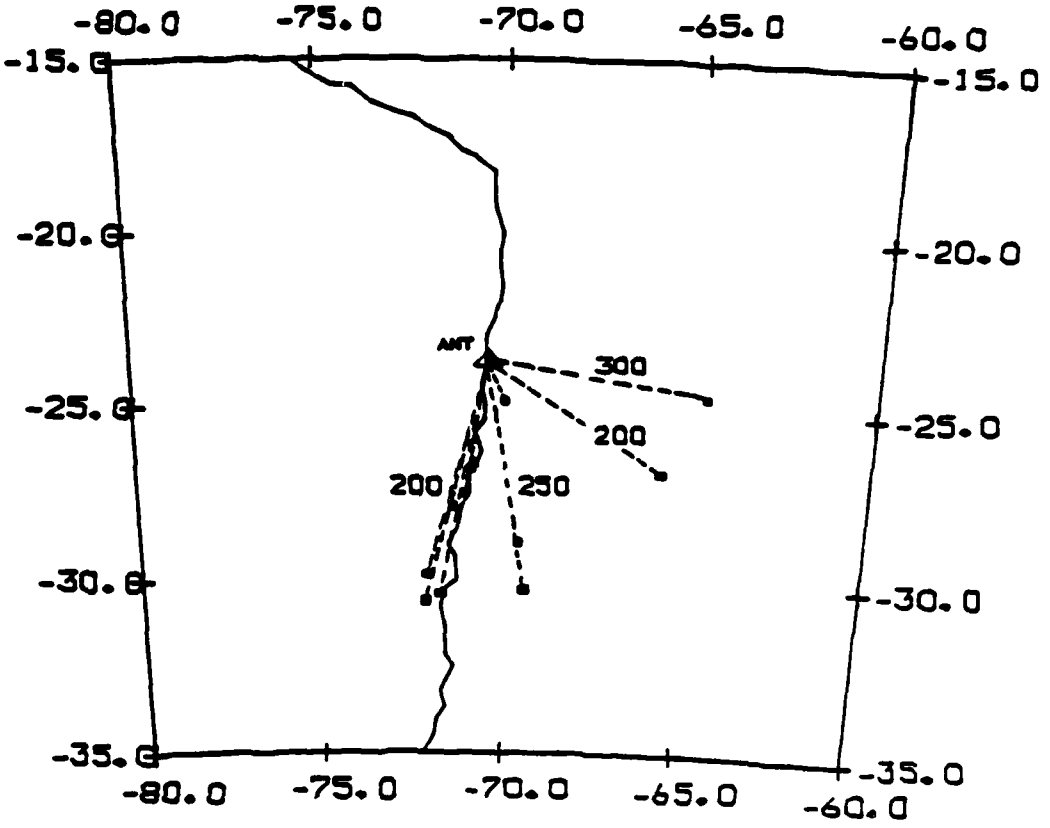

#13

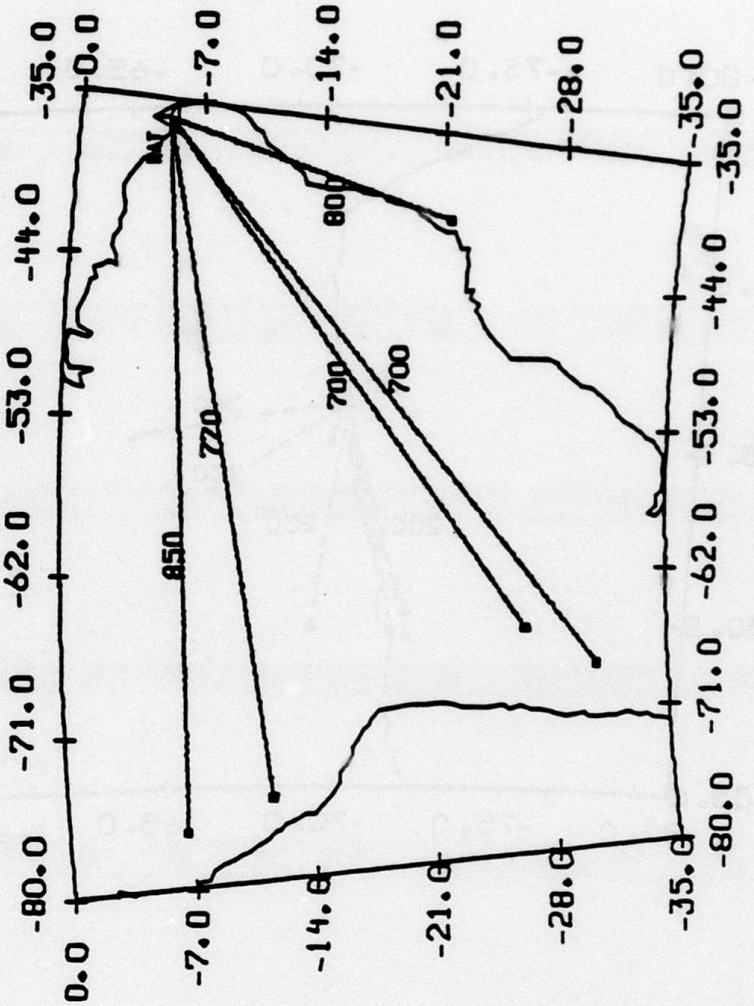

#14

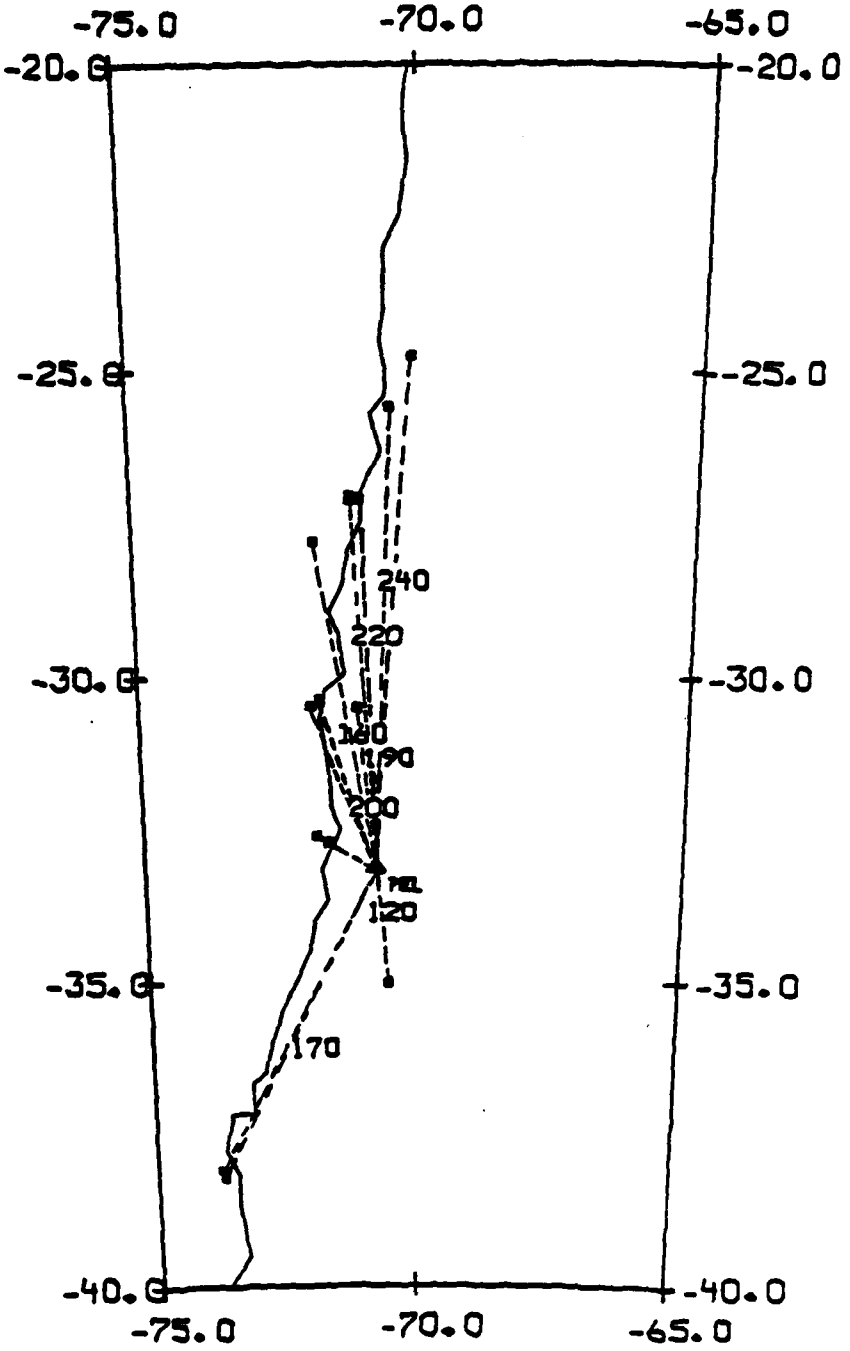
-75.0
-70.0
-65.0
-20.0
-20.0
-25.0
-25.0
-30.0
-30.0
-35.0
-35.0
-40.0
-40.0
-75.0
-70.0
-65.0
240
220
160
190
200
mm
120
170

#15

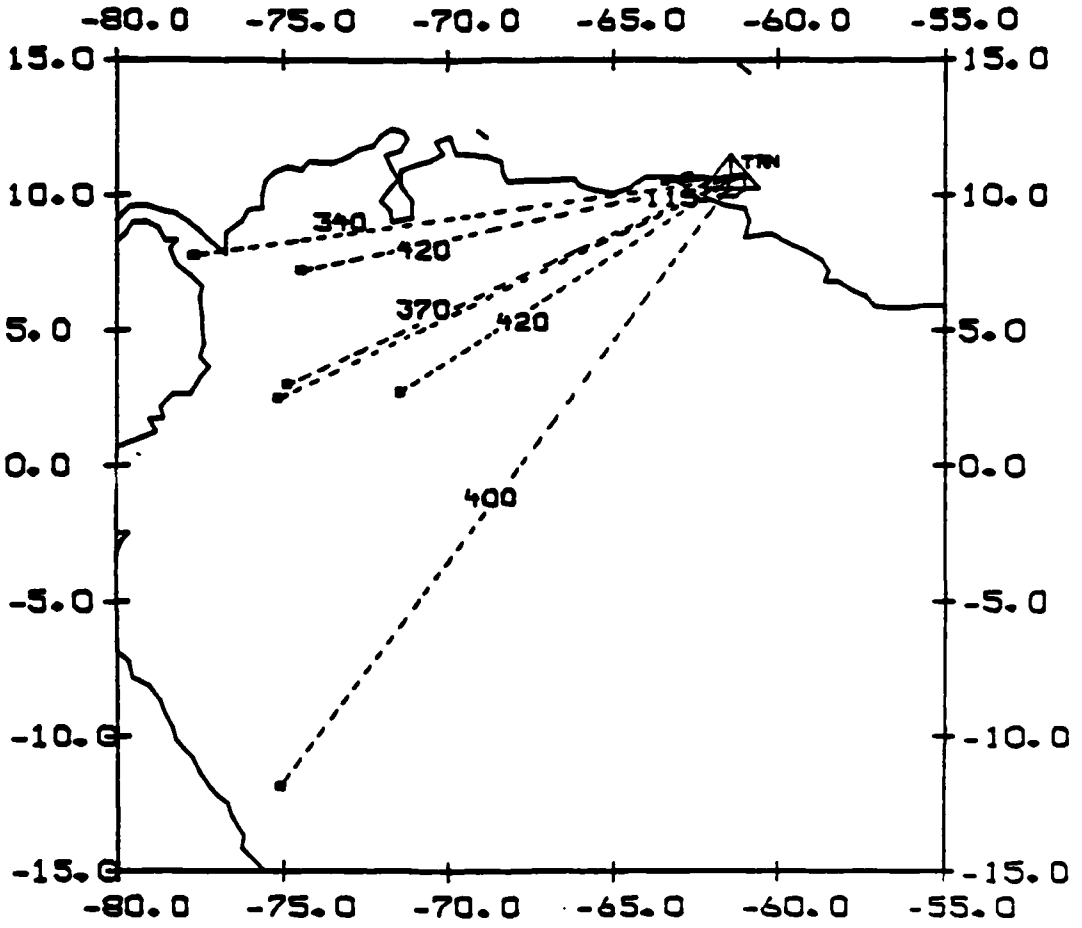
-80.0
-75.0
-70.0
-65.0
-60.0
-55.0
15.0
10.0
5.0
0.0
-5.0
-10.0
-15.0
TTN
340
420
370
420
400

#16

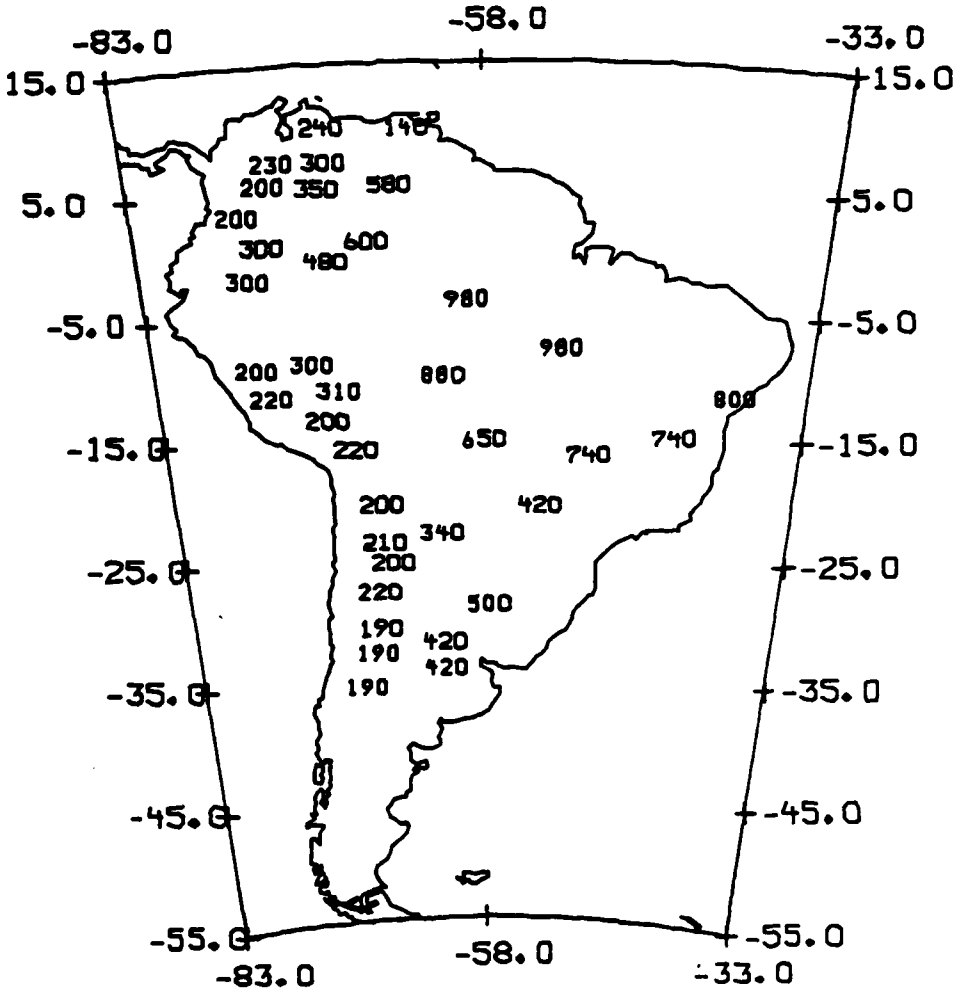
-83.0
-58.0
-33.0
15.0
5.0
-5.0
-15.0
-25.0
-35.0
-45.0
-55.0
240
230 300
200 350
580
200
300
600
480
300
980
980
200 300
880
220 310
200
220
650
740
740
200
420
210 340
200
220
500
190
420
190
420
190

#17

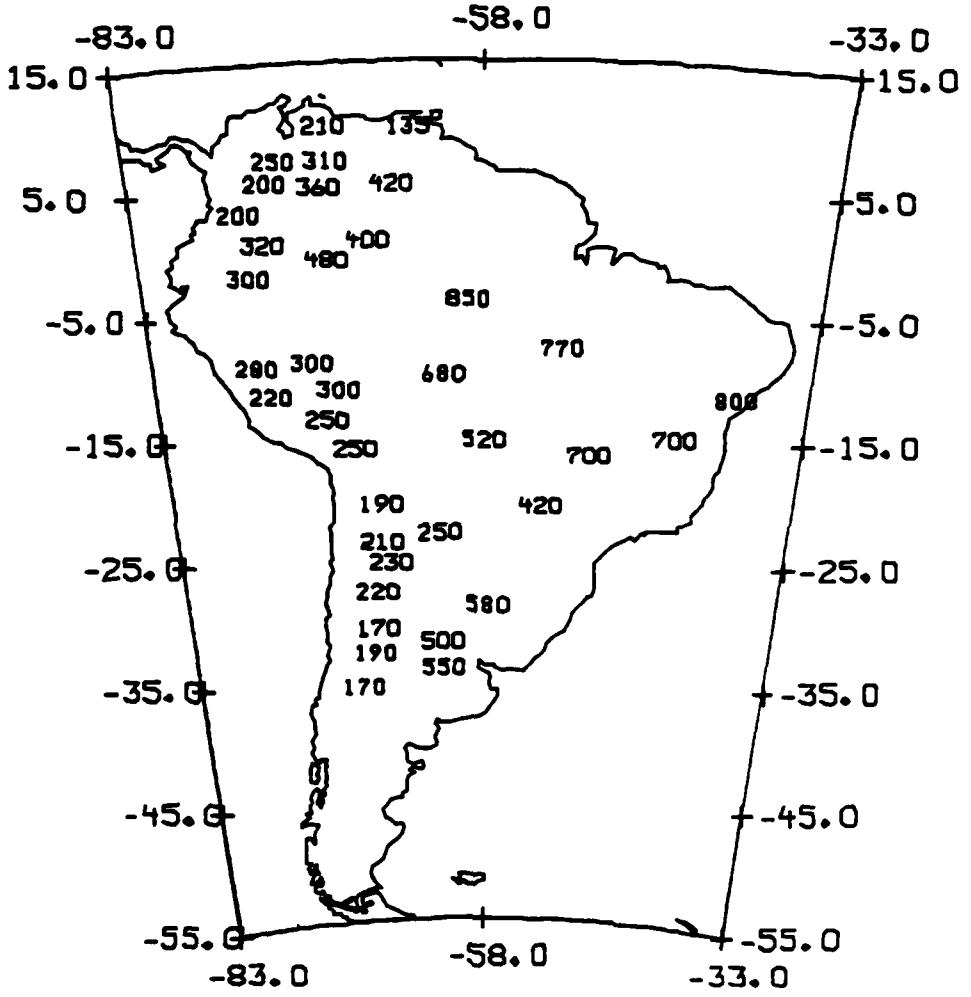
-83.0
-58.0
-33.0
15.0
5.0
-5.0
-15.0
-25.0
-35.0
-45.0
-55.0
210
135
250 310
200 360
420
200
320
400
480
300
850
770
280 300
680
220
300
250
808
250
520
700
700
190
420
210
250
230
220
580
170
500
190
550
170

#18

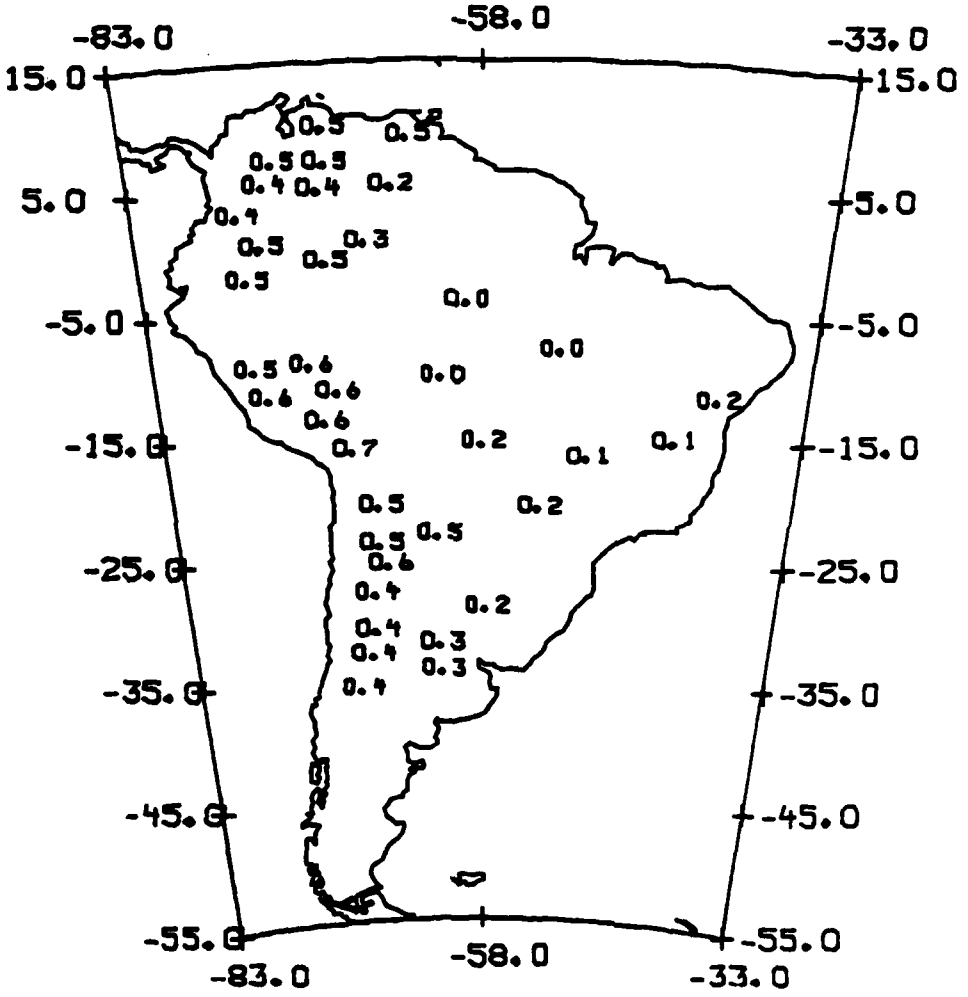

#19

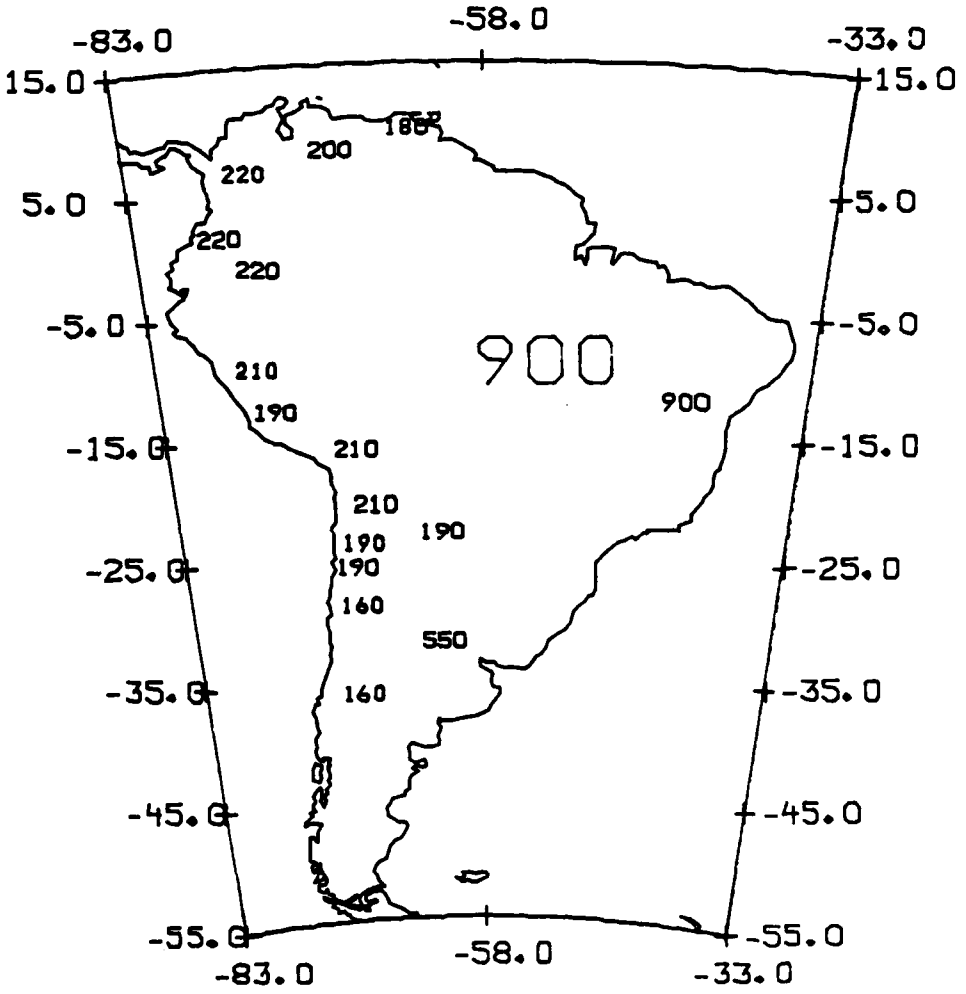
-83.0
-58.0
-33.0
15.0
5.0
-5.0
-15.0
-25.0
-35.0
-45.0
-55.0
900
900
200
220
220
220
210
190
210
210
190
190
190
160
160
550

#20

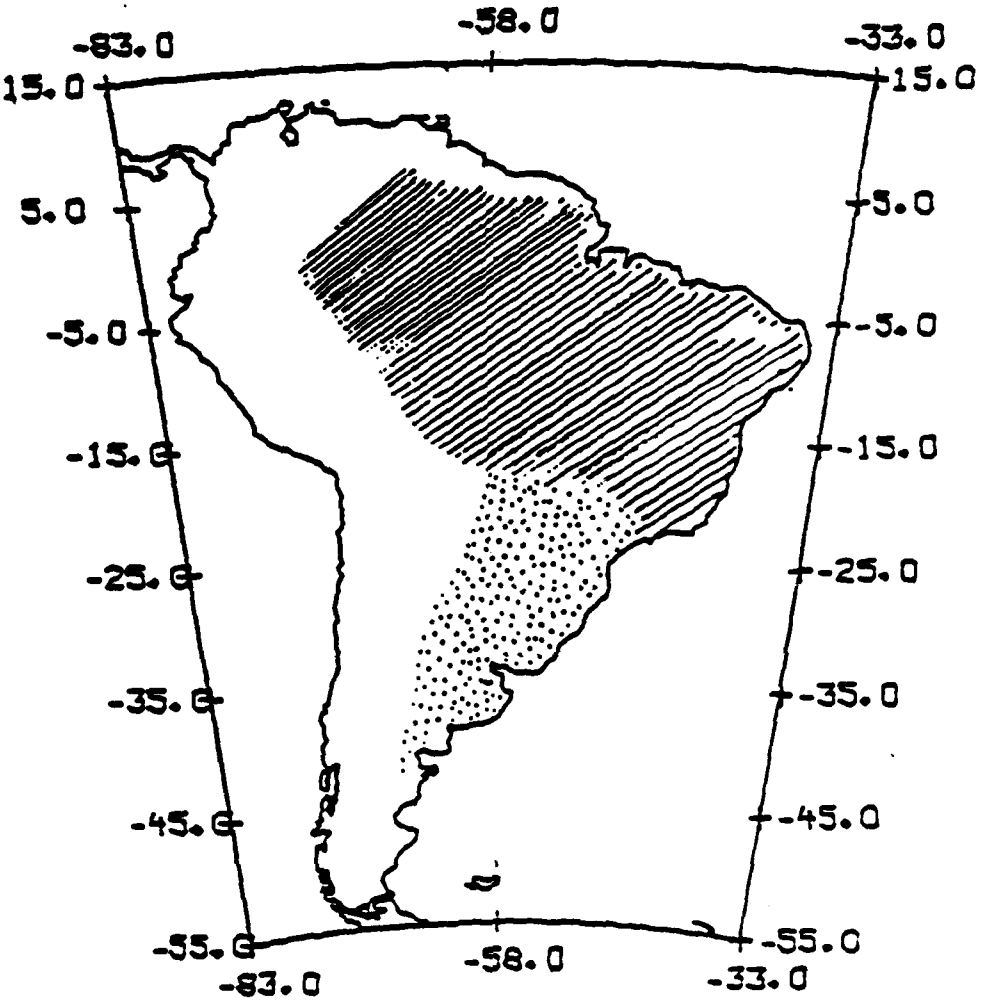

#21

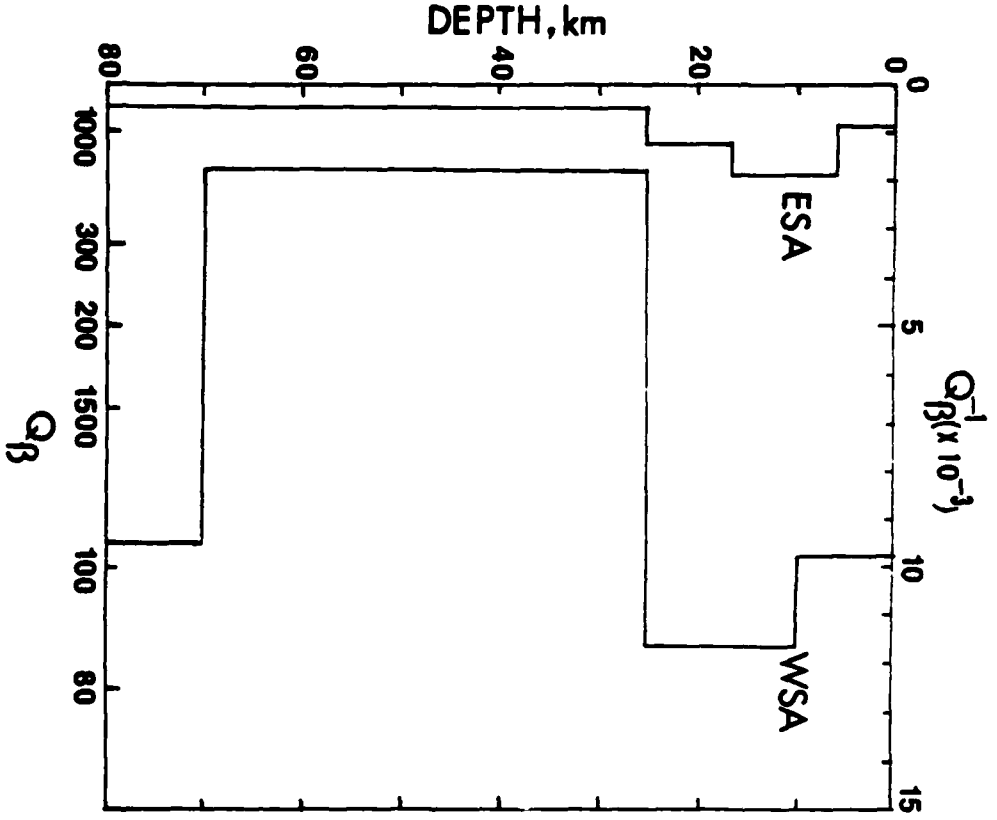
DEPTH, km
80
60
40
20
0
0
1000
300
200
1500
100
80
Q_β
ESA
WSA
5
10
15
Q_β^{-1} (x 10^{-3})

#22

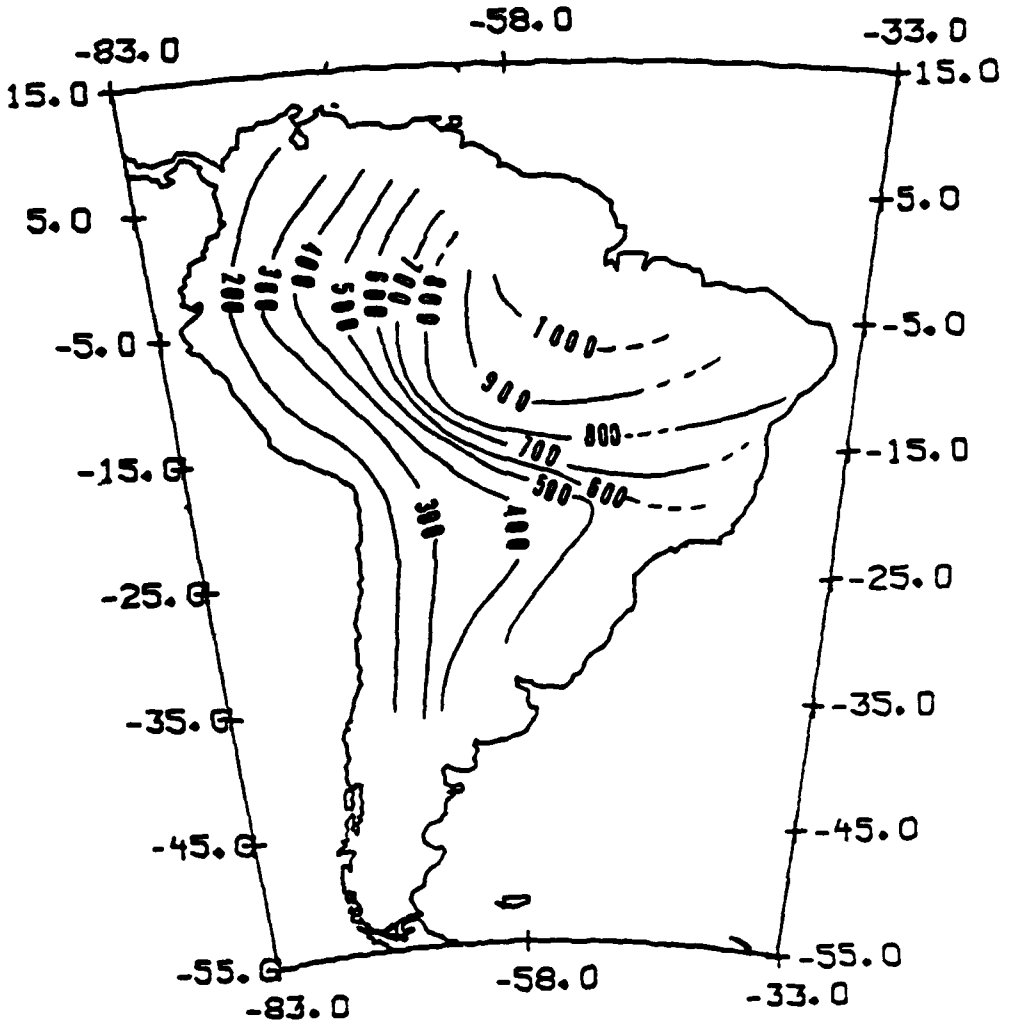
-83.0
-58.0
-33.0
15.0
5.0
-5.0
-15.0
-25.0
-35.0
-45.0
-55.0
1000
900
800
700
600
500

#23


90
75
60
45
10
0
10
20
30
40
50
SOUTH
AMERICAN
PLATE
NAZCA
PLATE
LEGEND
SHIELD
PHANEROZOIC
MESOZOIC-CENOZOIC

#24

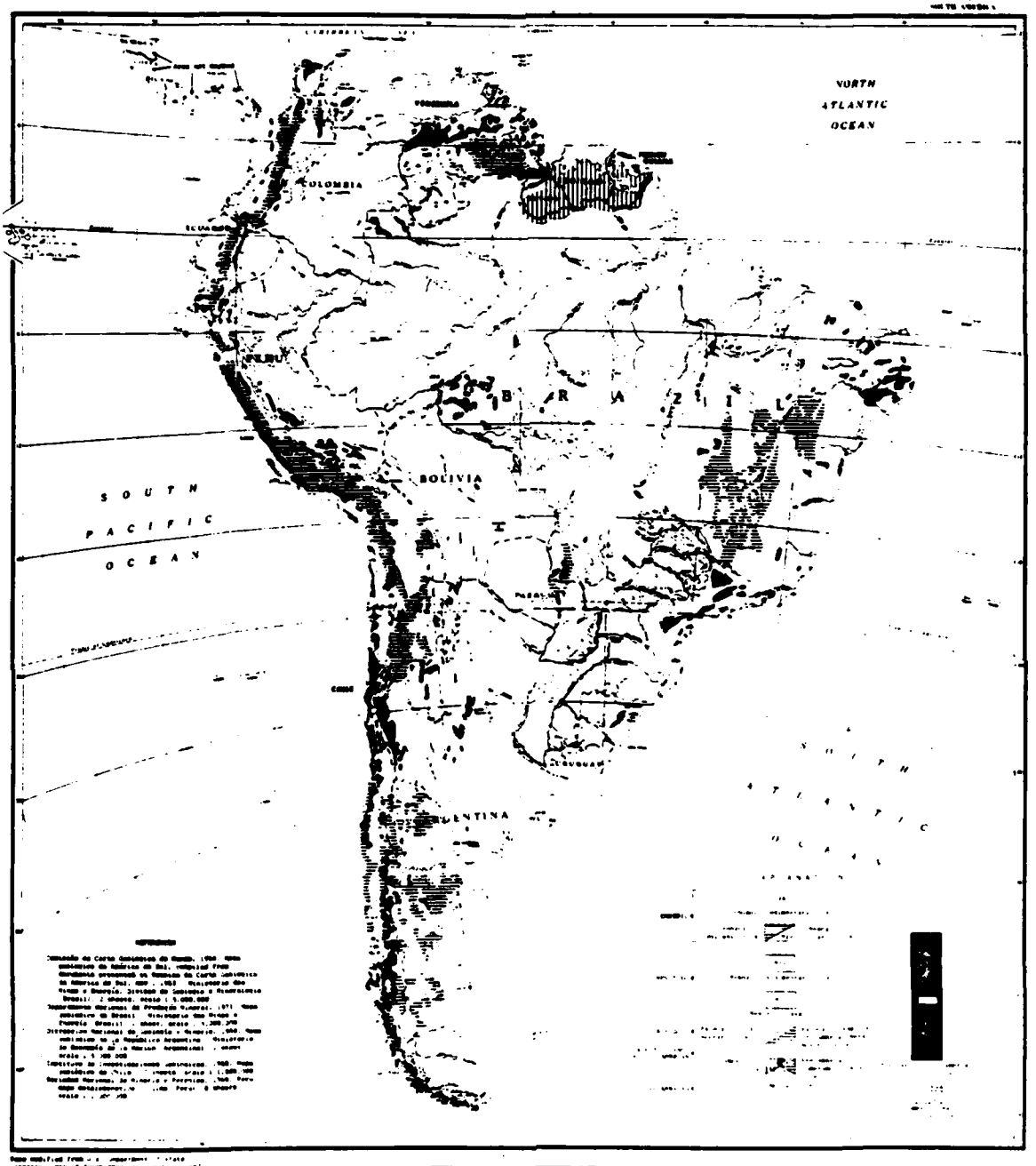

GEOLOGIC MAP OF SOUTH AMERICA

Compiled by

Geo R. Goudarzi

1972

#25

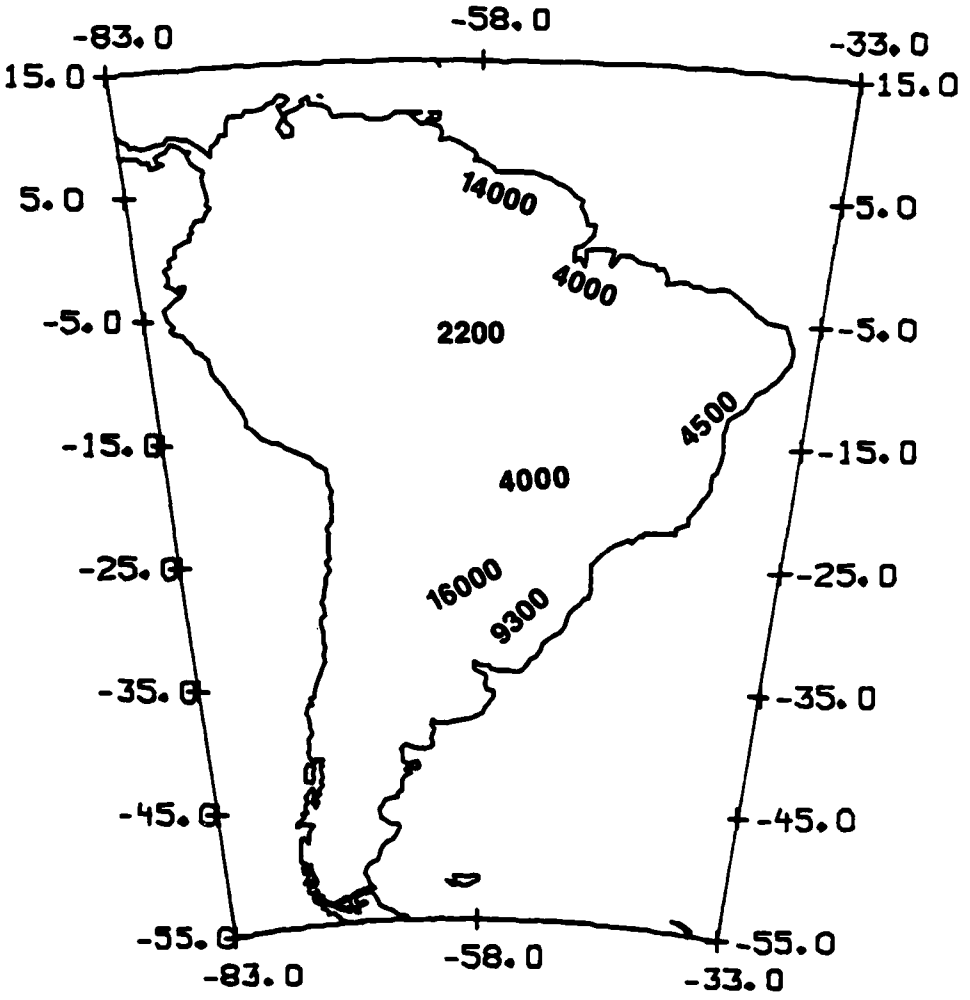
-83.0
-58.0
-33.0
15.0
5.0
-5.0
-15.0
-25.0
-35.0
-45.0
-55.0
14000
4000
2200
4500
4000
16000
9300

#26

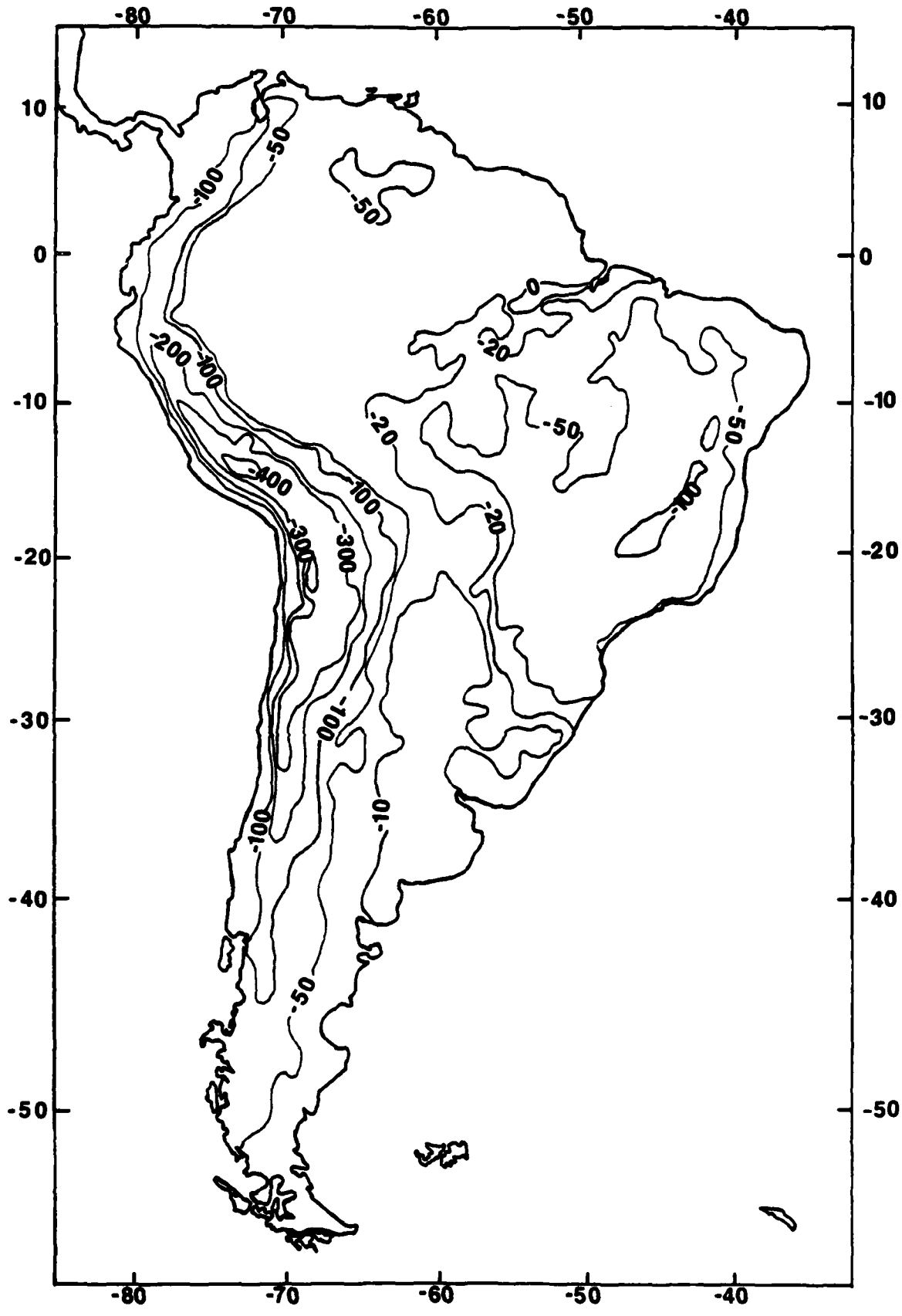
-80
-70
-60
-50
-40
10
0
-10
-20
-30
-40
-50
-50
-100
-50
0
-20
-200
-400
-20
-50
-50
-400
-100
-300
-300
-20
-100
-100
-10
-50

#27

Effect of Crustal Velocity Structure and Crustal Q Values on the Amplitudes and Wave Forms of Lg

by

B.J. Mitchell and H.J. Hwang

Introduction

The amplitudes and wave forms of the phase Lg are influenced by several factors, including velocity and Q structure of both crustal and sedimentary rock. Variations in these factors with depth, as well as lateral complexities along the path of travel are expected to play a role in the wave forms recorded at seismic stations. Our work over the period of this contract has been concerned with studying those factors which can be addressed using plane-layered models of the crust. Thus our results either ignore the effect of lateral complexities or consider them to be approximately modelled by layered models over their paths of travel.

In order to minimize the effect of lateral complexities, we have used two approaches. First, we have, as far as possible, used relatively short paths which avoid major lateral boundaries, such as continental margins or major boundaries between tectonic provinces. Second, we have used the early portions of observed Lg wave forms in the data analysis portion of our study. Thus we have used waves which are more coherent, and presumably less scattered, than the later portions of the Lg coda.

In the eastern United States, velocity and Q models have been found

which adequately predict observed surface wave phase velocities, group velocities and attenuation at both intermediate and short periods. Models have also been found which satisfy similar data for other regions, such as the Basin-and-Range province, although in the case of Q, the models are less reliably determined. We have studied various factors which affect the attenuation of higher mode Rayleigh waves (or Lg) in various period ranges. We will first discuss the effect of the velocity model on amplitudes and attenuation in both the eastern United States and Basin-and-Range. Second, we will attempt to see whether or not the observed regional variation of 1-Hz Lg in both eastern and western United States can be explained simply by the variations in thicknesses of sediments there. Third, we will test two Q models of the Basin-and-Range province to see if the rapid attenuation known to occur there can be explained by low-Q sediments over a Q-model similar to that for the stable regions in the eastern United States, or if it requires low Q values in the deeper crust.

Effect of Velocity Structure on Attenuation and Yield

Four velocity models derived from data in the central and eastern United States were used to compute short-period Lg synthetics. These are a simplified version of a model by Mitchell and Herrmann (1979), as well as models developed by McEvilly (1964), Herrmann (1979), and Taylor (1980). These are shown in Table 1. The simplified eastern United States model in that table (Mitchell, 1982) is composed of six layers, and was used, rather than the multi-layer model of Mitchell and Herrmann (1979), in order to save computation time.

All of the velocity models were combined with a Q model in which

compressional wave Q (Q_α) is 2000 and shear wave Q (Q_β) is 1000 at all depths. Short-period synthetics for these models were calculated using programs of Wang (1980). Our results indicated that only those models which include a surface-layer of low-velocity sediments produce realistic looking seismograms. Those models without sediments, and comprised of thick crustal layers, contain spike-like arrivals which are not observed on real seismograms. Examples for two models appear in Figures 1a and 1b. The variations in velocity structure can produce somewhat different amplitudes at a given distance from the source and can lead to small differences in magnitude. and consequently in yield, for this case in which the source is located at a depth of 5 km.

Synthetics were next computed for a velocity model of the Basin-and-Range province (Bache et al., 1978) and these were compared with those computed for the simplified eastern United States model. These models appear in Figure 2. Identical Q models were used for both regions, Q_β being set at 300 through the upper 18 km of the crust and 1000 at greater depths. Q_α was assumed to be twice as large as Q_β at all depths.

Table 2 gives magnitude differences produced by differences in velocity structure between the simplified EUS and Basin-and-Range model for a source at a depth of 0.5 km. The source corresponds to an explosion in the low-velocity sediment layer of each model. Although the magnitude differences for 1-Hz Lg are as large as 0.3 at a distance of 750 km. they become less consequential at greater distances. Table 2 also lists differences in m_b derived from spectral amplitudes of larger period values. At periods of 8 and 10 s, these differences are very

small, although they are larger at short periods.

Effect of Sediments on Q_{Lg} in the Eastern United States

Q values obtained from Lg amplitudes (Espinosa, 1981) and from the dispersion of the Lg coda (Singh and Herrmann, 1983) exhibit a similar regional variation across the United States. The map of Singh and Herrmann shows the highest Q values in the north and central United States, with gradual decreases extending both eastward and westward from there into the mid-Atlantic states and Great Plains. More rapid decreases occur along the Atlantic and Gulf coasts.

The distribution of sediments everywhere east of the Rocky Mountains (e.g. Sloss et al., 1960), especially that of young sandstones and shales, bears a resemblance to the areal distribution of the Q values from Lg coda waves.

In an attempt to see if the regional variation of Q for Lg waves could be explained simply by the effect of sediment distribution, an attempt was made to model those regions, using the crustal Q model of Mitchell (1980) overlain by various thicknesses of sediments, depending upon geographic region. It was assumed that crustal Q was frequency-dependent whereas the Q values of the sediments were not. It was also assumed that Q values of limestones and dolomites were similar to those of crustal rock and that in the low-Q sediments, sandstone and shales, Q_α is equal to Q_β.

Figure 3 (from Sloss et al., 1960) illustrates the distribution of sediments in the United States for the Cretaceous period. Shales and sandstones for that period thicken to the west and along the east and

Gulf coasts as compared with the north-central United States. Sediments from other periods exhibit other patterns. Combining these thicknesses with sediments of various other periods, we constructed models corresponding to regions in western Pennsylvania, Nebraska, and southern Louisiana. Values of Q were assigned to those sediments using the Q versus pressure curve of Winkler and Nur (1979) for partially saturated sandstone. Table 3 presents simplified Q models of sediments for the various regions. These were combined with the frequency-dependent Q models of Mitchell (1980) for the eastern United States. Table 4 compares Q values for Lg computed for those models, as well as for a model of the high-Q region in the central United States, and compares them with values observed by Singh and Herrmann (1983).

Our results indicate that it is very easy to obtain Q values for Lg waves which are as low or lower than those which have been observed, simply by using realistic Q values for sediments. In fact, our first results yielded Q values for Lg which were too low in all cases. These Q differences produced by regional variations of low-Q sediments can produce very large differences in m_b. Table 5 shows that these can be as large as 0.7 in severe cases.

These results suggest that Lg Q in stable regions can be estimated if we have a knowledge of near-surface geology.

Effect of Sediments on Q_{Lg} in the Western United States

Results of computations in the previous section indicate that the rather large regional variation of Q observed in the eastern and central

United States can be explained as being due in large part to variations in the thickness of surficial sediments. Variations of Lg Q values also occur in the western United States, although to a smaller extent. It will be important to know whether or not those variations are also produced by varying accumulations of sediment.

We first found a crustal model which produced Lg wave forms which are similar to those observed for paths across the Basin-and-Range province. The model found to be most satisfactory included a low-Q upper crust ($Q_\alpha = Q_\beta = 150$) and a higher-Q lower crust ($Q_\alpha = Q_\beta = 500$). This Q model was combined with the velocity model of Chen and Mitchell (1984) for that region. The Lg synthetic seismograms produced by that model are shown in Figure 4 for 4 distances.

Varying thicknesses of sediments (1, 2, and 4 km) were placed above that model as shown in Table 6 to see how that variation might affect Lg Q values. As in the previous section, Lg Q values were taken to increase with pressure in accordance with laboratory measurements.

Theoretically expected Q values for Lg are shown beneath each model. The maximum range is between 190 and 230. These results indicate that, in contrast to stable high-Q regions, such as the eastern United States, Lg Q values for regions with low-crustal Q values are not greatly affected by varying thickness of sediment, if losses due to scattering are ignored.

Q Structure in the Basin-and-Range Province

Mitchell (1975), in inverting intermediate-period attenuation data for the western United States, found that Q_β values in the upper crust

in the western United States were much lower than those in the eastern United States. Cheng and Mitchell (1981), using a new multi-mode method and paths nearly totally confined to the Basin-and-Range province found very low Q_β values (approximately 85) in the upper crust. Later work has, however, suggested that it may be possible to explain the fall-off of amplitudes at intermediate periods by thick layers of low-Q sediment overlying high-Q crust.

Two types of models were tested using both long-period and short-period seismograms. Long-period seismograms computed for the Bache et al. (1978) velocity model and the two Q models are nearly identical in form, so single station data at long periods cannot be used to distinguish between the two models.

The fall-off of 1-Hz Lg amplitudes was then determined from short-period synthetic seismograms predicted by the two models. The Q values for Lg in these cases are 550 for the model with the high-Q crust and low-Q sediments and 290 for the model with the low-Q crust. Thus it appears that the low Q values of Lg in the Basin-and-Range province cannot be due to low-Q sediments, but reflect low Q values in the upper crust. Moreover, a model in which Q_β varies with frequency is not required to explain both intermediate- and short-period data.

References

Bache. T.C., W.L. Rodi, and D.G. Harkrider, Crustal structure inferred from Rayleigh wave signatures of NTS explosions, Bull. Seism. Soc. Am., 68, 1399-1413. 1978.

Chan, J.J., and B.J. Mitchell, Shear velocity and Q_β structure beneath the western United States from fundamental- and higher-mode surface wave observations (Abstract), EOS, Trans. Am. Geophys. Union, 65, 244, 1984.

Cheng, C.C., and B.J. Mitchell. Crustal Q structure in the United States from Multi-mode Surface Waves, Bull. Seism. Soc. Am., 71. 161-181. 1981.

Espinosa. A.F., Seismic wave attenuation studies in conterminous United States, in Summaries of Technical Reports, Vol. XII. U.S. Geol. Survey Open-File Report 81-833, Menlo Park, CA, 1981.

Herrmann. R.B., SH-wave generation by dislocation sources - a numerical study. Bull. Seism. Soc. Am., 69, 1-15, 1979.

McEvilly. T.C., Central U.S. crust-upper mantle structure from Love and Rayleigh wave phase velocity inversion, Bull. Seism. Soc. Am., 54. 1997-2015, 1964.

Mitchell. B.J., Regional Rayleigh wave attenuation in North America, J. Geophys. Res., 81. 4904-4916. 1975.

Mitchell. B.J., Frequency dependence of shear wave internal friction in the continental crust of eastern North America. J. Geophys. Res., 85, 5212-5218, 1980.

Mitchell, B.J., Observations and synthesis of short-period Lg waves in the eastern United States, in Semi-Annual Technical Report No. 8, of Saint Louis University to DARPA/AFOSR, 1 April 1982 - 30 September 1982, 3-36. 1982.

Mitchell, B.J., and R.B. Herrmann, Shear velocity structure in the eastern United States from the inversion of surface waave group and phase velocities, Bull. Seism. Soc. Am., 69, 1133-1148, 1979.

Singh. S., and R.B. Herrmann. Regionalization of crustal coda Q in the continental United States. J. Geophys. Res., 88,. 527-538, 1983.

Sloss. L.L., E.C. Dapples, and W.C. Krumbein, Lithofacies Maps. An Atlas of the United States and Southern Canada, Wiley, 108 pp, 1960.

Taylor. S.R., Crust and Upper Mantle Structure of the Northeastern United States, Ph.D. Dissertation. Massachusetts Institute of Technology, 288 pp, 1980.

Winkler. K., and A. Nur. Pore Fluids and Seismic Attenuation in Rocks, Geophys. Res. Lett., 6, 1-4, 1979.

Table 1

Eastern and Central United States Velocity Models

Simplified EUS Model

h	α	β	ρ
0.25	2.42	1.30	2.30
0.75	4.91	2.71	2.67
6.00	6.19	3.47	2.75
18.00	6.38	3.67	2.90
18.00	7.17	3.98	3.00
---	8.10	4.58	3.30

McEvilly (1964)

h	α	β	ρ
11.00	6.10	3.50	2.70
9.00	6.40	3.68	2.90
18.00	6.70	3.67	2.90
24.00	8.15	4.67	3.30
40.00	8.20	4.47	3.30
180.00	8.20	4.45	3.30
---	8.70	4.80	3.60

Herrmann (1979a)

h	α	β	ρ
1.0	5.00	2.89	2.50
9.0	6.10	3.52	2.70
10.0	6.40	3.70	2.90
20.0	6.70	3.87	3.00
---	8.15	4.70	3.40

Taylor

h	α	β	ρ
15.0	6.00	3.50	2.70
10.0	6.60	3.80	2.80
10.0	6.80	3.80	2.85
40.0	8.10	4.50	3.30
---	8.20	4.70	3.30

Table 2

Magnitude Differences

EUS and B & R Velocity Models

Source depth = 0.5 km

Δm_{bLg}

Distance	SP	LP			
		4 s	6 s	8 s	10 s
500 km	0.16	0.24	0.26	0.02	0.07
750	0.31	0.26	0.23	0.07	0.06
1000	0.22	0.22	0.29	0.07	0.06
1250	0.13	0.27	0.29	0.03	0.03
1500	0.07	0.31	0.23	0.02	0.06

Table 3

Sediment Q Models

Pennsylvania		Nebraska		Louisiana	
h	$Q_\beta (= Q_\alpha)$	h	$Q_\beta (= Q_\alpha)$	h	$Q_\beta (= Q_\alpha)$
100 m	30	100 m	30	100 m	30
200	50	200	50	200	50
300	75	300	75	300	75
		400	100	3900	100

Table 4

Lg Q Values for Four Regions

	Central U.S.	Pennsylvania	Nebraska	Louisiana
Computed	1190	710	680	570
Singh and Herrmann (1983)	1000-1300	≈1000	≈850	400-600

Table 5

Effect of Sediment Q Values on m_{bLg}

m_{bLg} Differences Compared to Simplified EUS Model

Distance	Pennsylvania	Nebraska	Louisiana
500 km	-0.21	-0.03	-0.33
750	-0.05	-0.09	-0.58
1000	-0.05	-0.27	-0.70
1250	-0.02	-0.29	-0.69
1500	-0.06	-0.24	-0.72

Table 6

W.U.S. Q Models and Lg Attenuation
for Varying Thickness of Sediments

1 km of sediments			2 km of sediments			4 km of sediments		
h,km	Q_α	Q_β	h.km	Q_α	Q_β	h.km	Q_α	Q_β
0.1	30	30	0.1	30	30	0.1	30	30
0.2	50	50	0.2	50	50	0.2	50	50
0.3	75	75	0.3	75	75	0.3	75	75
0.4	100	100	1.4	100	100	3.4	100	100
20.0	150	150	20.0	150	150	20.0	150	150
	500	500		500	500		500	500
$\gamma = 4.00 \times 10^{-3}$ km^{-1}			$\gamma = 4.80 \times 10^{-3}$ km^{-1}			$\gamma = 4.30 \times 10^{-3}$ km^{-1}		
$Q_{Lg} = 230$			$Q_{Lg} = 190$			$Q_{Lg} = 215$		

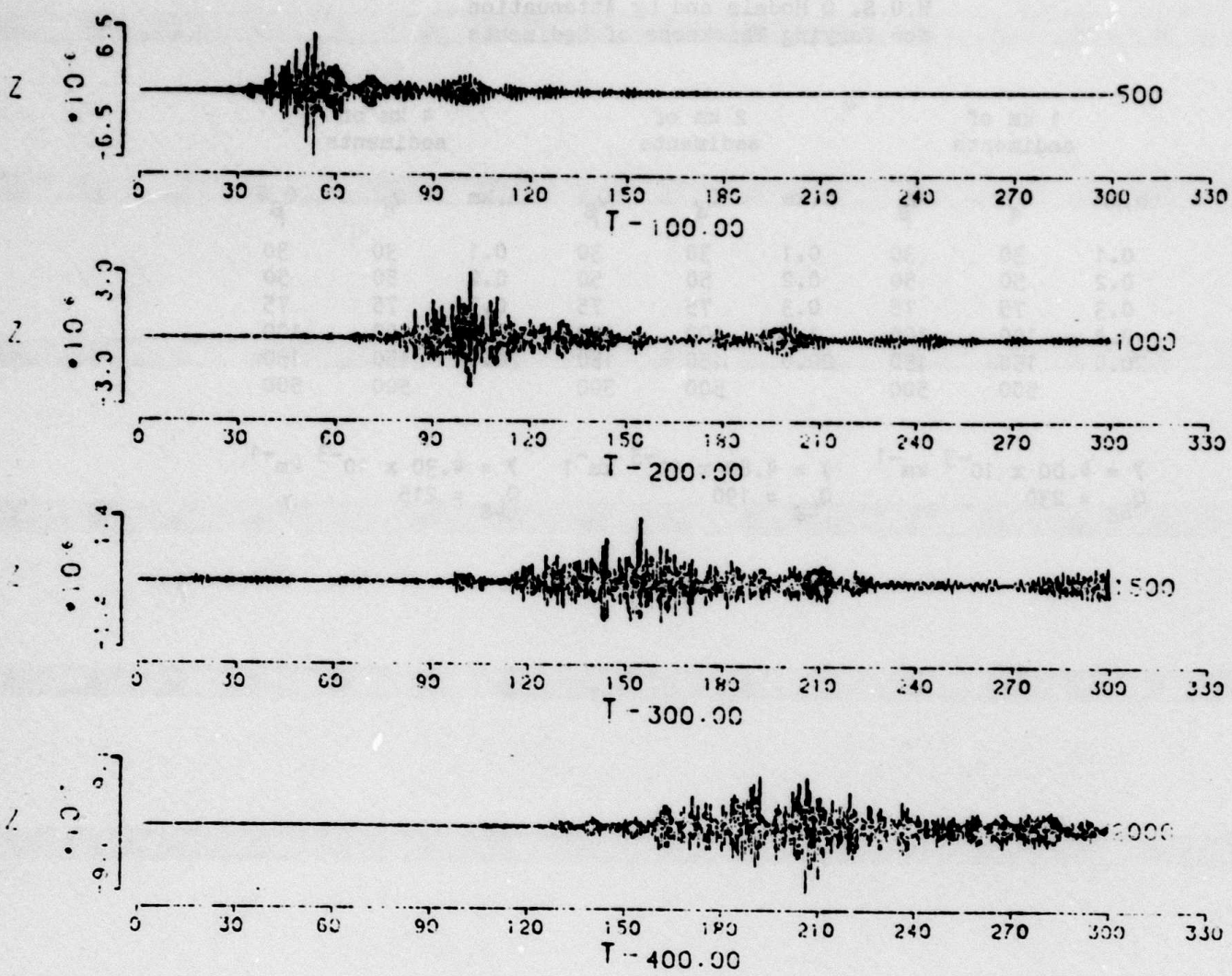

Figure 1a. Vertical component synthetic seismograms at 4 distances for the Simplified EUS model. Q_α = 2000 and Q_β = 1000 at all depths.

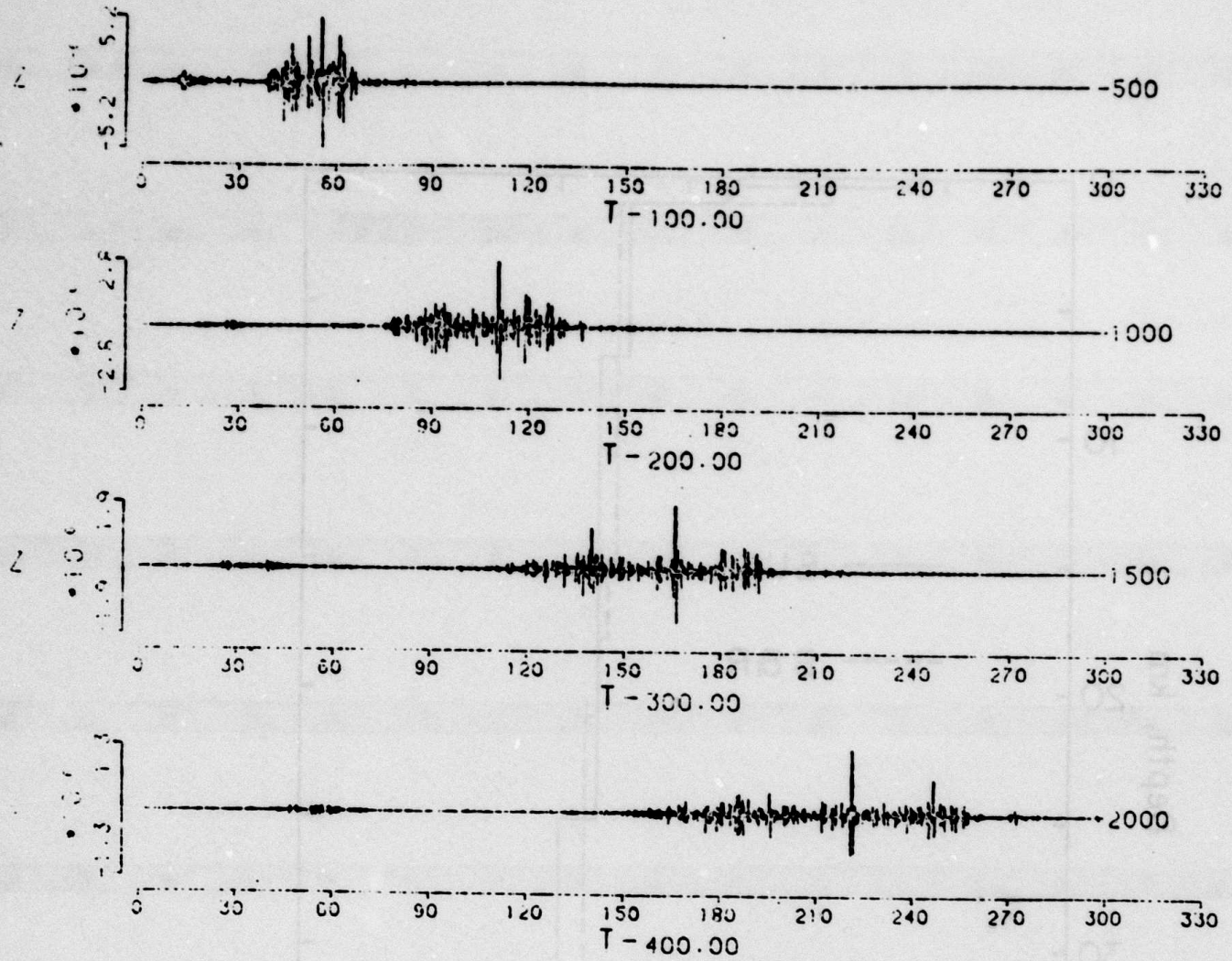

Figure 1b. Vertical component synthetic seismograms at 4 distances for the velocity model of McEvilly (1964). Q_α = 2000 and Q_β = 1000 at all depths.

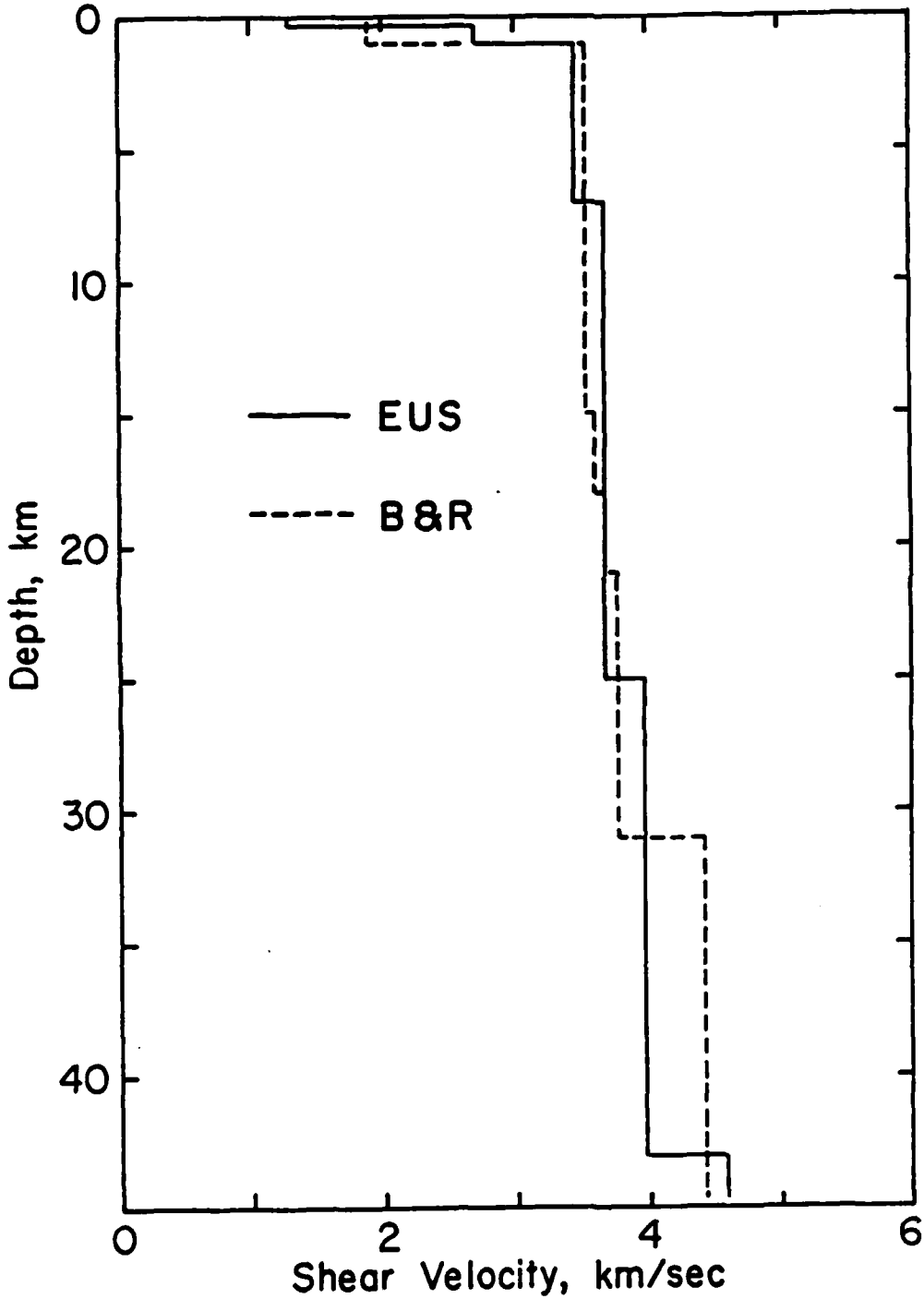

Figure 2. Shear velocities for simplified eastern United States model (Mitchell, 1982) and Basin-and-Range model (Bache et al., 1978)

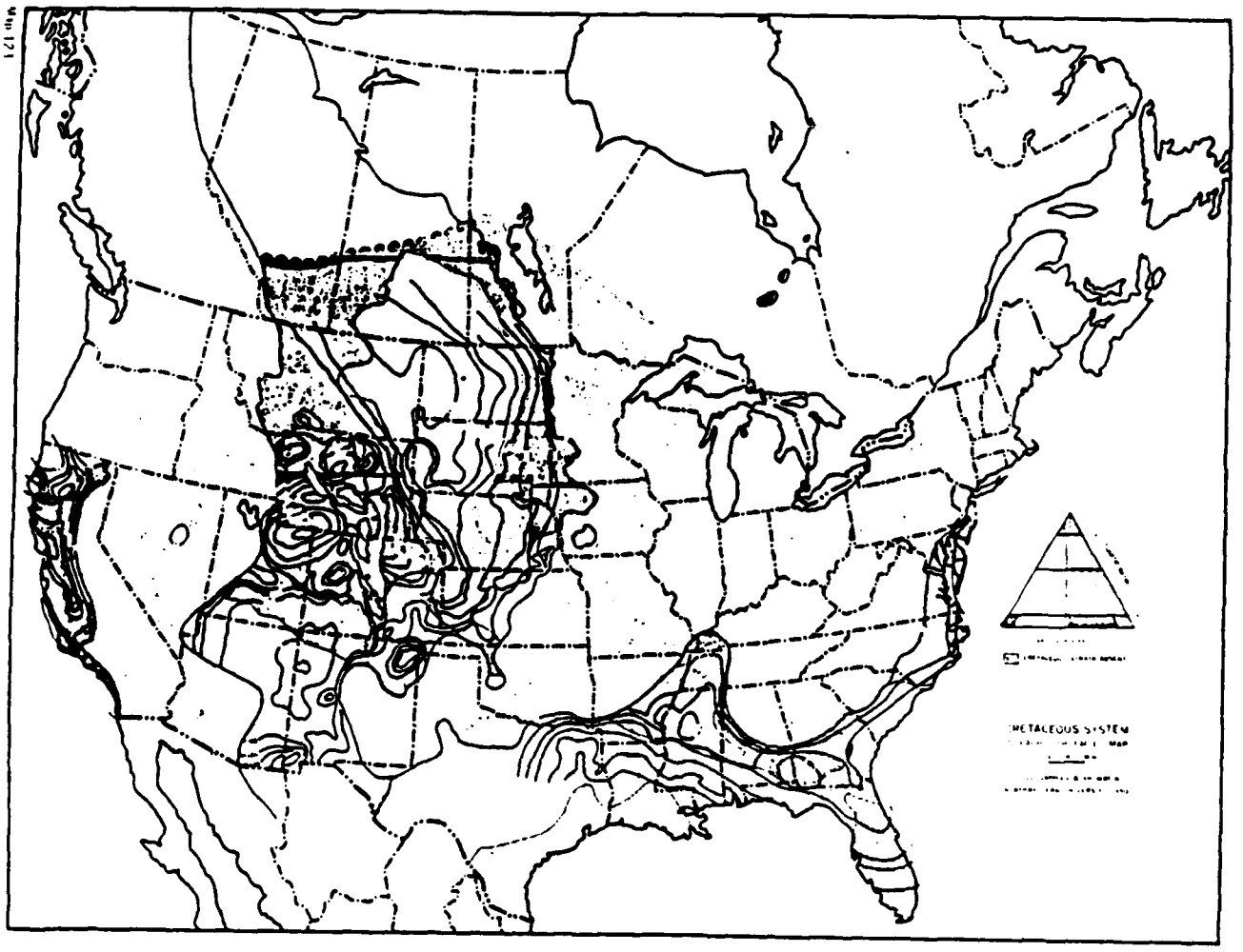

Figure 3. Isopach-lithofacies map for the Cretaceous system (from Sloss et al., 1960).

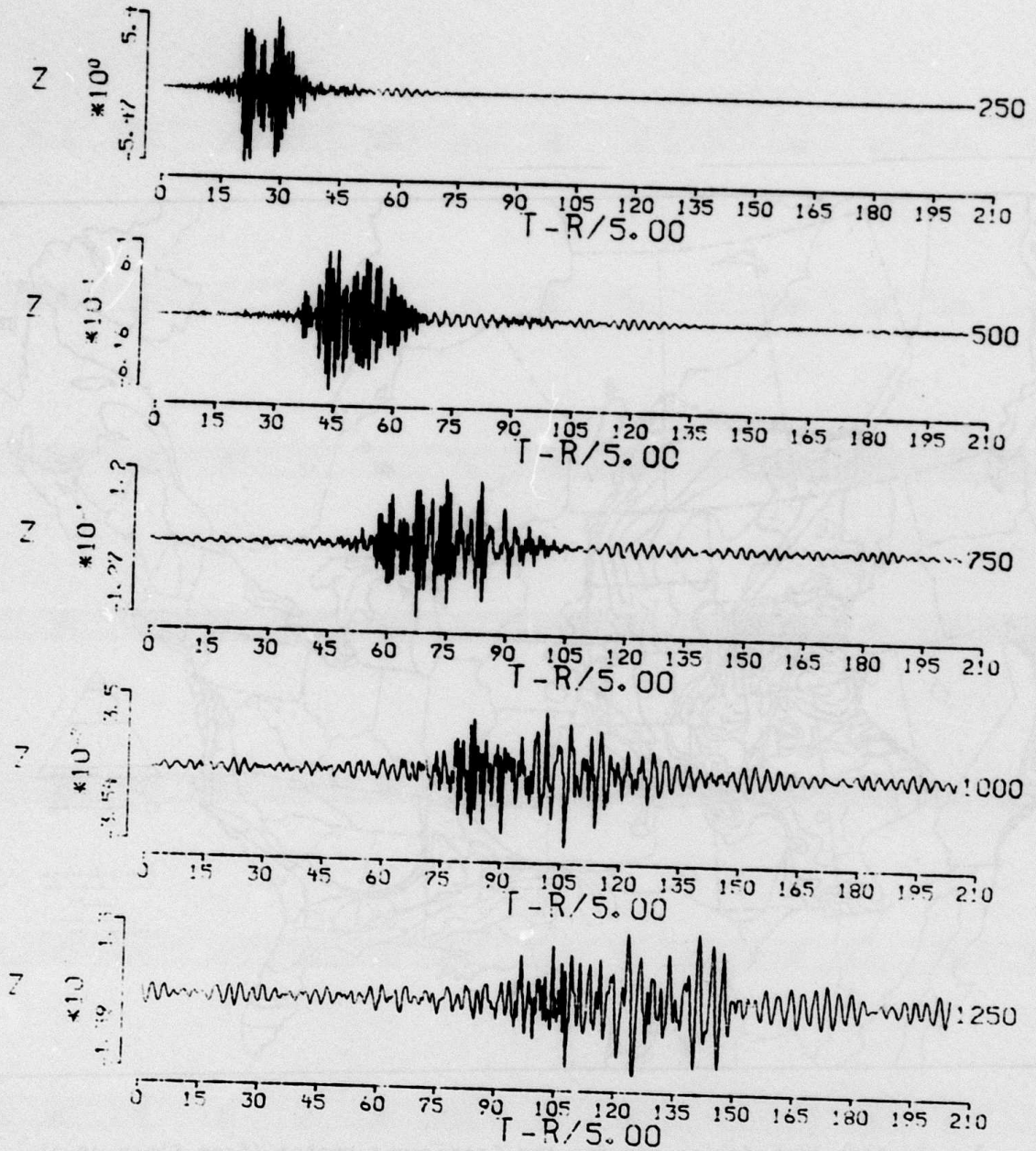

Figure 4. Synthetic Lg seismograms for a Basin-and-Range model with Q_α and Q_β values of 150 in the upper crust and 500 in the lower crust and upper mantle.

Summary of Studies on the Frequency Dependence of Q_β in the Continental Crust

by

E.O. Osagie, H.J. Hwang and B.J. Mitchell

One of the first observations to be made when regional studies of attenuation began in a systematic way in the mid-70's was that shear wave Q values (Q_β) in the crust obtained from intermediate-period surface waves can vary by large amounts from region to region (Mitchell, 1975; Cheng and Mitchell, 1981). Q values for 1-Hz Lg waves were also found to vary regionally in much the same way that Q_β from surface waves were found to vary. Studies such as that of Singh and Herrmann (1983) presented maps of 1-Hz Q values which showed low values of Q for Lg waves in the same region where low values of Q_β in the upper crust had been found.

Q_β has also been found to be frequency-dependent in the upper crust (Mitchell, 1980). The degree of that frequency dependence varies regionally, being higher in regions of high Q_β and lower in regions of low Q_β in the United States (Mitchell, 1981).

The purpose of the present report is to discuss preliminary attenuation data obtained at intermediate periods from South America and from India. Both regions have large areas which are tectonically stable as well as large areas which have undergone extensive tectonic activity. It should therefore be possible to verify whether our results for stable and active regions of North America are also applicable to other continents.

Data Acquisition and Processing

Seismograms which included well-developed fundamental-mode Rayleigh waves were obtained for several earthquakes in both South America and India. The events were selected such that they were situated on a common great circle path between two seismograph stations.

For the selection of events, a computer program was used to search the tape of USGS PDE epicenters for events located within 4 degrees of arc of the azimuth of a line joining two seismograph stations. The program obtains a set of earthquakes for each of the station pairs used. A manual selection was then made from this set of events on the basis of magnitude, distance to the station, and depth. The data used were vertical component seismograms recorded by instruments of the World-Wide Standard Seismograph Network (WWSSN).

Spectral amplitudes and group velocities of the fundamental-mode Rayleigh wave were obtained by the multiple-filter technique (Dziewonski et al., 1969). The recorded seismograms were digitized at irregular intervals and a sampling interval of 1.0 sec was then obtained by linear interpolation of the digitized points. Digitization started 1 or 2 minutes before the arrival of the surface waves and extended to times corresponding to group velocities of about 2.2 km/sec. The length of the digitized record depends on the length and character of the dispersed wave, but most often it is 8-10 minutes long.

Attenuation at Intermediate Periods

Attenuation coefficients were computed from amplitude spectra using the two-station method (Ben-Menahem, 1965). An advantage of the two-

station method is that it does not require a knowledge of the source or the velocity structure along the path of propagation. Several individual determinations along the same path, however, can show large fluctuations due to multipathing. The attenuation coefficients are obtained using the equation

(1)

where A refers to spectral amplitude, I to instrument response, r to distance in km, and Δ to distance in degrees. The subscripts 1 and 2 refer to values at the near and more distance stations, respectively.

Preliminary Rayleigh wave attenuation coefficients determined for the eastern and western portions of South America appear in Figure 1. The scatter in the data is reflected in standard deviation bars which accompany the mean values at each period. It is quite apparent that the attenuation coefficients for western South America are substantially higher than those for eastern South America, especially at shorter periods between 20 and 40 seconds. The values for eastern South America are similar to, and perhaps slightly lower than, those previously determined for eastern North America. The values for western South America are similar to those obtained in tectonically active regions of North America (Mitchell et al., 1977) or Eurasia (Yacoub and Mitchell, 1977). Similar attenuation coefficient values have been obtained for the stable and tectonically active regions of India from the portion of the available data from that region which has been analyzed up to now.

Inversion of Q_β

The equations of Anderson et al. (1965) were used to invert the attenuation coefficient data, assuming that Q_β is independent of frequency. In order to utilize those equations, a velocity model is required for the region of study. Phase velocities were obtained using the two station method. Across the eastern region of South America, they are very close to the phase velocities of the Canadian shield (Brune and Dorman, 1963). The phase velocities determined for the western portion of South America agree closely with values determined for that region by James (1971). Because of the agreement of phase velocities observed in the present research with those obtained from earlier models, we use those velocity models to compute partial derivatives to be used in the inversion process for Q_β.

Models of Q_β were obtained for both eastern and western South America (Figure 2). The Q_β values for western South America appear to be lower at all depths than those for eastern South America, although at greater depths in the crust it is not possible to resolve the differences between the two regions. The data for western South America appear to require a low Q zone in the upper mantle whereas the data for eastern South America do not. Because of the similarity of the attenuation data for India, it is also expected that crustal Q_β values will be lower in tectonically active regions than in stable regions of that sub-continent.

Attenuation of 1-Hz Lg

The models shown in Figure 2 were used to compute the attenuation

and Q values for 1-Hz Lg and to compare them with previously determined observed values (Raoof and Nuttli, 1983). Programs written by C.Y. Wang and R.B. Herrmann (Wang, 1981) were used to compute synthetic seismograms, corresponding to short-period instruments of the World-Wide Standard Seismograph Network (WWSSN), and to measure the amplitude fall-off with distance to determine attenuation coefficients and Q values. This method allows us to determine Q values for Lg predicted by various models in much the same way that Q is determined from real seismograms.

Synthetic seismograms of 1-Hz Lg waves were computed for the models of both eastern and western South America (Figures 3 and 4). The seismograms for western South America not only fall off more rapidly with distance than those for eastern South America, but also have lower predominant frequencies, especially at greater distances. The models predict values of Q for Lg recorded on short-period WWSSN instruments to be 480 and 290, respectively, for eastern and western South America.

The Q value of Lg predicted by the model of eastern South America (480) is substantially lower than those observed by Raoof and Nuttli (1983). This result implies that Q_β in the crust beneath eastern South America is substantially higher at high frequencies (near 1-Hz) than at lower frequencies. This result is similar to that of Mitchell (1981) for eastern North America. By contrast, the Q value of Lg predicted by the model of western South America is similar to that observed by Raoof and Nuttli (1983). Q_β in the crust beneath western South America, therefore, does not vary significantly with frequency over the frequency range considered in this report. These results are consistent with ear-

lier results in North America (Mitchell, 1981), where Q_β values in the crust of the tectonically active region of western North America do not vary greatly with frequency whereas they do in the stable craton of eastern North America. Preliminary results for stable and tectonically active regions of India also seem to be consistent with that pattern.

References

Anderson, D.L., A. Ben-Menahem, and C.B. Archambeau, Attenuation of seismic energy in the upper mantle. J. Geophys. Res., 70. 1441-1448, 1965.

Ben-Menahem, A., Observed attenuation and Q values of seismic surface waves in the upper mantle. J. Geophys. Res., 70, 4611-4651, 1965.

Brune, J., and J. Dorman. Seismic waves and earth structure in the Canadian shield, Bull. Seism. Soc. Am., 53, 167-209, 1963.

Cheng, C.C., and B.J. Mitchell. Crustal Q structure in the United States from multi-mode surface waves, Bull. Seism. Soc. Am., 71, 161-181. 1981.

Dziewonski, A., S. Block, and M. Landisman, A technique for the analysis of transient seismic signals, Bull. Seism. Soc. Am., 59, 427-444, 1969.

James, D.E., Andean crustal and upper mantle structure. J. Geophys. Res., 76. 3246-3271. 1971.

Mitchell. B.J., Regional Rayleigh wave attenuation in North America. J. Geophys. Res., 81, 4904-4916, 1975.

Mitchell, B.J., Frequency dependence of shear wave internal friction in the continental crust of eastern North America, J. Geophys. Res., 85, 5212-5218, 1980.

Mitchell. B.J., Regional variation and frequency dependence of Q_β in the crust of the United States, Bull. Seism. Soc. Am., 71. 1531-1538, 1981.

Mitchell, B.J., N.K. Yacoub, and A.M. Correig, A summary of seismic surface wave attenuation and its regional variation across continents and oceans, in AGU Mono. 20. The Earth's Crust, edited by J.G. Heacock, 405-425, 1977.

Raoof. M., and O.W. Nuttli. Attenuation of high frequency Lg waves in South America (abstract), Earthquake Notes, in press. 1983.

Singh. S., and R.B. Herrmann, Regionalization of crustal coda Q in the continental United States, J. Geophys. Res., 88, 527-538, 1983.

Wang, C.Y., Wave Theory for Seismogram Synthesis, Ph.S. Dissertation, Saint Louis University, 235 pp, 1981.

Yacoub, N.K., and B.J. Mitchell, Attenuation of Rayleigh wave amplitudes across Eurasia. Bull. Seism. Soc. Am., 67, 751-769, 1977.

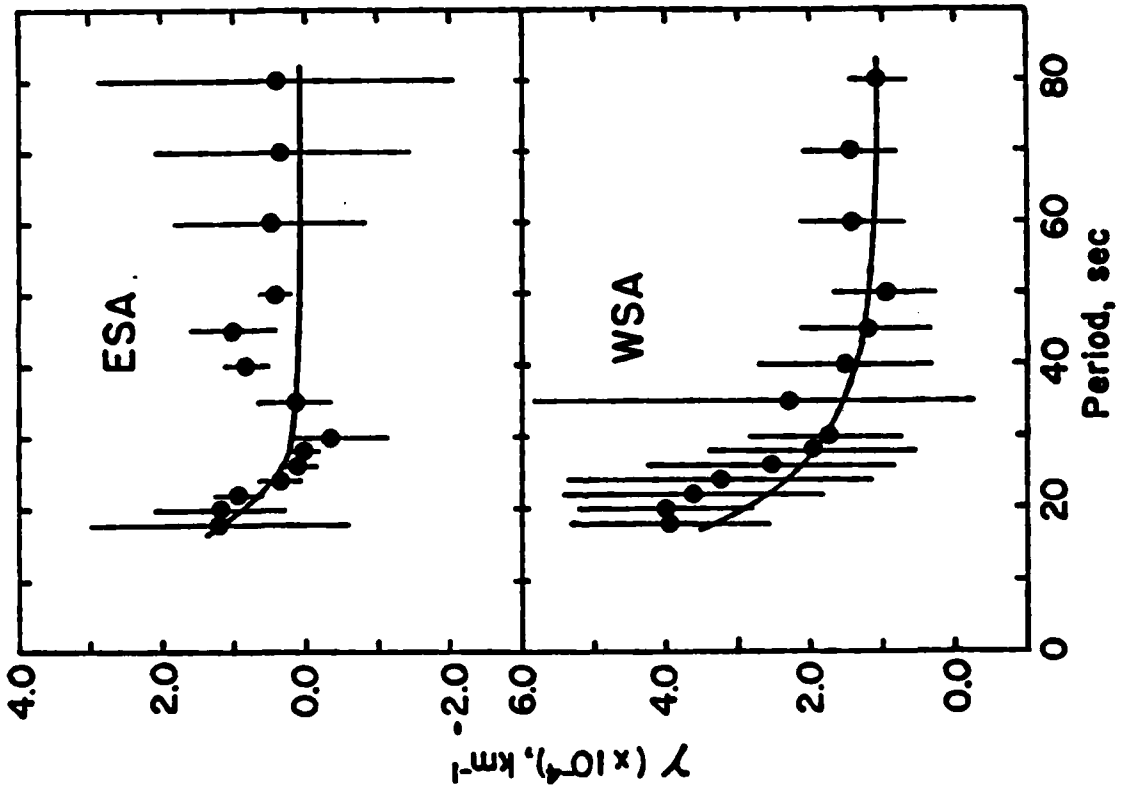

Figure 1. Rayleigh wave attenuation coefficients for paths in eastern and western South America. Circles denote observed values, vertical lines indicate standard deviations, and the curved lines are theoretical values corresponding to the models in Figure 3.

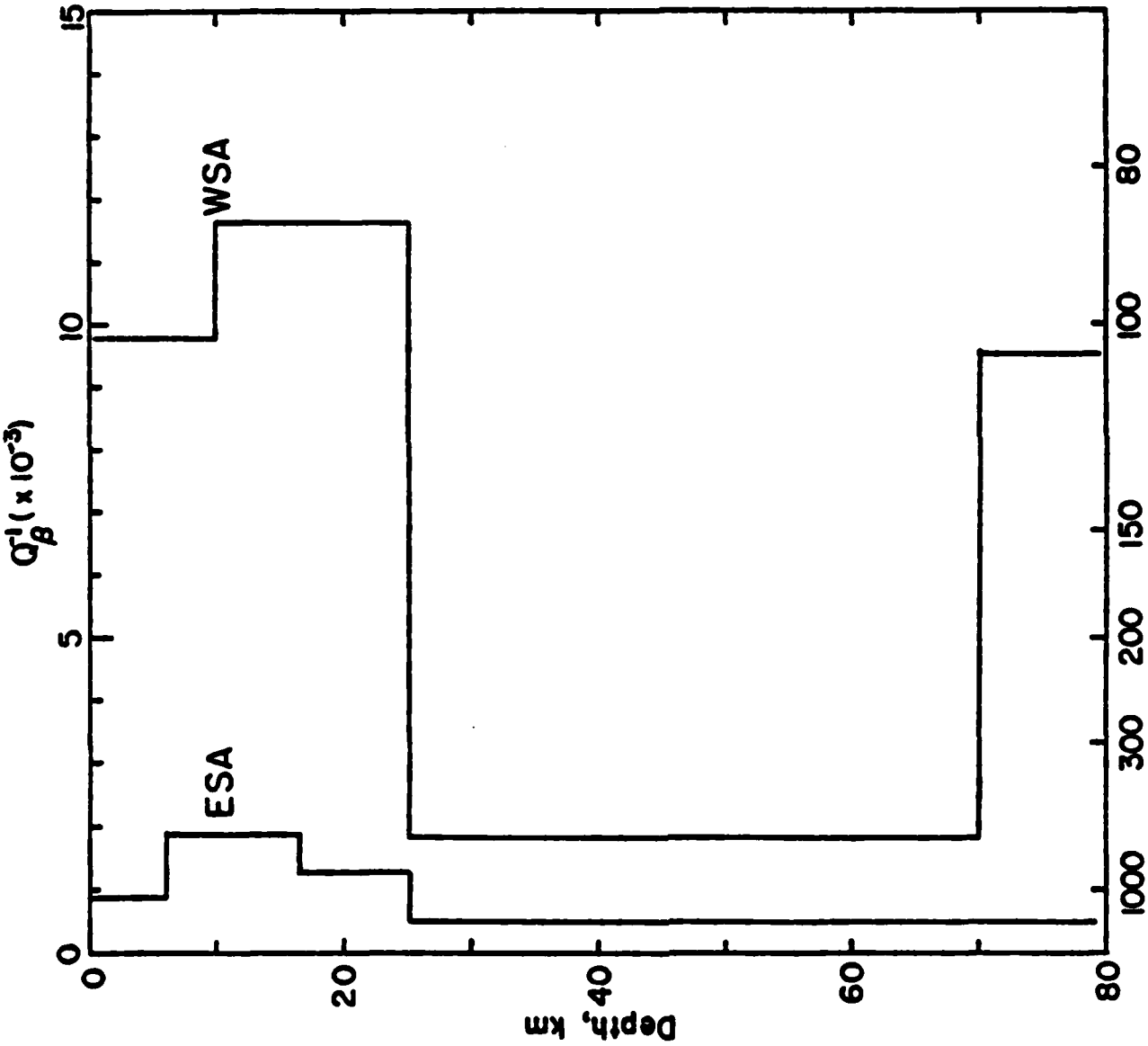

Figure 2. Models of anelasticity for eastern and western Southern America.

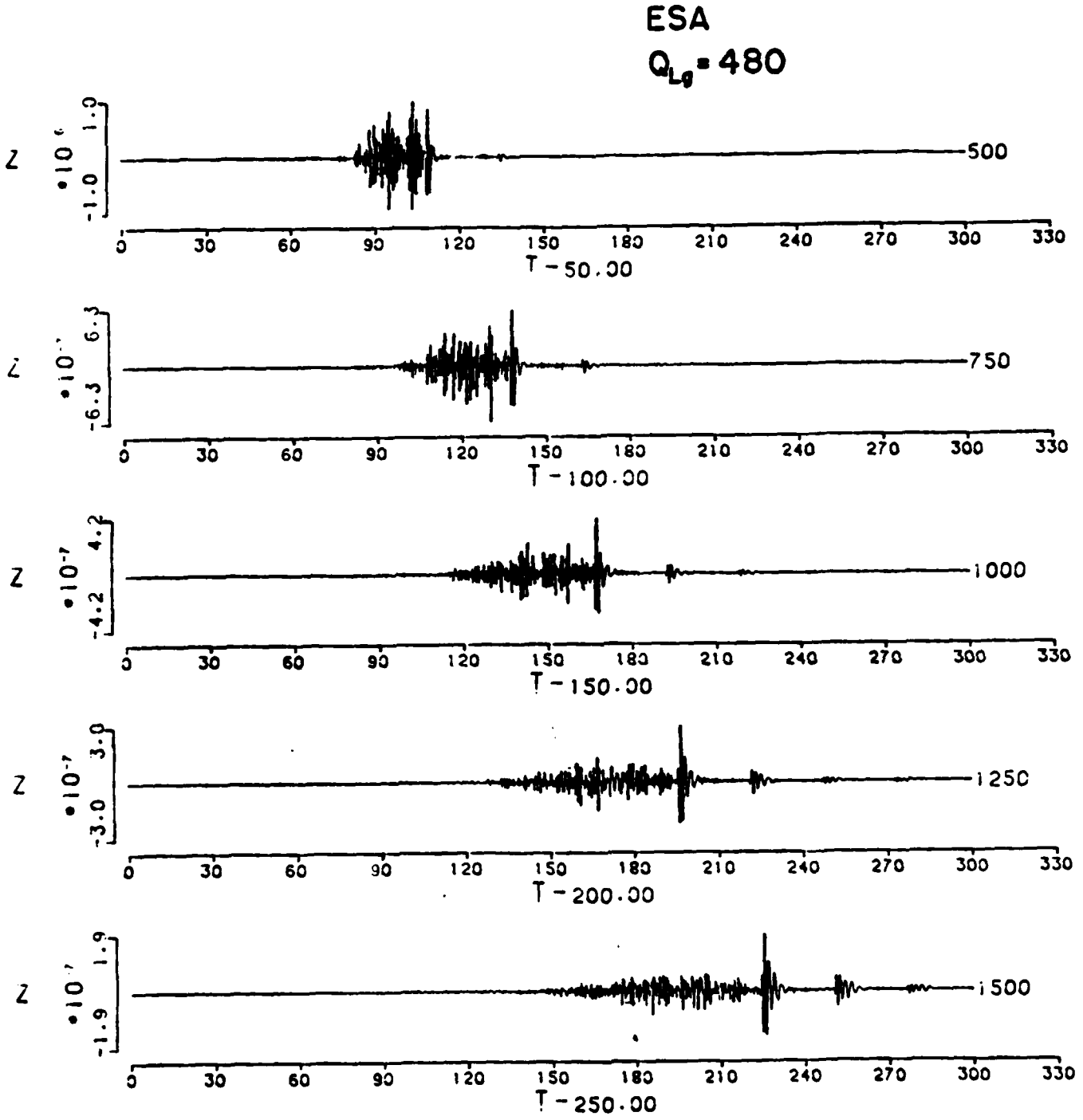

Figure 3. Synthetic seismograms for paths across eastern South America for the phase Lg as recorded on short-period WWSSN seismographs.

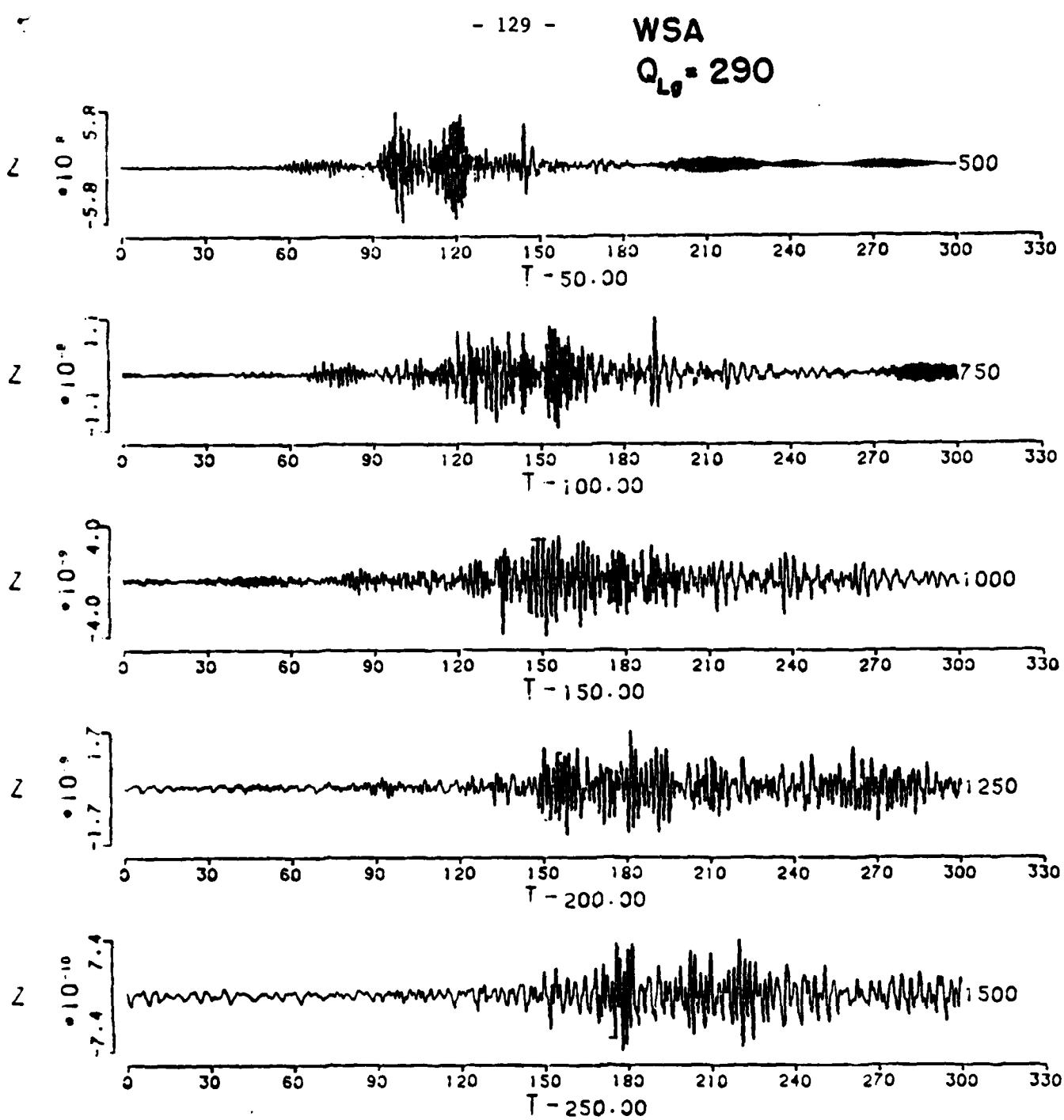

Figure 4. Synthetic seismograms for paths across western South America for the phase Lg as recorded on short-period WWSSN seismographs.